MICROBIOLOGICAL REVIEWS, Mar. 1978, p. 114-160
0146-0749/78/0042-0114$02.00/0

Vol. 42, No. 1
Printed in U.S.A.

Anatomy and Chemistry of Spirochetes

STANLEY C. HOLT

Department of Microbiology, University of Massachusetts, Amherst, Massachusetts 01003

INTRODUCTION

Biologists have been fascinated with the complexity and multitude of morphologies that exist in the microscopic world ever since van Leeuwenhoek observed "very little animalcules" in 1674 (57). Among the numerous observations and recordings made by van Leeuwenhoek some appear to be of spirochetes; in 1681 he wrote to the Royal Society (57, letter 34) on a host of subjects, including the "animalcules" found in his feces during a bout with diarrhea. Dobell suggests that it is here, in letter 34, that van Leeuwenhoek "... in no uncertain terms (described) the discovery of intestinal protozoa and bacteria of man." In addition, letter 34 describes for the first time organisms that "... had a very nimble motion, and bent their bodies serpentwise and shot through the stuff as quick as a pike through the water" and that were, presumably, spirochetes. After examining material removed from the teeth of an old man, van Leeu-

wenhoek noted, "I found an unbelievably great company of living animalcules aswimming more nimbly than any I had ever seen up to this time. The biggest sort (whereof there were a great plenty) bent their body into curves in going forwards..." It is probable that this large bent organism (reference 57, Fig. G, letter 39, 17 September 1683) was a spirochete, possibly *Spirochaeta buccalis* (*Borrelia buccalis*).

The majority of observations of spirochetal morphology in the early years of bacteriology were made on organisms of medical importance—for example, *Treponema pallidum* obtained from a lesion. Early investigators, notably Zuelzer (239), Dobell (56), and Noguchi (150), began the morphological investigations of spirochetes by employing light microscopy. Morton and Anderson (143, 144) were the first to use the electron microscope in an examination of *T. pallidum* Nichols and *Leptospira*. The literature concerned with spirochete morphology to 1960 has been reviewed by Babudieri (9–11), to which the reader is referred for detailed information.

The potential of the electron microscope as a tool for analysis of biological ultrastructure was widely realized only in the 1950s, when the resulting information could be associated with the chemical analyses of isolated cell fractions such as cell walls, membranes, mitochondria, flagella, and nuclei. Patterns of structural-functional relationships emerged, which may be reaching their zenith in sophisticated studies of membrane-nucleoid associations (126). The full force of structure-function investigations are seen in the attempts to localize enzyme complexes, for example, and discern their in vivo roles by integrated morphological, biochemical, and genetic analysis.

Order Spirochaetales. The term spirochetes will be used to encompass this group of flexuous, thin, gram-negative, chemoheterotrophic, helical-shaped organisms, which differ morphologically from other procaryotes by the presence of an axial fibril, known also as an endoflagellum, axistyle, or axial filament (12, 192, 193). Members of the group thus far examined invariably possess an outer sheath, which surrounds the cell, a protoplasmic cylinder, consisting of the cell wall, cell membrane, and the enclosed cytoplasm, and the axial fibril. Some, or all, of the basic spirochetal structural features are seen in even the earliest electron micrographs (5, 25, 49, 116, 117, 128, 140, 142–144, 173, 191, 226, 233) and are shown in micrographs and diagrams in Fig. 1, 2, and 3. By current definition, any procaryotic cell with an axial fibril is considered a spirochete. However, no longer is overall cell outline, as deduced from light microscopy, sufficient to mark an organism as a spirochete; witness the members of *Spiroplasma* that (Fig. 1k and 2b) have a gross morphology strikingly similar to those classically associated with *Spirochaetales*.

The members of the order *Spirochaetales* are grouped into five genera, *Spirochaeta*, *Cristispira*, *Treponema*, *Borrelia*, and *Leptospira*, and the genera are separated from one another on the basis of morphological and physiological traits (34, 192, 193).

Descriptions have been based on organisms growing under very different environmental conditions, and thus different physiological conditions, but several morphological traits appear to be stable and sufficiently distinctive to serve as key characteristics for generic differentiation. Among these are the wavelength of the coils, the presence or absence of terminal (polar) hooks, the shape of the cell poles, and the number of axial fibrils. In general, the dimensions vary from 0.1 to 3 μm in diameter and 3 to 500 μm in length. *Spirochaeta* (Fig. 1b and h) cells are 0.2 to 0.75 by 5 to 500 μm, with uniform amplitude of the coils; the cell poles are relatively straight with rounded ends. Two axial fibrils, one at each end of the cell, are present. *Cristispira* (Fig. 1a) range in size between 0.3 and 3 by 30 and 150 μm; the cell poles may be rounded, tapered, or pointed and possess a characteristic rigid spicule. As many as several hundred axial fibrils are normally present at each cell pole. *Treponema* strains (Fig. 1e, g through j) range in size from 0.09 to 0.5 by 5 to 20 μm, and cells of several of them have irregular wavelength along the coil; cell poles are rounded or tapered, and each characteristically possesses from three to five axial fibrils (45, 93, 95, 96, 98, 188). *Borrelia* strains (Fig. 1f) as large as 1 by 25 μm have been observed; the coils of *Borrelia* cells are longer and looser than those of the treponemes; cell poles are tapered or pointed, and each bears 15 to 20 axial fibrils. The *Leptospira* (Fig. 1c) range in size between 0.1 by 6 and 0.1 by 20 μm. Characteristics of the genus include the regular, tight coiling of the central portion; either one or both of the cell poles take the form of a hook and a single axial fibril at each pole of the genus.

Particularly for members of the genera *Treponema* and *Leptospira*, the degree to which the same or different organisms may have been assigned the same or different names is often uncertain. It will be my practice in this essay to refer to organisms by the names used in papers dealing with their anatomical details; whether this practice will have the desired result of avoiding the arbitrary "lumping" of independent isolates, which may indeed differ from one another

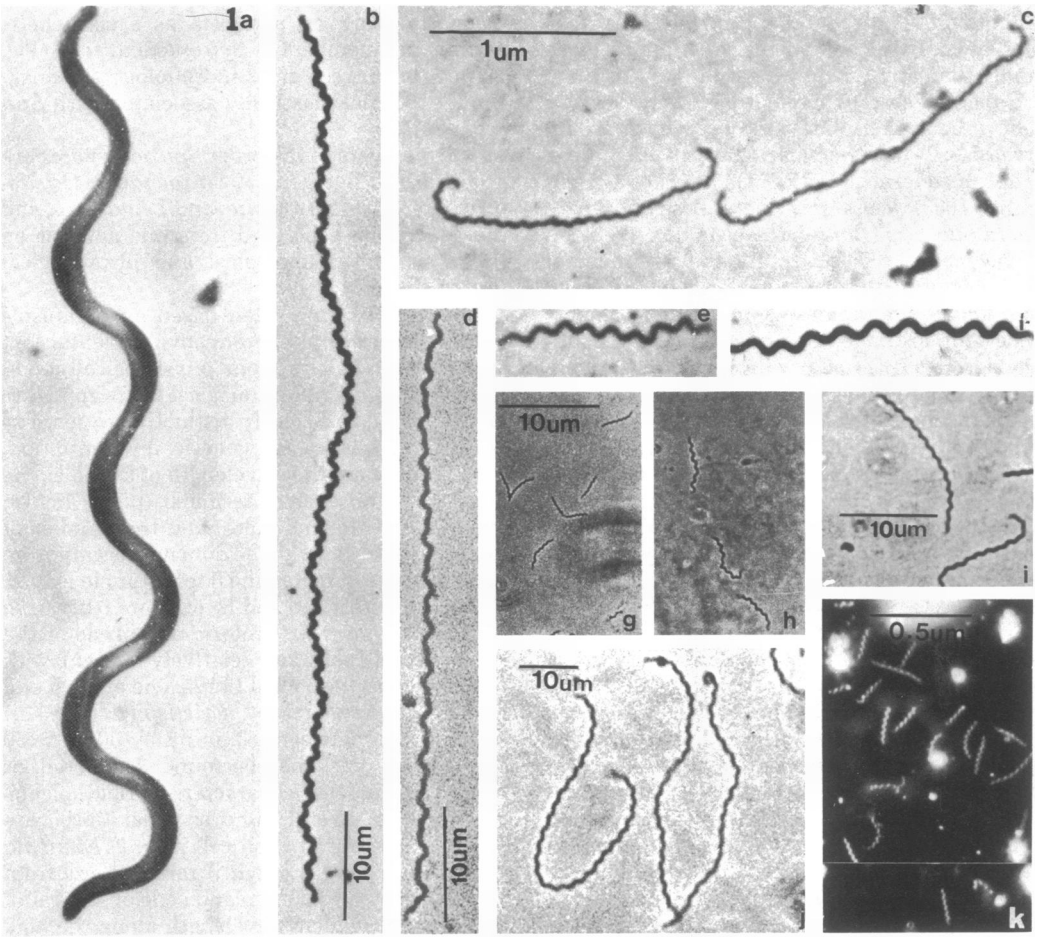

FIG. 1-24. *The following abbreviations are used: axial fibril, AF; axial fibril core, AFC; outer sheath, OS; axial fibril sheath, AFS; protoplasmic cylinder, PC; axial fibril insertion pore, IP; electron-opaque particles, P; cytoplasmic membrane, CM; mesosome, M; cytoplasmic tubule, CT; rhapidosome, R; honeycombed proximal hook, PH; insertion disks, D; axial fibril neck, C; axial fibril-associated membrane, Mm; striated tubules, ST; peptidoglycan, Pg; adjacent outer sheaths, DOS; cytoplasmic fibrils, CF; perimural fibrils, PF; cytoplasmic region, CR; helical lipoprotein layer, H; treponemes, T; collagen fibers, CL; pinocytotic vesicle, PV; intracellular space, I; spirochetes, S; microvilli, MV; cytoplasmic membrane bleb, CYB; residual desmosomes, RD; protozoan flagellum, F; Pyrsonympha membrane, Pm; transitional zone, TZ; vesicles, V; potassium phosphotungstate, KPTA; uranyl acetate, UAC; ammonium molybdate, NH_4MoO_4. All figures reproduced here are done with appropriate permission.*

FIG. 1. *Phase-contrast photomicrographs of representative spirochetes. (a) Cristispira species from the crystalline style of Cryptomya californica; (b) S. plicatilis; (c) L. interrogans icterohaemorrhagiae with characteristic hooked ends; (d) intermediate type B spirochete found occurring with S. plicatilis; (e) irregularly coiled, pointed-end T. pallidum from rabbit testes; and (f) B. anserina from chicken blood. T. zuelzerae from logarithmic growth phase and S. stenostrepta are seen in (j) and (i), whereas the very small T. denticola and S. litoralis are seen in (g) and (h). (k) Dark-field photomicrograph of suckling mouse cataract agent (Spiroplasma) in chorioallantoic fluid from 4-day-infected embryonated hen eggs. (a, c, e, f) are from D. Kuhn, Bergey's Manual of Determinative Bacteriology, 8th ed; (b, d, g, h) from reference 20; (i, j) from reference 34; and (k) from reference 215.*

in important ways, will undoubtedly be known only after careful, future comparative taxonomic studies have been undertaken.

OUTER SHEATH

Hardy and Nell (81) along with Turner and Hollander (216, 217) provided some of the earliest evidence for the presence of an outer sheath in spirochetes on the basis of antibody-agglutination studies. *T. pallidum* Nichols, freshly isolated from rabbits, were not agglutinated by treponeme-specific antibodies, although aged

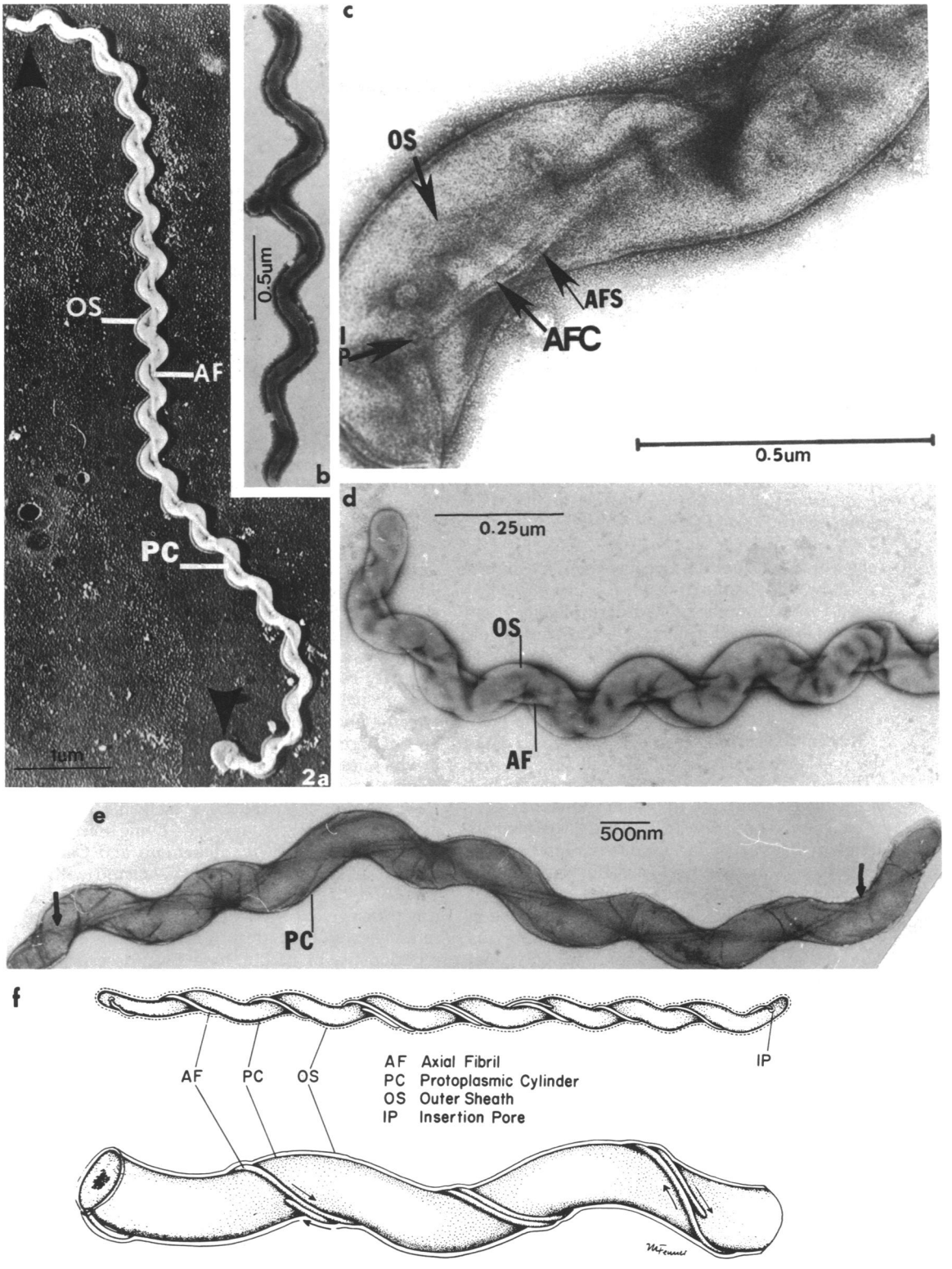

FIG. 2. *Electron micrographs and interpretative drawing of representative spirochetes and Spiroplasma. (a) Chromium-shadowed L. interrogans icterohaemorrhagiae with cell poles, characteristically hooked (arrows). (b) Suckling mouse cataract agent (Spiroplasma) in chorioallantoic fluid. Note the absence of axial fibril. (c) S. stenostrepta Z1; (d) L. interrogans B16. In (c), the axial fibril core and axial fibril sheath are evident. (e) T. zuelzerae—the axial fibrils that extend for most of the cell length and wind with the protoplasmic cylinder are in a 1-2-1 (arrows) arrangement and overlap in the central region of the cell. (f) Basic anatomical components of spirochetes as interpreted from electron micrographs; surface views. (c through e) UAC, negative stain; (b) KPTA, negative stain. (a) is from reference 191; (b) from reference 215; (c) from reference 90; (d) from reference 147; and (e) from reference 113.*

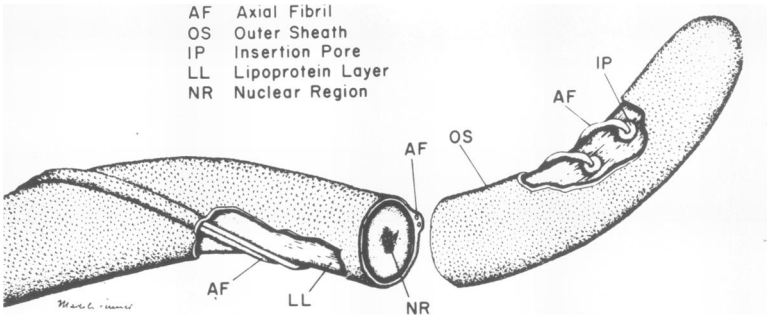

3

FIG. 3. *Diagramatic representation of a typical spirochete as interpreted from electron micrographs. An outer sheath envelopes the cell. The axial fibrils are between the outer sheath and the layers of the protoplasmic cylinder (depicted here as a lipoprotein layer, as found in S. stenostrepta) and insert into the cylinder by way of an insertion pore.*

cells were agglutinated. Because heated cells did not show this change in seroreactivity, they proposed that a nonreactive external physical barrier was lost from the aging cell. The then available electron microscopic studies were consistent with this interpretation.

Location and General Morphology

Negative stains. The outer sheath is seen as the most external layer of the cell (Fig. 2a and c through e, 4a through c, 5a and e through g, 6a, b, and d through f). In preparations that were not extracted or chemically treated, this sharply delineated layer varies in fine structure from smooth and nontextured, e.g., in *Spirochaeta stenostrepta* (Fig. 2c and 7e), to a morphologically complex layer of polygonal subunits as in *S. aurantia* (Fig. 4a; reference 31), *S. litoralis* (88), and *T. microdentium* (96). The polygonal subunits are approximately 8 nm in diameter and are separated by a 2-nm space. These or different anatomical features might be looked for in the strains not yet examined. Listgarten and Socransky (128) observed, in an as yet uncultivated large spirochete associated with acute necrotizing ulcerative gingivitis, an outer sheath they characterized as being "pinstriped" (Fig. 4b and d). These parallel stripes (15 to 16 nm wide and separated by a 5- to 6-nm space) may result from a folding of the outer sheath such that two layers with polygonal subunits are nearly superimposed on one another. In other small- and intermediate-size spirochetes, the outer sheath subunits were also polygonal, but had a diameter of 0.8 nm and were separated by a 0.2-nm space. A central core in the polygonal subunits often could be discerned (129). In two cultivable treponemes, *T. refringens* and *T. genitalis*, the outer sheath (referred to by Hovind-Hougen [95] as the RS or SL layer) of enzyme- or detergent-treated cells contained holes, rings, pits, or depressions arranged either pentagonally or hexagonally in tightly packed rows. The center-to-center spacing of this substructure varies between 4 and 10 nm; the pits have a mean diameter of approximately 5 nm (95–98).

The outer sheaths of *S. plicatilis*, all *Borrelia* species, and *T. phagedenis* strains so far examined are characterized by a lack of structural detail (20, 94, 95). A large free-living spirochete (designated type B by Blakemore and Canale-Parola; reference 20) found associated with *S. plicatilis* (20) contains fibrillar elements that run transversely across the cell (Fig. 4c and e; reference 20). Fine, transverse striations, having a periodicity of 4.5 nm, have been described by Birch-Anderson et al. (18) in the outer sheath of *Leptospira interrogans* pomona.

In most cases, treatment of spirochetes with surface-active agents and/or enzymes results in a dramatic alteration or rearrangement of the outer sheath. Thus, for example, when *T. genitalis* is treated for short (30 s to 1 min) periods with sodium deoxycholate, not only is the outer sheath substructure disorganized to reveal pits (see above), but thin fibrils, approximately 2 nm in diameter, are also seen. Similarly, when *T. phagedenis* and *T. vincentii* are treated with the myxobacter AL-1 protease or the detergent Tee-pol, the outer sheath is likewise altered to expose a fine structure of closely apposed, parallel zigzag fibers (95). The fibers are separated by a space approximately 8 nm wide. Similar treatments also disorganized the outer sheath substructure

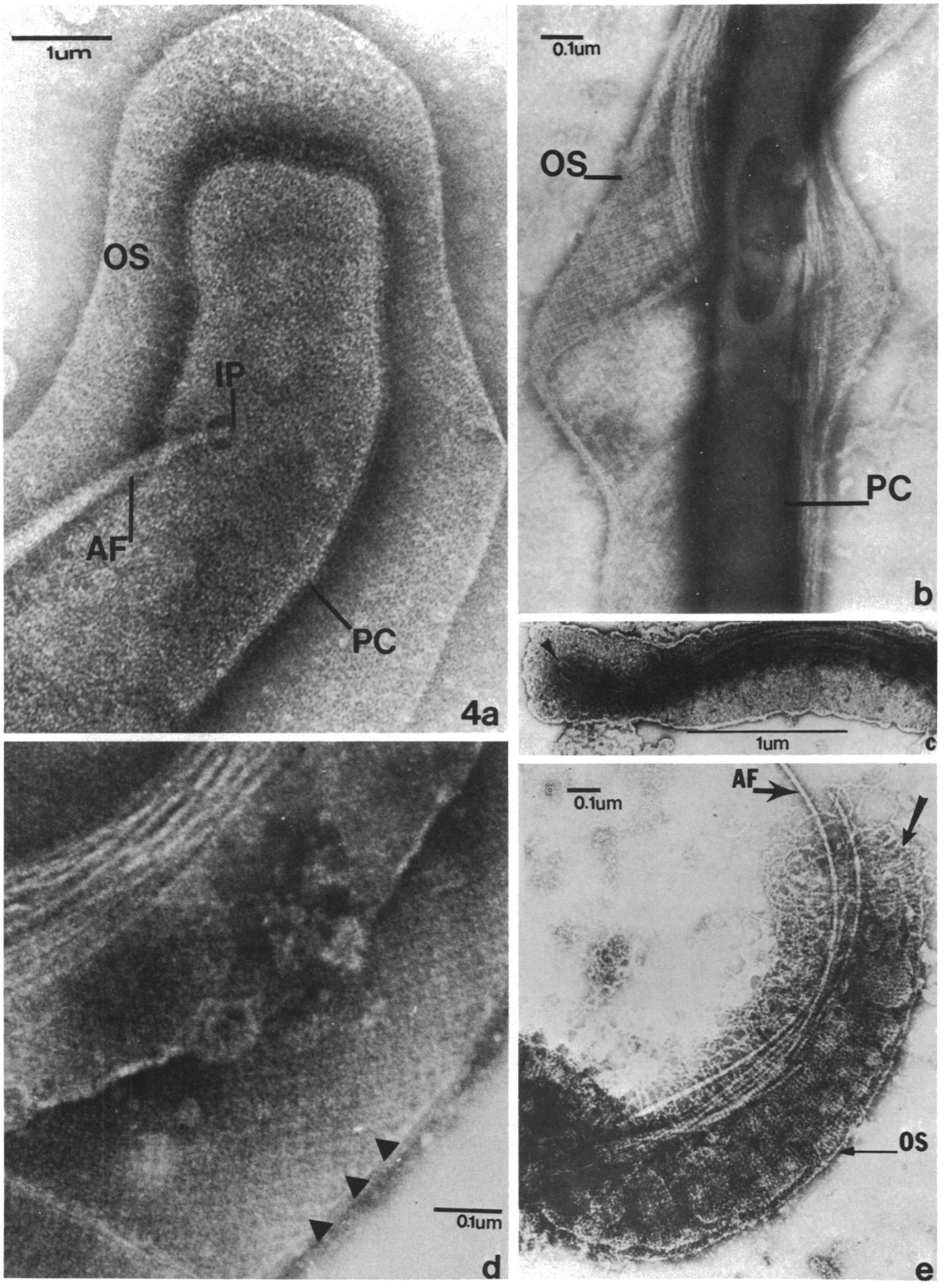

FIG. 4. *Electron micrographs of negatively stained portions of S. aurantia J1 (a), a large spirochete from gingival debris (b, d), and the type B spirochete (c, e) found associated with S. plicatilis. The outer sheath in the spirochetes varies from polygonal (a) to pinstriped (b). The pinstriped arrangement gives way to a cross-hatched pattern where the stripes overlap at the cell periphery (triangles, d). The type B spirochete (c, e) has a striated or fibrillar outer sheath (e, arrow). The axial fibril is located below the layers of the outer sheath (e) and inserts directly into the axial fibril insertion pore (a). (a through c) NH_4MoO_4; (b, e) KPTA. (a) is from reference 31; (b, d) from reference 128; and (c, e) from reference 20.*

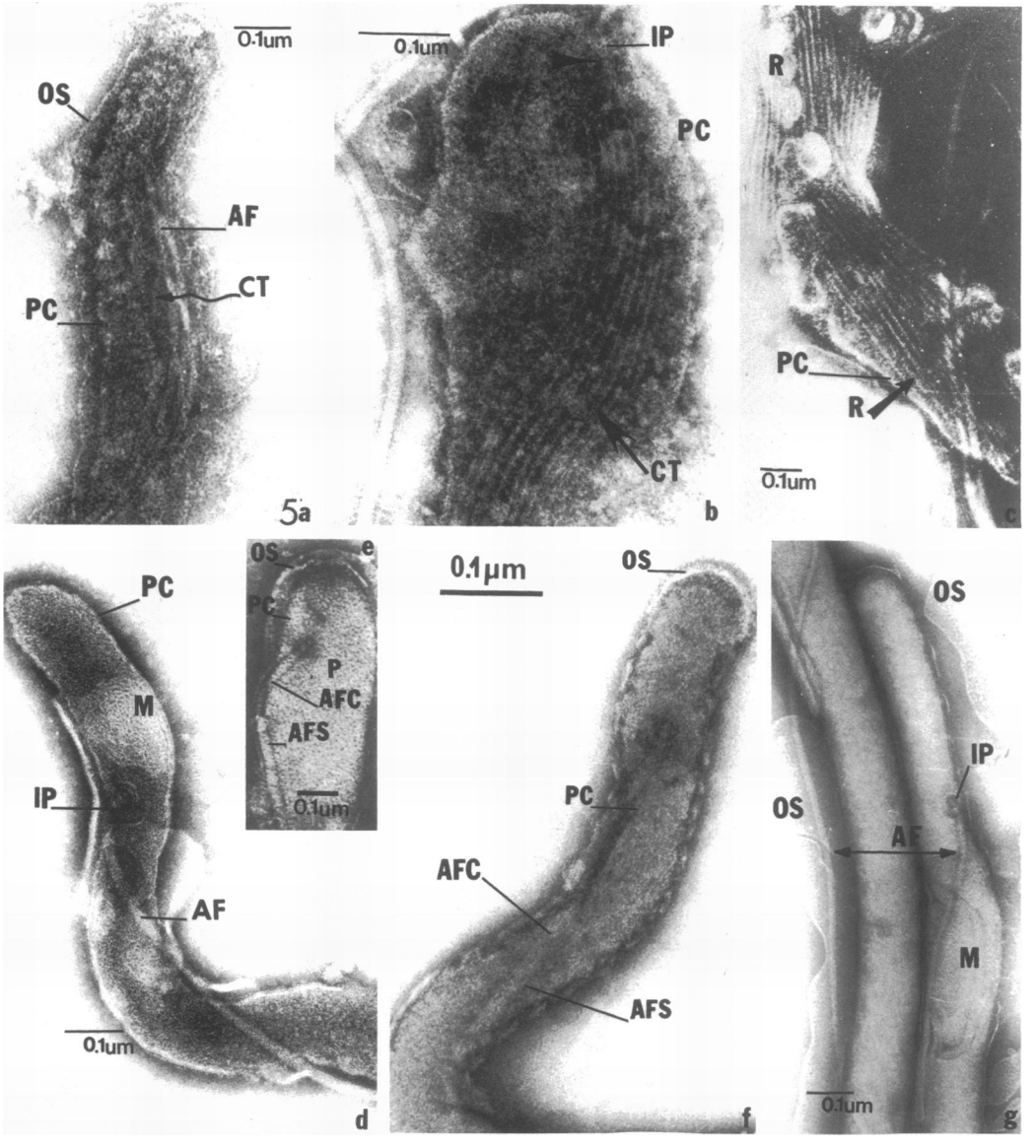

FIG. 5. *Electron micrographs of negatively stained preparations of protoplasmic cylinder contents and axial fibril arrangements. At least three axial fibrils are apparent in T. calligyrum (a), whereas Leptospira B16 (d), pomona (f), and S. aurantia (e, g) each contain one axial fibril inserted into the insertion pore at one cell pole. In (d, f, and g) the outer sheath has been removed or disrupted; note the underlying protoplasmic-cylinder components. The axial fibril makes a sharp bend as it enters the protoplasmic cylinder (a, d, e). Note that the axial fibril sheath ends at the proximal hook, revealing the naked axial fibril core (e through g). T. calligyrum treated with sodium deoxycholate or the myxobacter AL-1 protease (a and b, respectively) displays cytoplasmic tubules in the protoplasmic-cylinder interior. Short rods, similar to rhapidosomes, are seen in SDS-treated S. litoralis (c). (a, b, f, g) NH_4MoO_4; (c, d) KPTA; (e) UAC; (f) glutaraldehyde fixation, NH_4MoO_4 stain. (a, b) are from reference 96; (c, e) from reference 113; (d) from reference 147; and (f) from reference 18.*

in *T. minutum* and *T. microdentium*, although in the other cultivable treponemes these detergents had little, if any, visible effect.

One must be cautious in interpreting details of fine structure because attention must be paid not only to the physiological condition of the cells being examined but also to physical and chemical treatments, including the stains used, their pH, and the method of staining. Whether a given reagent acts as a positive or negative

stain depends not only upon the pH, but also on the isoelectric point of the component molecules, among many factors (9, 25, 48, 71, 91, 92, 224). The need for these considerations can be shown in, e.g., *S. aurantia*. Exponential-phase cells stained directly in the growth medium had little if any structural detail in the outer sheath, whereas cells washed free of growth medium displayed polygonal fine structure in the outer sheath (Fig. 4a). Whether or not such manipulation removes a surface (slime) layer (see reference 81) masking this substructure, blocks stain penetration, or generates artifacts is unknown.

Thin sections. The profile of the outer sheath is seen as a unit membrane (169; Fig. 7a through d and g through j). In many species, e.g., *L. interrogans, S. aurantia, S. litoralis*, and *T. zuelzerae*, the outer sheath appears loose (Fig. 5a, c, g, and i) or tight fitting (Fig, 7b and d), depending upon the fixation procedure. The tight-fitting sheath is seen in glutaraldehyde + osmium-fixed cells and may be the result of immobilization of outer sheath proteins by glutaraldehyde as a consequence of protein cross-linking and membrane protein stabilization (76); the loose-fitting sheath is seen when cells are fixed directly in the slow-penetrating fixative osmium (114, 147), which is a much less effective cross-linking reagent. *S. stenostrepta*, on the other hand, possesses a loose-fitting outer sheath even after double fixation in glutaraldehyde + osmium (R. Joseph, Ph.D. thesis, University of Massachusetts, Amherst 1971). Do these apparent differences in outer sheath ultrastructure reflect differences in either its chemical composition or linkage to the underlying protoplasmic cylinder? With both fixation procedures (glutaraldehyde; glutaraldehyde + osmium), the outer sheath is preserved as a unit membrane composed of two 5- to 8-nm electron-dense layers separated by an electron-transparent region of similar dimension.

Although an outer sheath was said to be absent in thin sections of *T. pallidum* Nichols (205), Johnson and co-workers (109) have shown quite clearly the presence of a triple-layered outer sheath in their strain of *T. pallidum* Nichols. It seems likely that these conflicting reports stem from examination of freshly isolated cells fixed with a minimum of preparatory steps (109), as opposed to the examination of cells fixed after extensive manipulative steps (205).

The recent experiments of Zeigler et al. (237), utilizing a ruthenium red fixation and staining technique, have demonstrated the existence of an external layer associated with the outer sheath of *T. pallidum* Nichols, but not with *T. phagedenis* Reiteri or *T. refringens* Nichols. Ruthenium red-staining material is usually regarded as some form of acid mucopolysaccharide (22, 23, 132, 133). *T. pallidum* Nichols, grown in testicular tissue, showed a thick electron-dense layer after ruthenium red fixation; interconnecting fibrils were also found between adjacent cells. This outer ruthenium red-positive layer was retained on cells fixed with 1% glutaraldehyde even after several washings (112); without glutaraldehyde fixation, the cells lost both this outer electron-dense material and the outer sheath. Whether or not this material may be of importance in bacterial adhesion, as are other extracellular polymers for other organisms in other habitats (69, 158), is yet to be determined.

T. refringens Nichols and *T. phagedenis* Reiteri were "ruthenium red negative," but this finding does not rule out the presence of other, different extracellular surface-associated materials. It is also unclear if these materials are produced by the spirochete or formed by the host in response to the spirochete.

It appears, at least in *T. pallidum* (111), that the outer sheath contributes to the morphological integrity of the treponemes, because exposure of washed cells to trypsin, lysozyme, butanol, or complement results in loss of structural integrity of almost all (92%) of the cells, whereas unwashed cells are considerably more resistant to these treatments (90% survive treatment).

The outer sheath may occupy the same relative position as the capsule of nonspirochetal procaryotes, but there are distinct ultrastructural differences. In *Klebsiella* (199), for example, the capsule is fibrillar, as is the capsule of *Diplococcus* (*Streptococcus*) *pneumoniae* (13), as are also the M proteins of streptococci (67); none of these have the unit membrane construction of the spirochete outer sheath type.

Isolation and Characterization

Solubilization and reaggregation. The outer sheaths of *T. phagedenis* Kazan 5, *T. scoliodentum*, *T. denticola*, *T. refringens*, and *L. interrogans* (biotypes pomona, canicola, Hund, Utrecht IV, and Hebdomadis A) are all sensitive to low concentrations of either sodium dodecyl sulfate (SDS) or phosphate buffers (7, 110, 147, 209, 228, 238). Treatment of whole cells with SDS results in disaggregation of the outer sheath membrane into its subunits, whereas exposure of whole cells to phosphate buffer results in release of the outer sheath from the protoplasmic cylinder as "flakes" or large membrane sheets (Fig. 8c; reference 238); the myxobacter AL-1 protease also releases large fragments or "flakes" of the outer sheath (97). When the

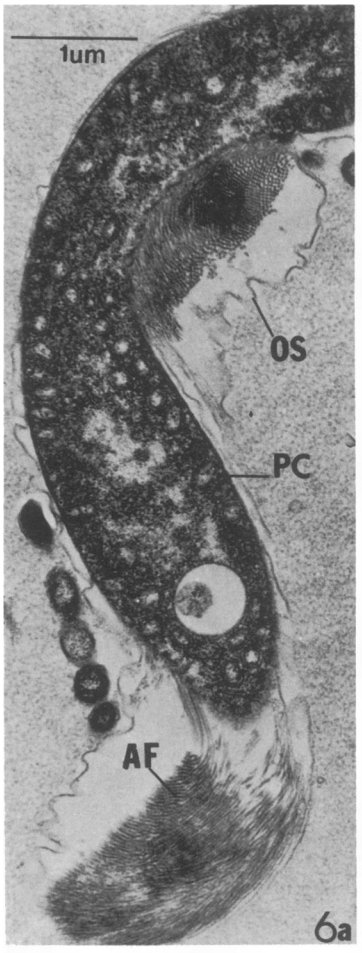
1um
OS
PC
AF
6a

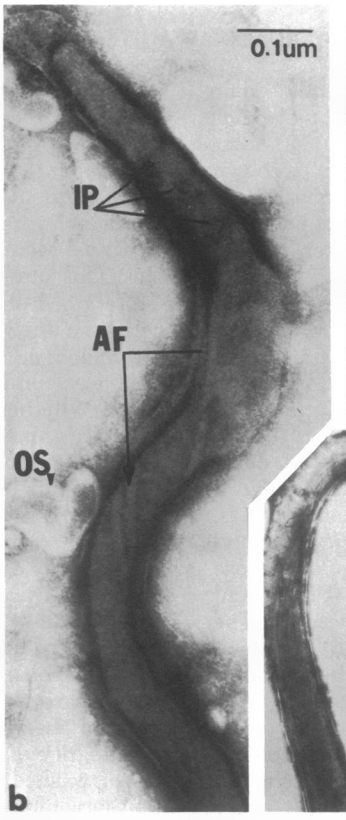
0.1um
IP
AF
OS
b

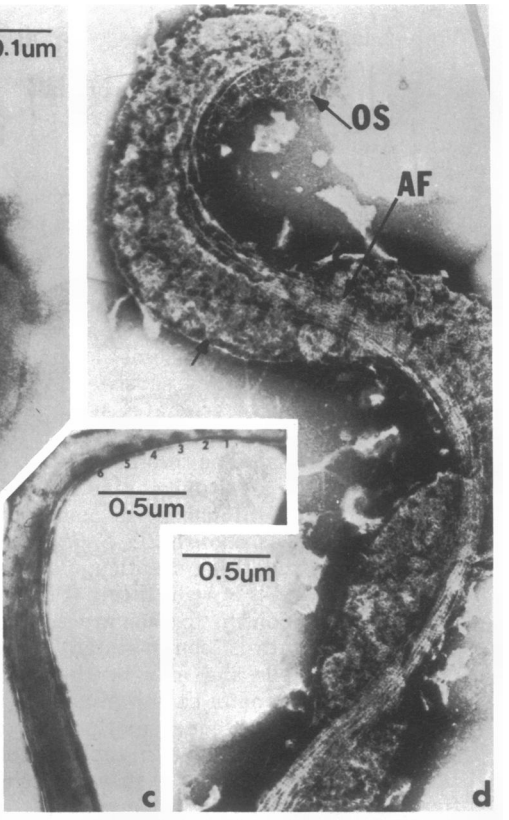
OS
AF
0.5um
0.5um
c
d

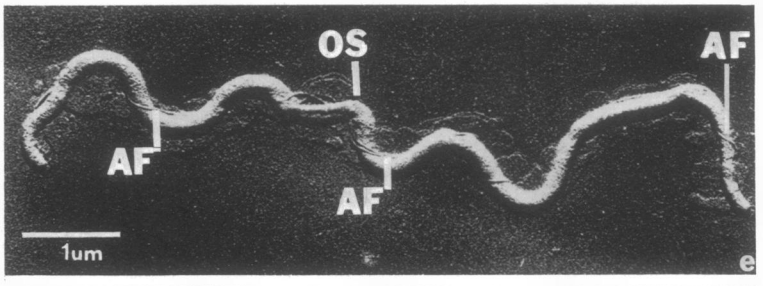
OS
AF
AF
AF
1um
e

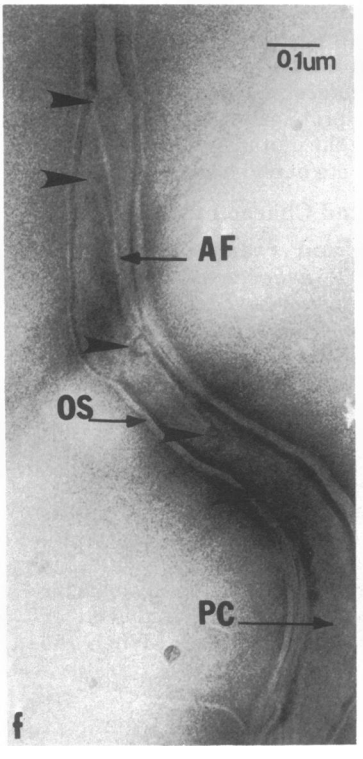
0.1um
AF
OS
PC
f

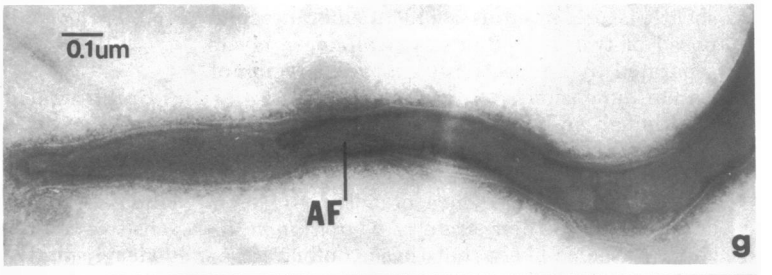
0.1um
AF
g

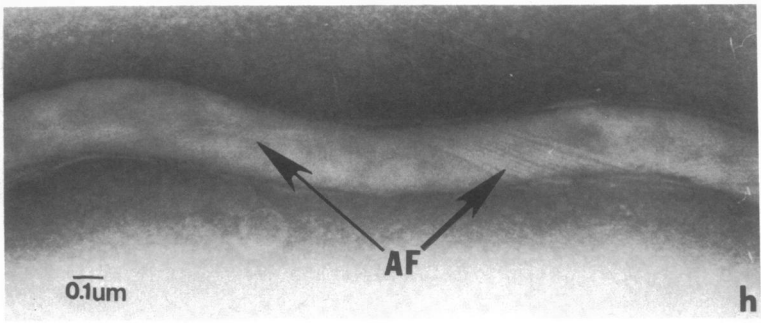
AF
0.1um
h

detergent-treated outer sheath material is dialyzed against distilled water, some (0.4% of cell dry weight) reaggregation results.

The extent of reaggregation appears for the most part to be dependent upon cation concentration (110), since addition of $MgCl_2$ to the dialysis menstruum results in an increased yield of reaggregated membrane, approaching 23% of the cell dry weight at Mg^{2+} concentrations of 20 mM or greater. However, at Mg^{2+} concentrations between 5 and 80 mM, there is visible loss of the trilaminar membrane configuration and a change in the appearance of an amorphous globular mass (Fig. 8b). It seems possible that the inability of the dissociated outer sheath to reform into the classical unit membrane could be the result of a large cation-charge effect, which favors a random globular protein-lipid reaggregation and thus prevents membrane re-formation. Both di- (Mg, Mn, Ca, Cu) and tri- (Fe, Al) valent cations are capable of reaggregating dissociated treponeme outer sheath material, and exposure to the chelating agent ethylenediaminetetraacetic acid (EDTA) results in resolubilization of the outer sheath. Thus, cations could function to bridge proteins and lipids into globular units, and EDTA could be acting to chelate these weak cationic bridges. In sharp contrast to the cation requirement for sheath reaggregation in the treponemal species, the dissociated outer sheath of *L. interrogans* canicola Hund Utrecht IV does not require addition of cations to the distilled water-dialysis system for membrane aggregation (7); thus the two may differ chemically (e.g., lipid content), as may also the sheaths of other spirochetes not yet studied. Electron microscopic examination of this distilled water-reaggregated sheath reveals the presence of small amounts of trilaminar membrane (Fig. 8a), which cytologically resemble the outer sheath membrane of intact cells. The large mass or sheets of outer sheath membrane material recovered after exposure of *L. interrogans* pomona to phosphate buffer (Fig. 8c) is seen in thin section to consist of typical unit membranes (Fig. 8d). Zeigler and Van Eseltine (238) have called attention to the five-layered membrane seen in their electron micrographs of isolated, thin-sectioned outer sheath. The extra layer could, as the authors (238) state, "... be an artifact produced by ultracentrifugation." In *L. interrogans* Hund Utrecht IV, the isolated, reassociated outer sheath consists of either three or five layers (7). Exposure of nonpathogenic *L. interrogans* Patoc 1 to 90% ethanol releases the outer sheath with classical trilaminar ultrastructure, although an occasional five- and seven-layered membrane is observed.

Chemical composition. The sensitivity of the outer sheath to organic solvents and detergents suggests that it is a chemically complex structure, and not of the rather simple composition of a typical procaryotic capsule, as was also suggested by ultrastructural comparisons.

However, only a few investigators have concerned themselves with the chemical composition of the outer sheath (157, 228, 238), and, as will be seen, it is not yet certain whether the same structures, or different preparations of similar structures, have been examined. Zeigler and Van Eseltine (238) exposed *L. interrogans* pomona to 0.01 M phosphate buffer, pH 7.2, and the separated outer sheath was isolated by isopycnic KBr and CsCl density gradient centrifugation, as well as zonal centrifugation in sucrose gradients. The banded material had a density of 1.25 g/cm^3 in the three gradient supports.

The isolated material from both *L. interrogans* pomona and *T. phagedenis* contains protein, lipid, and carbohydrate (228, 238) and is similar to outer membranes of gram-negative bacteria (178). The quantitative distribution of these components varies between the genera: *L. interrogans* pomona contains, by weight, 46% protein, 27% carbohydrate, and 22% lipid in the outer sheath (238); a *T. phagedenis* Kazan 5 outer sheath (isolated by SDS treatment and reaggregated by dialysis in 20 mM $MgCl_2$) consists of 60 to 73% protein, 4 to 5% lipid, and 1 to 2% carbohydrate, by weight (228). The reaggregated outer sheath material contains nearly half the amount of glucosamine and galactosamine

FIG. 6. *Electron micrographs. Cristispira thin section (a) shows many axial fibrils internal to the outer sheath. Negative stains of T. pallidum Nichols (b); a spirochete from the brush border of colonic mucosa of healthy monkey, Macaca mulatta (c); type B spirochete (d) showing many axial fibrils. Note different number of fibrils; in (c) the insertion pores are numbered 1 through 6 and are arranged in a single row at the cell pole (see also Fig. 4c). Shadowed cell of distilled water-treated T. zuelzerae (e); the outer sheath has been fragmented to reveal the single axial fibril originating at the end of each cell pole. Note the 1-2-1 axial fibril arrangement. B. hermsii (negative stains) with characteristic pointed ends (f, g) and numerous axial fibrils (g, h). In (f) the fibrils insert along the protoplasmic cylinder (arrows). (a) Kellenberger-Ryter fixation, UAC-lead stained; (b, c) Formalin fixation, KPTA; (d) unfixed cell, NH_4MoO_4; (e) osmium-vapor fixation, gold-palladium shadow-cast; (f through h) glutaraldehyde fixed, NH_4MoO_4. (a) is from reference 174; (b) from K. Hovind-Hougen, unpublished; (c) from reference 208; (d) from reference 20; (e) from reference 15; and (f through h) from S. C. Holt, unpublished.*

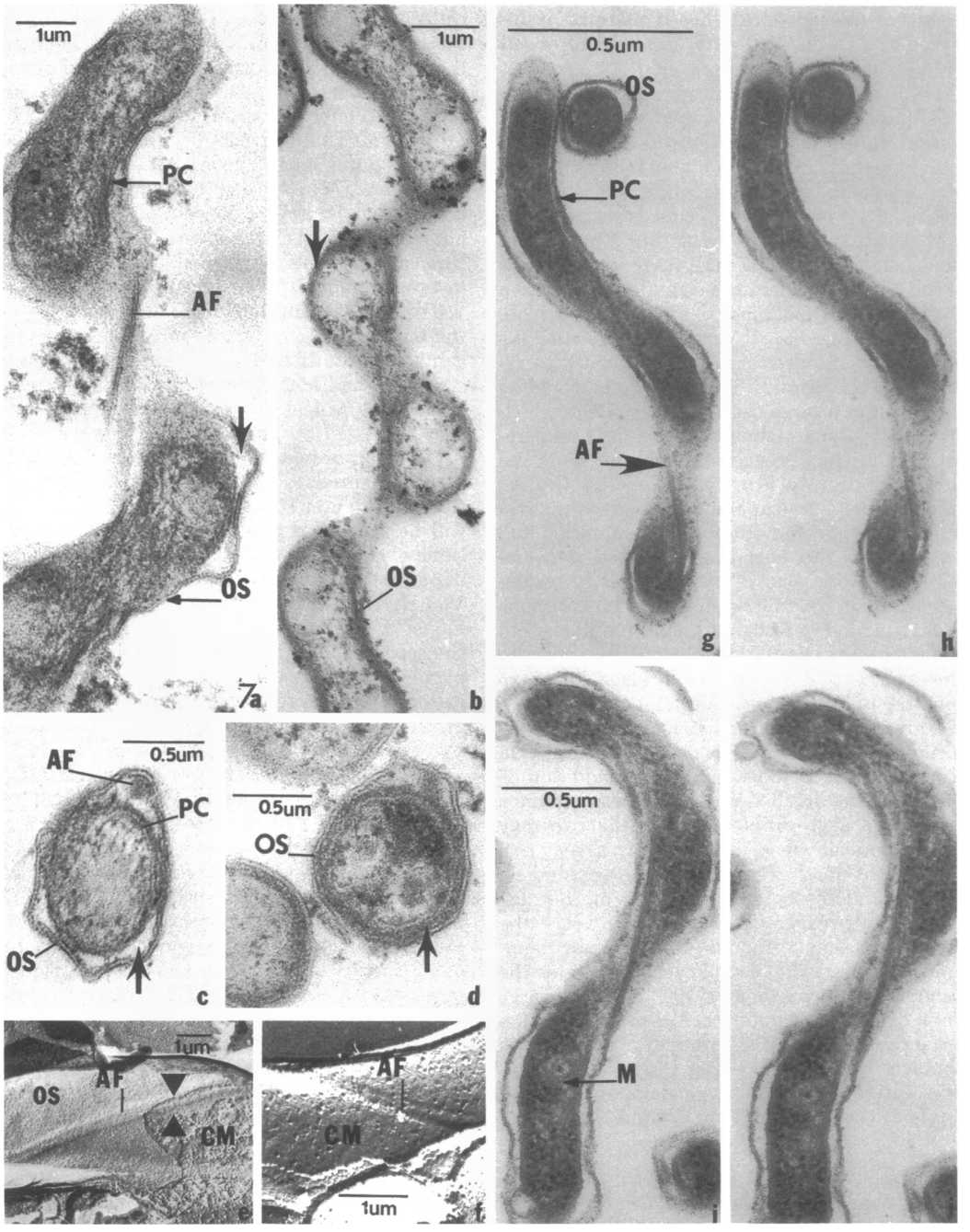

FIG. 7. *Electron micrographs of thin sections of chemically fixed cells of L. interrogans B16 (a through d) and S. stenostrepta Z1 (g through j). Leptospira fixed only in osmium has a loose-fitting outer sheath (a, c) and an empty or electron-transparent periplasm (arrow), whereas cells fixed in glutaraldehyde + osmium display a tight-fitting outer sheath (b, d) and an entrapped electron-dense periplasm (b, d arrows). Stereo-electron micrographs of S. stenostrepta (g through j) reveal the protoplasmic cylinder to be tubular, with the axial fibril lying below the outer sheath and above the layers of the cell envelope. Freeze-etch replicas of L. interrogans B16 (e, f) reveal the axial fibril to be situated between the nontextured outer sheath and the particle-covered outer surface of the cytoplasmic membrane. Both outer and inner fracture faces with axial fibril images (f) are clearly seen, as is also the multilayered nature of the outer sheath (e, triangles). Thin sections stained with UAC and lead citrate. (a, b) are from 147; and (c through j) from S. C. Holt, unpublished.*

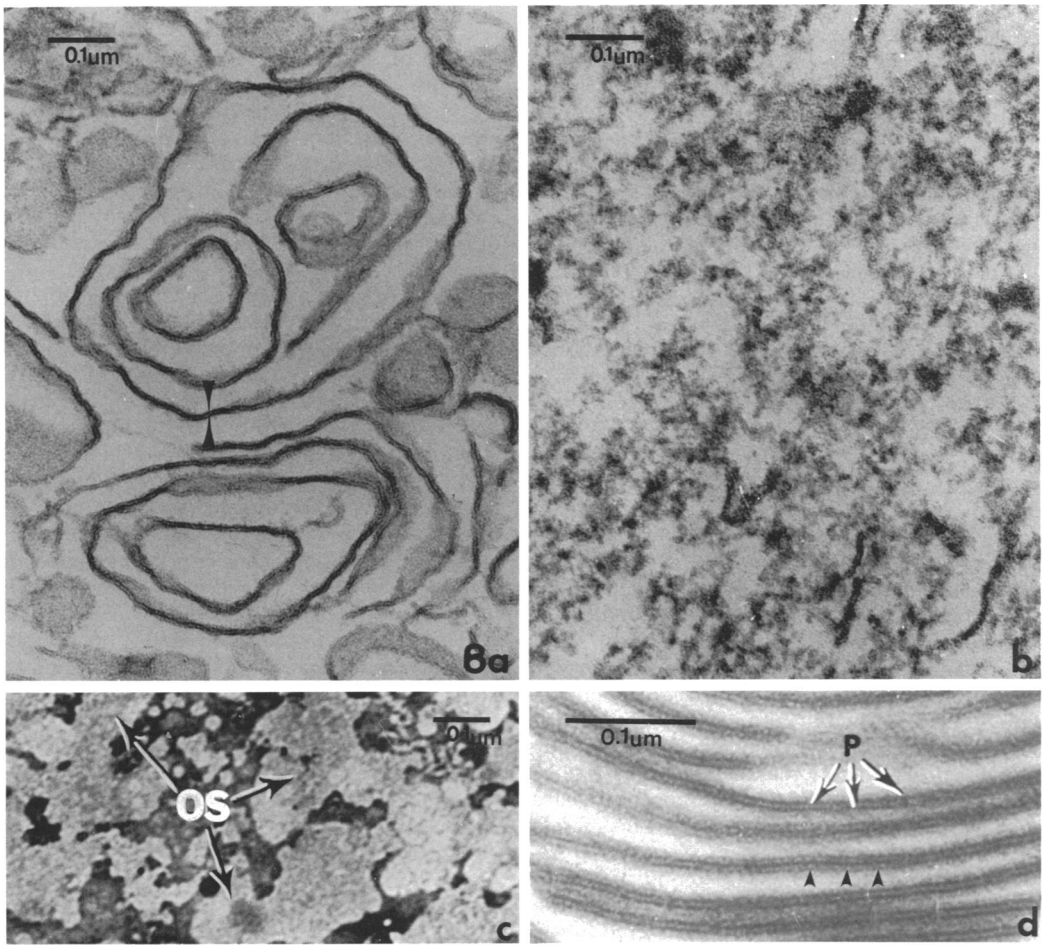

FIG. 8. *Electron micrographs of thin sections and negative stains of isolated outer sheaths. (a) "Solubilized" outer sheath from T. phagedenis after distilled water dialysis. Note reaggregated unit membranes (arrows). Addition of 5 mM Mg^{2+} to the dialysis system results in (b) the loss of unit membranes and reaggregation of an amorphous material. Negative-stained outer sheath of L. interrogans pomona (c) after sucrose density zonal centrifugation showing large sheets of membrane. Thin section of this isolated outer sheath (d) reveals unit membranes, along with small, electron-dense particles. In some areas (arrows) the sheath appears to have five layers. (a, b) Osmium fixation, UAC stained; (c) KPTA, negative stain; and (d) glutaraldehyde + osmium fixation, UAC-lead citrate stained. (a, b) are from reference 110; and (c, d) from reference 238.*

found in whole-cell preparations, and thus the purity of these preparations must be regarded as equivocal, as must also their possible identity with outer membranes of other gram-negative bacteria. Until a specific marker for the outer sheath is recognized, the precise chemical composition of the sheath will be uncertain. The spirochetal peptidoglycan constituents, L-ornithine and muramic acid (see below), were not detected in what should be regarded as the outer sheath of *T. phagedenis* (228) or *L. interrogans* pomona (238).

Essentially all lipid found in the outer sheath of *L. interrogans* pomona is phospholipid, with almost 98% of it occurring as phosphatidylethanolamine (238). The major fatty acids comprising the phosphatidylethanolamine are hexa- and octadecenoic acids (56 and 34%, respectively). In contrast, *T. phagedenis* Kazan 5 phospholipid consists predominantly of phosphatidylcholine (57%) with "lesser amounts" of phosphatidylethanolamine. Monogalactosyl diglyceride accounts for 43% of the polar lipid. Palmitic and oleic acids are the two major fatty acids present in *T. phagedenis*.

The large differences in total amounts of protein, lipid, and carbohydrate could reflect either significant differences between leptospires and treponemes, or differences in the degree of purity of this outer sheath material. Indeed, taken to-

gether, the noted differences in chemical composition and disaggregation-reaggregation behaviors make likely future demonstrations of physical and/or chemical differences in pure sheath preparations from leptospires and treponemes.

There are no known functions ascribed to the outer sheath. One might imagine that it could function as a primary permeability barrier. If the space, apparent in electron micrographs, between the outer sheath and the outer layers of the protoplasmic cylinder were the equivalent of the periplasmic space in other gram-negative cells (37, 38, 44, 86, 87, 148), then the role proposed for the outer sheath takes on added significance. A search for hydrolytic enzymes and their cytochemical localization will clarify their possibly significant role in the breakdown of polymers, especially for host-associated spirochetes.

Since the outer sheath is the most external layer of spirochetes, it may interact with host defense mechanisms. Auran et al. (7) have found that the sheath of *L. interrogans* canicola is immunogenic. Hamsters immunized with "purified reaggregated sheath" are protected against lethal doses of virulent *L. interrogans* canicola. The site of antibody-complement activity has been determined to be the outer sheath (6), but since solubilized and reassociated material of uncertain purity were used as immunogens, care must be exercised in the interpretation of this data.

Bharier and Rittenberg (17) found that antisera against *T. zuelzerae* cells immobilized the organisms, whereas antisera against axial fibrils did not, and hence they suspected that at least part of the immobilizing activity of the anti-cell sera was caused by antibodies reacting with some cell component other than axial fibrils—possibly the outer sheath. Whether the outer layers of the spirochete play a role in cell motility or merely impede the passage of axial fibril antibody into the underlying axial fibrils is uncertain. Bharier and Rittenberg (17) also suggested that immobilization of *T. zuelzerae* could be due to a distortion of the cell surface or to steric hindrance resulting from the presence of large amounts of antibody attached to the cell surface. Clearly, comparative localization studies of anti-cell and anti-fibril antibody would be of immense value.

LPS

Several reports in the literature indicate the presence of a lipopolysaccharide (LPS) layer in spirochetes (39, 50, 54, 107, 159). Jackson and Zey (107) employed the classical (230) hot phenol extraction procedure to extract LPS from *T. pallidum* Nichols. As judged by electron microscopy, such extracts contain several morphological entities—14-nm-diameter spherical particles, as well as ribbon- and doughnut-shaped structures. The ribbon configuration is more predominant when LPS has been lyophilized (107) before performance of electron microscopic techniques. Such morphological features are similar to those found in LPS isolated from other gram-negative cells (e.g., see references 131, 189).

The precise physical location of spirochete LPS is not known; for treponemes suggestive evidence for its location exists (J. Pillot, Ph.D. thesis, University of Paris, Paris, 1965). Pillot observed that in *T. pallidum* Reiter the peptidoglycan layer was external to the plasma membrane, which had been stripped of its outer sheath. In addition, these outer sheathless cells retained their helical shape, a characteristic usually considered to be determined by peptidoglycan. Isolated outer sheath was, however, elastic and thus presumed in vivo to be external to the peptidoglycan layer. The outer sheath contained, in addition to protein and lipid, polysaccharides that were both antigenic and immunologically specific for treponemes, suggesting to Pillot an LPS component.

Isolated outer sheath of *L. interrogans* pomona, which is assumed to contain the LPS, is known to contain hexoses, pentoses, hexosamine, and 6-deoxyhexose (238). Similar chemical constituents have been reported by Schneider (186), Rothstein and Hiatt (172), Schricker and Hanson (187), Kondo and Ueta (121), and Shinagawa and Yanagawa (190) in whole cells of *Leptospira*. Two constituents, heptose and 2-keto-3-deoxyoctonoic acid, which have been found in many LPSs, were absent from *L. interrogans* pomona (238). Similar lack of heptose and/or 2-keto-3-deoxyoctonoic acid has been reported for the LPS of *Neisseria catarrhalis* (4) and several free-living myxobacteria (171, 227), and thus it is quite possible that the LPS of spirochetes have biological activity quite different from that found in the enteric bacteria and several *Neisseria* (200). This has been seen for the *L. interrogans* canicola LPS, which when tested for endotoxic activity in mice was negative, whereas LPS extracted from *Escherichia coli* prepared in an identical fashion was endotoxic (66).

AXIAL FIBRIL

General Morphology and Location

The axial fibril (Fig. 9a through d and j through l) is morphologically similar to the procaryotic flagellum (Fig. 9i and 10e; references 1-3, 43) in that it consists of two basic compo-

nents: a shaft and its covering sheath, and an insertion apparatus that is differentiated into a terminal knob composed of a proximal hook and insertion disks or bulbous "annular swellings." Since, however, there are no unequivocal demonstrations of a role in motility for the axial fibrils, it seems unwise to imply such a function with such terms as flagellum or endoflagellum, and thus only the term axial fibril will be retained for use in this discussion.

The shaft may be either filamentous or globular in substructure and, thus, strikingly similar to the substructure seen in the bacterial flagellar shaft (2, 3, 43). However, unlike the bacterial flagellum, the shaft or filament of the axial fibril is a totally "internal" structure that lies between the inner layer of the outer sheath and the outermost layer of the protoplasmic cylinder (Fig. 2f, 3, 5a, d, f, and g; 7a through j). The axial fibril(s) winds around the protoplasmic cylinder (Fig. 2f) and, in most spirochetes, overlaps near the center of the cell (Fig. 2e; references 90, 95, 96, 106, 108, 113, 128, 160, 173, 233), although the axial fibrils of the leptospiral species thus far examined do not appear to overlap (18, 98).

Size. Like bacterial flagella, the diameter of individual axial fibrils does not vary appreciably in the different spirochetes and thus bears no relationship to the cell size or the number of fibrils per cell. The axial fibril found in *Cristispira* has a diameter of approximately 18 nm (174), similar to that in *Leptospira* (147), when the measurement is of the axial fibril without the coat (see later), and *Treponema* (15, 17; Pillot, Ph.D. thesis, 1965). *S. stenostrepta*, *S. aurantia*, *S. litoralis*, and *T. zuelzerae* axial fibril diameters range between 15 and 21 nm, whereas those of the oral spirochetes *T. macrodentium*, *T. microdentium*, *T. denticola*, and *T. oralis* vary from 15 to 19 nm (96, 128, 145); *T. phagedenis* Reiteri and *T. pallidum* (99, 231) are similar (16 to 22 nm). The internal location of the axial fibrils makes accurate length measurements difficult in intact cells, and length measurements of isolated fibrils, which may be fragmented, may be misleading.

Sheath and core. The shaft or filament portion of the axial fibril usually consists of an outer covering or sheath that encloses an internal core (Fig. 5e and f, 9e, 11D). After physical removal of the outer covering, the core remaining has a range of diameters of approximately 10 to 16 nm according to the species involved (see, e.g., 18, 20, 90, 96, 99, 100, 147). The close physical relationship between these two components is clearly seen in Fig. 9e. In both *T. pallidum* Nichols and *S. stenostrepta* the core is composed of longitudinal rows of globular subunits (106, 113). These globular subunits are seen clearly in freeze-etched preparations of purified axial fibrils of *S. stenostrepta* (Fig. 10f), and are arranged in a right-handed helix (113). In *S. plicatilis* (20), the core is approximately 10 nm in diameter and is covered by a sheath, 15 to 20 nm in diameter, which has a slight granular substructure and thus is also in contrast to the striated sheath covering the axial fibril (Fig. 9g) in *T. zuelzerae*. This entire, striated, close-fitting covering (Fig. 9f and g) surrounding the axial fibril has been observed by Birch-Andersen et al. (18), Bladen and Hampp (19), Holt and Canale-Parola (90), Hovind-Hougen (95), and Nauman et al. (147). Jackson and Black (106) have observed similarly striated axial fibril coverings in *T. pallidum* Nichols. Whether this striated sheath is an actual feature of the native axial fibril or represents an experimentally induced artifact is unclear. It is essential to recognize that the striated layer (sheath) was only observed in cells that had been in some way perturbed; hence, the striated sheath may represent fragments of the outer sheath that broke away or rolled up and around the axial fibril either during growth or during sample preparation (Fig. 9h). Birch-Andersen et al. (18) have observed that in *L. interrogans* pomona the outer envelope (sheath) consists of the triple-layered membrane (described previously), as well as an additional layer. Striated tubules are observed to be distributed randomly over the electron microscopic grid surface and often enclose fragmented axial fibrils. Speculation about the origin of these striated tubules has also been discussed by Bladen and Hampp (19) and Chang and Faine (36), who are in agreement with Birch-Andersen et al. (18) in suggesting that the tubules are fragments of the outer sheath. Anderson and Johnson (6) have also observed sheathed fragments with a periodicity of 0.4 nm after treatment of whole cells of *L. interrogans* canicola with complement and antibody.

A sheath has not been observed surrounding the 13-nm-diameter axial fibril in *Borrelia recurrentis* or *B. merionesi* (94). Joseph and Canale-Parola (113), in an experiment modeled after that of Glauert and Lucy (72), were able to prepare striated lipid assemblies that were morphologically similar to the striations seen covering fibrils of broken-cell preparations (cf. Fig. 9f through h and m and n). Since these striated lipid assemblies were prepared by mixing, on an aqueous layer, sterols (cholesterol, lecithin, and saponin) which are not known to be present in spirochetes, care must be exercised in the interpretation and extrapolation of this artificial lipid-bilayer data to the striated material associated with axial fibrils. Bharier et al. (15) did not find a striated sheath in *T. zuelzerae* thin

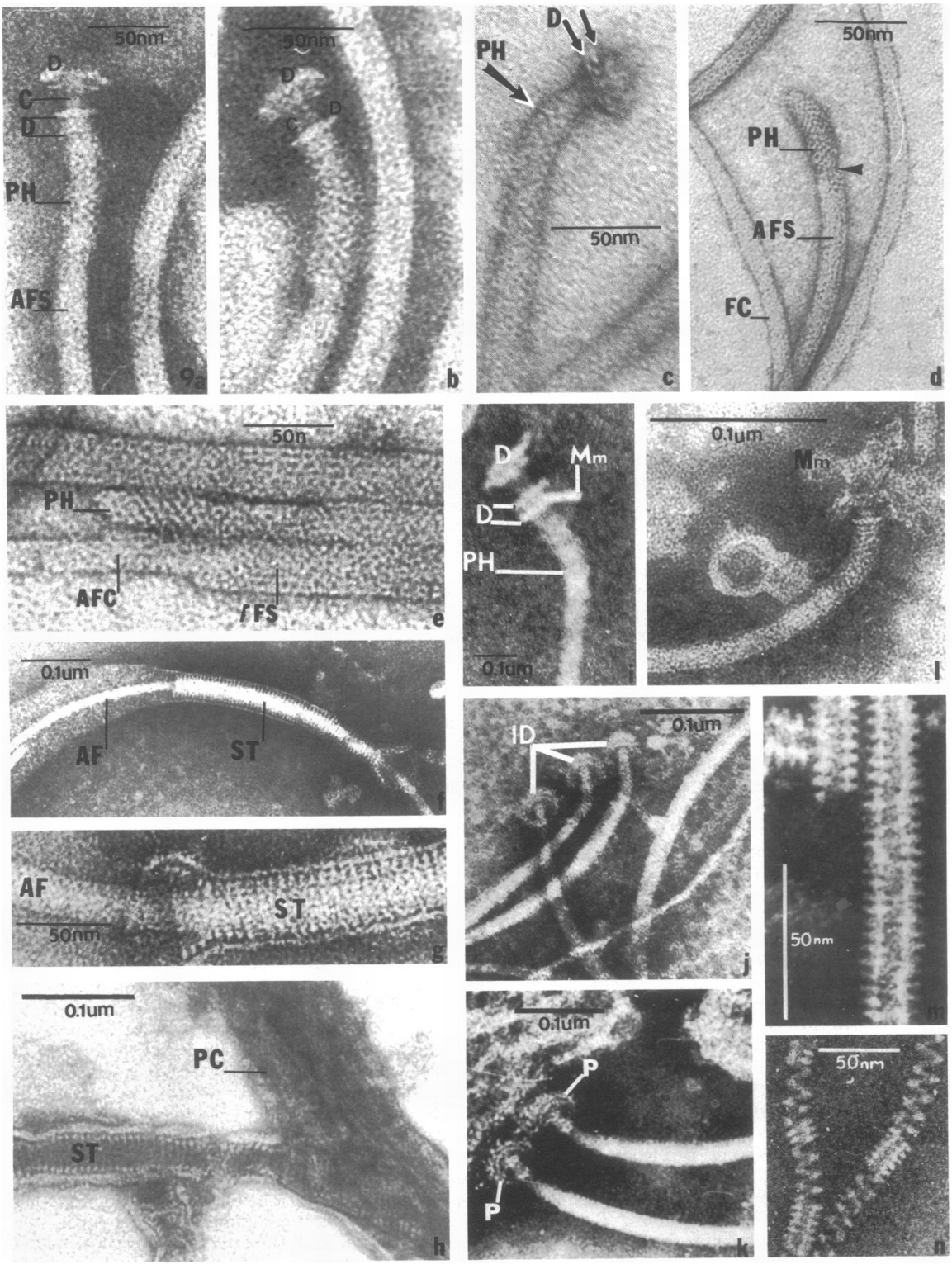
50nm
D
C
D
PH
AFS
a
50nm
D
C
D
b
D
PH
50nm
c
50nm
PH
AFS
FC
d
50n
PH
AFC
FFS
e
D
Mm
D
PH
0.1um
i
0.1um
Mm
l
0.1um
AF
ST
f
AF
ST
50nm
g
0.1um
PC
ST
h
ID
0.1um
j
50nm
m
0.1um
P
P
k
50nm
n

sections. However, these authors noted an electron-transparent space surrounding the axial fibrils. This space might well be, or have housed, an axial fibril sheath; since this striated sheath may be of high lipid content (leptospiral striated "tubules" float on 20 to 60% sucrose gradients), it is quite possible that much of the sheath is extractable by lipid solvents used in preparative procedures for electron microscopy. It is also possible that a lipid-rich sheath would not stain readily and therefore not be visible in thin sections viewed in an electron microscope. The use of the water-soluble resins that do not require organic solvents should make important contributions to a resolution of these uncertainties.

Insertion apparatus. This structure is differentiated into a terminal knob, composed of a proximal hook, and insertion disks or bulbous "annular swellings."

Proximal hook. Proximal to the filament or shaft portion of the axial fibril is a hook (Fig. 9a through d) with a honeycombed surface. The hook is usually slightly larger than the shaft (14 to 17 versus ca. 13 nm), varies in length between 40 and 70 nm, and bends sharply toward, and into, the protoplasmic cylinder (18, 88, 90, 93–99, 101, 106, 108, 113, 128, 147).

Insertion disks. This proximal hook is continuous with the insertion disk(s) by means of a narrow 9-nm-wide and 16-nm-long neck. The number of insertion disks varies with the genus: *Leptospira* usually have three to five closely apposed 20- to 26-nm-diameter disks, whereas *Spirochaeta* have three disks, each approximately 40 nm in diameter. Similar insertion disks have been observed by Listgarten and Socransky (128) in several of the oral spirochetes. In some *T. pallidum* Nichols strains, only one flat disk of approximately a 30- to 35-nm diameter has been observed (93), although Jackson and Black (106) have observed a 60-nm-diameter insertion disk in their cultures. The disks in the cultivable treponemes number either one or two and average approximately 30-nm in diameter (95–97). In *B. merionesi* and *B. recurrentis*, there appear to be at least two insertion disks with diameters of 30 to 35 nm (94). Some insertion disks consist of electron-dense, round plates, approximately 30 nm in diameter, surrounded by less electron-dense rings, 10 to 15 nm in diameter. The rings are said to possess some substructure that, however, is not readily apparent in the published micrographs (94).

The disks are inserted into a subterminal hole or depression in the protoplasmic cylinder near the ends of the cell (Fig. 2c, e, and f, 4a and c, 5a and d through g). In those spirochetes that contain multiple axial fibrils (Fig. 6b through d and f), the insertion point of the outermost fibril varies between 0.08 and 0.15 μm from the cell pole (98).

Characterization of Purified Axial Fibrils

Isolation and purification. Axial fibrils free of any apparent contamination, as revealed by electron microscopy, have been prepared from *Leptospira* B16 (147), *S. stenostrepta, S. zuelzerae,* and *S. litoralis* (113), *T. zuelzerae* (16), and *T. phagedenis* Reiteri (14, 79).

The techniques used for axial fibril isolation and purification involve prior removal of the cell's outer sheath with either *n*-butanol or phosphate buffer and subsequent cell lysis and fibril release by either (i) detergent action, (ii) freeze-thawing, (iii) blending in an omnimixer, or (iv) breakage of fibrils into fragments by ultrasound. The axial fibrils are purified either by banding in KBr, CsCl, and/or RbCl density gradients or by elution from diethylaminoethyl-cellulose columns.

Morphology. The isolated fibrils vary in length, a result of the isolation procedure, and have a mean diameter of 18 nm (Fig. 10a, b, and d).

FIG. 9. *Electron micrographs of negatively stained, isolated axial fibrils, striated tubules, and bacterial flagella. Axial fibrils from L. interrogans B16 (a, b, d, e, and l) and S. stenostrepta Z1 (c) showing axial filament sheaths attached to honeycombed proximal hooks. Insertion disks (a through c, j through l) are attached to the hook through a narrow axial fibril neck. A disk-free honeycombed proximal hook with enveloping axial fibril sheath that covers the axial fibril core is seen in (d). Note that the sheath terminates at the proximal end of the hook (arrow). An axial fibril membrane fragment is attached to the distal end of the axial fibril in (l). Axial fibrils of T. pallidum Nichols (j, k) are mushroom-shaped and contain small electron-opaque particles either attached to or in close apposition to the rim of the insertion disks. The flagellum from Rhodospirillum rubrum (i) consists of two paired disks connected to the flagellar hook by a narrow neck; a piece of cytoplasmic membrane is possibly attached to one of the disks. In (f, g), striated tubules surrounding axial fibril fragments from S. stenostrepta and T. zuelzerae are seen; the tubules appear as a series of ringed elements enclosed by the sheath. As seen in (h), the striated tubule may originate from the surface of the protoplasmic cylinder. "Striated tubules" formed in vitro by sterol flotation on an aqueous layer are seen in (m, n) and resemble the striated tubules from S. stenostrepta and T. zuelzerae. (a, b, d, and e) are from reference 147; (c, f) from reference 90; (g, m, n) from reference 113; (h, l) from S. C. Holt, unpublished; (i) from reference 43; and (j, k) from reference 106.*

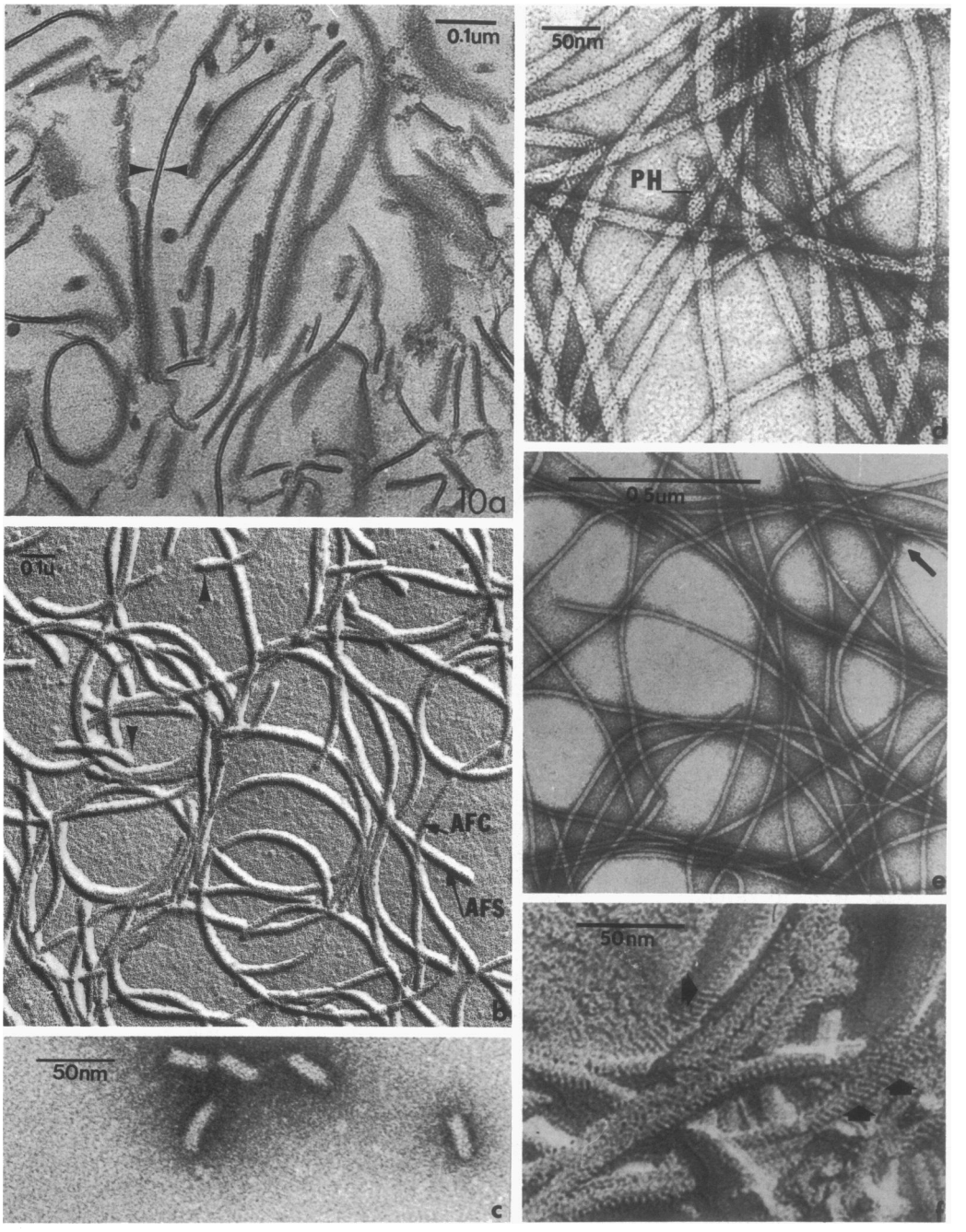

FIG. 10. *Electron micrographs of purified axial fibrils from L. interrogans B16 (a, b) and S. stenostrepta (d, f) and flagella from E. coli (e). The double-track construction of the axial fibrils is apparent in the thin section (a, small arrows). The outer surface of the leptospiral axial fibril is smooth after carbon-platinum shadow-casting (b), and the axial fibril sheath, core, and proximal hooks (arrows) are apparent. Freeze etch of S. stenostrepta axial fibrils (f) reveals a right-handed helical substructure (f, arrows) that is also seen clearly in UAC-stained material (d) where the subunits of the fibrils appear globular; characteristic honeycombed proximal hook is seen. The E. coli flagella (e) are smooth surfaced and hooked (arrow). Purified proximal hooks from S. stenostrepta axial fibrils treated with 0.1 N NaOH and stained with UAC (c). (a) Glutaraldehyde + osmium fixation, UAC-lead citrate stained. (c, d, f) are from reference 113; (e) from reference 55; (a, b) from R. K. Nauman, S. C. Holt, and C. D. Cox, unpublished.*

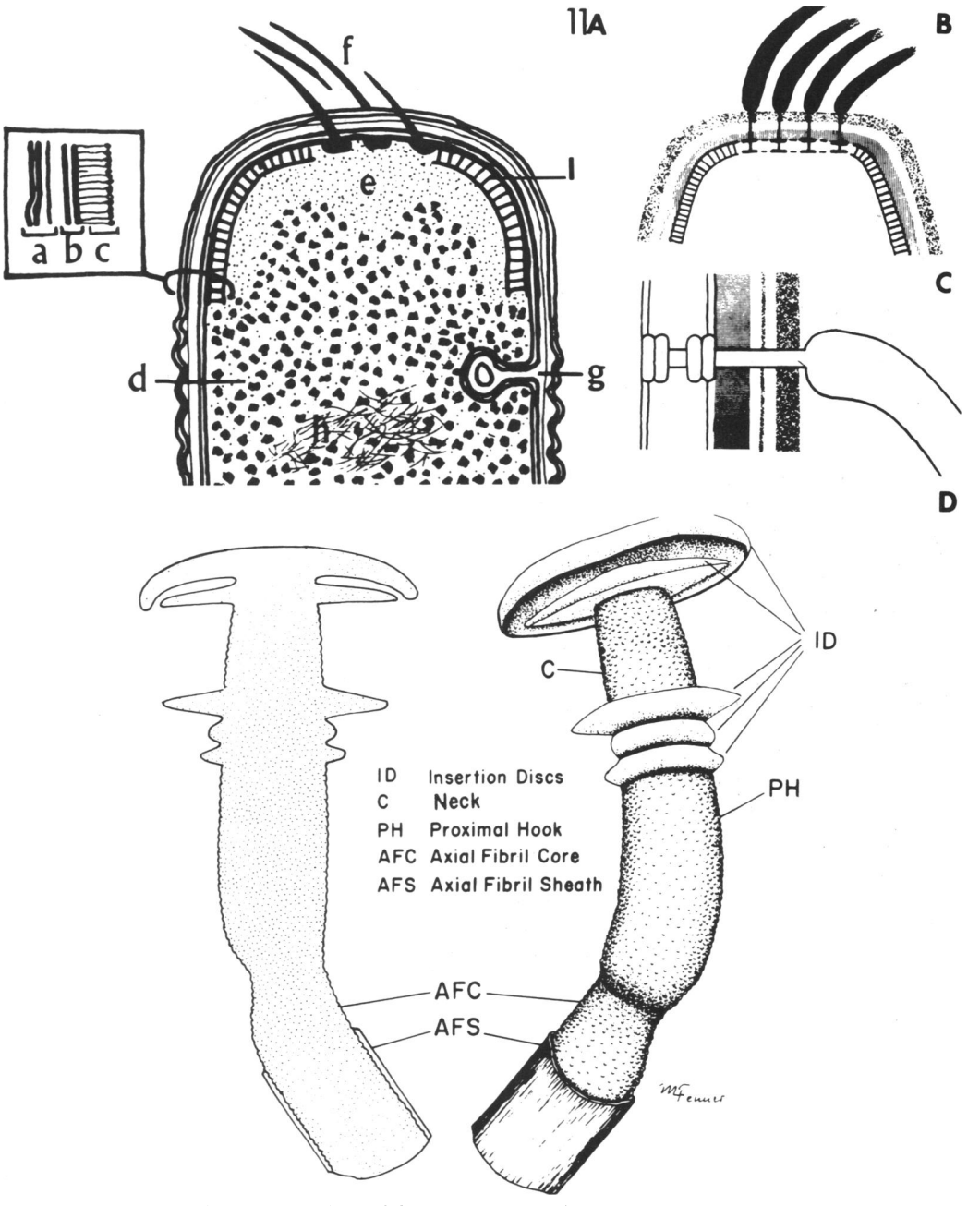

FIG. 11. *Diagramatic representations of the polar regions of (A) Aquaspirillum serpens, (B, C) a spirillum, and (D) the proximal portion of spirochete axial fibril. In (A), the flagella (f) pass through the cell wall (a) and cytoplasmic membrane (b) and associate in the polar membrane (c), which is associated with the cytoplasmic membrane through "linkers" (l). In (B, C), the relationship between the basal portion of spirilla flagella and the polar or flagellar membrane (c) is seen. Note in (C) that flagella are anchored via disks to the membrane and that the disks are interconnected through a narrow neck that connects to the major portion of the flagellum. The spirochete (D) axial fibril core is covered by a sheath in Leptospira (not apparent in all spirochetes). The axial fibril core narrows as it enters the proximal hook region of the fibril. The elliptical insertion disks anchor the hook to the layer of the protoplasmic cylinder. The proximal insertion disks are separated from the inner disks by a neck. (A) is from reference 146; and (B, C) from reference 43.*

In *Leptospira* B16 (147), the purified axial fibril observed by negative staining is multilayered and consists of an inner core approximately 13 to 16 nm in diameter, surrounded by an outer 7- to 8-nm coat (Fig. 9b, d, and e, 10b). This coat is not apparent in thin sections (Fig. 10a), perhaps because it has been removed in preparative procedures. The *S. stenostrepta, S. aurantia, S. litoralis,* and *T. zuelzerae* purified axial fibril consists of a 17- to 23-nm-diameter strand covered by a 21- to 23-nm-diameter sheath (i.e., Fig. 5e, and 9c); *T. phagedenis* Reiteri axial fibrils do not appear to be enclosed in such a sheath.

Physical and chemical characteristics. The buoyant density of axial fibrils from *Leptospira* B16, *S. stenostrepta, S. litoralis,* and *T. zuelzerae* varies between 1.27 and 1.30 g/cm^3 (16, 113, 147). Such densities are similar to those obtained for pure proteins (1.30 g/cm^3), and chemical analysis reveals that the fibrils are composed almost entirely of protein, with only trace amounts of hexose- and pentose-positive material present. A small amount of hexose (<1% measured as anthrone-positive material) was consistently found associated with the fibrils. In addition, small amounts (0.05 μmol/mg of protein) of phosphorus were found in the *S. stenostrepta* axial fibril. The significance, if any, of their presence is yet unclear.

Amino acid analysis reveals that, in general, the axial fibrils are chemically very similar to bacterial flagella (35, 104, 138). They are rich in aspartic and glutamic acids, alanine, leucine, and glycine and lack tyrosine, tryptophan, and cysteine; perhaps the most striking similarity is the absence of cysteine and tryptophan. In *S. stenostrepta* (113) and *T. zuelzerae* (16), the absence of these two amino acids has been verified by using analytical procedures that would not destroy them. Cysteine as half-cystine is present in very small amounts in *T. phagedenis* Reiteri, and tryptophan is either absent or present at very low levels. The absence of cysteine suggests that the macromolecular structure is not stabilized by disulfide bridges.

Electrophoretic characterization. The purified axial fibrils are dissociable into their protein subunits at both acid and alkaline pH and by addition of urea. Polyacrylamide gel electrophoresis of these protein subunits reveals the presence of two protein bands in *S. stenostrepta, T. zuelzerae,* and *T. phagedenis* Reiteri (16, 79, 113).

The two protein bands from *T. zuelzerae* axial fibrils vary in intensity with the fibril preparation used. The intensity of staining of the slower-migrating band is EDTA dependent; at EDTA concentrations of 10^{-3} M, the slower-migrating band is not clear. Bharier and Rittenberg (16) attribute this to aggregating of the slower-migrating protein and suggest that the slow-migrating band possibly represents different aggregation states of the faster-moving band. Bharier and Allis (14) have observed at least three protein-staining bands in SDS-gels of *T. phagedenis* Reiteri axial fibrils. When glycine-acetate buffer or a pH of 12 is used, only one major protein band is observed. In contrast, SDS-acrylamide gel electrophoresis of *Leptospira* B16 axial fibrils resolves six protein bands (147). It should be noted that Nauman et al. (147) used 0.05 M glycine · HCl (pH 2.4) as the acid buffer and 0.01 M NaOH + 0.05 M KCl (pH 12) as the alkaline buffer in their SDS-acrylamide gel electrophoretic analyses. Further, the fact that the leptospiral axial fibril and coat is larger than that found in *S. stenostrepta* and *T. zuelzerae* (20 to 25 versus 15 to 18 nm, respectively) may be responsible for this threefold increase in the number of proteins. The small number of protein bands observed in dissociated axial fibrils of *T. zuelzerae, S. stenostrepta,* and *T. phagedenis* Reiteri is again similar to findings with bacterial flagella, for both alkali- and acid-dissociated flagella of *Spirillum serpens* and *Bacillus subtilis,* when examined by acrylamide gel electrophoresis, form one protein band (138).

The only molecular weights available for dissociated axial fibril subunits are from *T. zuelzerae* and *T. phagedenis* Reiteri, which are approximately 32,000 to 36,000 (14, 16); such values are similar to those for flagellin subunits from *Proteus vulgaris* (35).

Physical and chemical effects on axial fibrils. A large number of tests have been done on the effects of a wide variety of chemical agents (acids, alkalis, hydrogen bond-breaking compounds, etc.) on the integrity of purified axial fibrils (16, 113, 147). The fibrils are most susceptible to hydrogen bond-breaking compounds and protein denaturants, whereas the nucleases and proteases appear to have little, if any, effect. Susceptibility to these reagents, along with the absence of cysteine residues, strongly reinforces the absence of covalent (disulfide), stabilized tertiary structure in the fibril. Heating of purified axial fibrils from both *Leptospira* B16 and *T. zuelzerae* at 60°C also results in their partial dissociation, and this activity may be consistent with the interpretation. The thermal stability of bacterial flagella of mesophiles was much less than that of the flagella of axial fibrils, the former being completely dissociated at 60°C (139). *S. stenostrepta* purified axial fibrils, on the other hand, are not affected by heating at 60°C (113); this presumably indicates a nonuniformity of axial fibril structure among the spirochetes.

The proximal hooks of bacterial flagella (2), *S. stenostrepta, S. litoralis,* and *Leptospira* B16 are resistant to the chemical dissociation that affects the axial fibril shaft (Fig. 10c). The basis for this difference in chemical sensitivity between the shaft and hook is unexplored but could well reflect differences in either chemical composition or macromolecular structure (tertiary folding) of the proximal hook. Although the function of the proximal hook is unknown, it could be an intermediary in energy transfer, as envisaged for bacterial flagella (2), or it could serve as an anchor. It is, clearly, an appendage onto which the other components of the axial fibril are linked.

Function. The probable function of the axial fibril and its associated structures (Fig. 11D) is still unclear.

The association of the disks with the cytoplasmic membrane could have functional significance for the axial fibril just as in the case of the procaryotic flagellum. The disks may insert into the membrane as a ball-joint socket and thus be able to rotate freely, permitting the shaft per se to rotate as well, and thus function in cell movement. Energy required for movement could be generated in the cytoplasmic membrane portion of the protoplasmic cylinder and could then be transmitted to the shaft through the insertion disks. The disks could, in addition to rotating, vibrate, and the force generated could be transmitted to the axial fibril filament. Berg's (13a) recent model of "how spirochetes may swim" also envisions rotation of the axial fibrils, which in turn results in rotation of the semirigid protoplasmic cylinder within the external, flexible sheath. None of these considerations establish the fact of fibril rotation.

A close anatomical association between the flagellum and the cytoplasmic membrane has been observed in both gram-positive and other gram-negative bacteria. In several models for the insertion and anchoring of the bacterial flagellum (Fig. 11A through C; references 43, 146), the flagellum passes through the cell wall-cell membrane (cell envelope) near a polar membrane. Perhaps axial fibrils, too, are anchored directly to the membrane layers of the protoplasmic cylinder. In general, the insertion apparatus in *Spirochaeta, Treponema,* and *Borrelia* is morphologically very similar to that observed in gram-positive cells (55), whereas *Leptospira* have an insertion apparatus more like that of gram-negative cells (43).

How energy, presumably generated in the cell membrane, is in some way transmitted to the axial fibril is as yet unclear.

The significance of the lamellar bodies seen within the confines of the protoplasmic cylinder (Fig. 5d and g and see 16b) and close to the proximal insertion disks is unknown, but they may play a role in energy production. Similar structures have been observed by others in several spirochetes (115, 147, 164, 167).

As already mentioned, the observations of Bharier and Rittenberg (17) cast doubt upon association of motility solely with the axial fibril(s), and speculation about mechanism(s) of energy transfer to the locomotion apparatus may have to be more complex than envisioned currently. Perhaps a careful study of the effects of chemicals that uncouple energy production will clarify the phenomenon.

PROTOPLASMIC CYLINDER

Basic Morphology

Directly beneath the outer sheath is the protoplasmic cylinder, which consists of the cell wall, cytoplasmic membrane, and enclosed cytoplasmic contents (Fig. 2a, e, and f, 3, 4a and b, 5 through 7, 12a and g, and see 17a, c and d). In the now classical electron microscopic study of the structures of *Treponema, Borrelia,* and *Leptospira,* Pillot and Ryter (160) referred to the cell wall-cell membrane complex as the "parietocytoplasmic membrane," since it was morphologically similar to the cell wall-cell membrane characteristic of gram-negative bacteria. This complex consists of two electron-dense layers separated by an electron-transparent layer, approximately 9 to 12 nm in thickness (Fig. 12g). In some spirochetes, for example *S. stenostrepta* and *S. litoralis,* the outer electron-dense layer appears asymmetric, being almost twice as thick as the inner layer (114). The basis for this asymmetry is revealed by high-resolution electron microscopy of glutaraldehyde + osmium-fixed cells where the outer dense layer is seen as at least two layers, each approximately 3-nm thick (Fig. 12a and b). In contrast to glutaraldehyde + osmium fixation, fixation of *S. stenostrepta* in osmium does not resolve these two outer protoplasmic-cylinder layers; rather the outer layer appears homogeneous. A similar asymmetry has been observed in *T. genitalis* (97).

Presence and Location of the Peptidoglycan Layer

The presence of a mucopeptide layer in several spirochetes was reported by several investigators after chemical analyses to determine the presence of eubacterial peptidoglycan components (70, 160, 212, 234). These investigators determined the presence of muramic acid and glucosamine in *B. duttoni, L. interrogans* biflexa, *L. interrogans* icterohaemorrhagiae, and in *T. phagedenis* Reiteri.

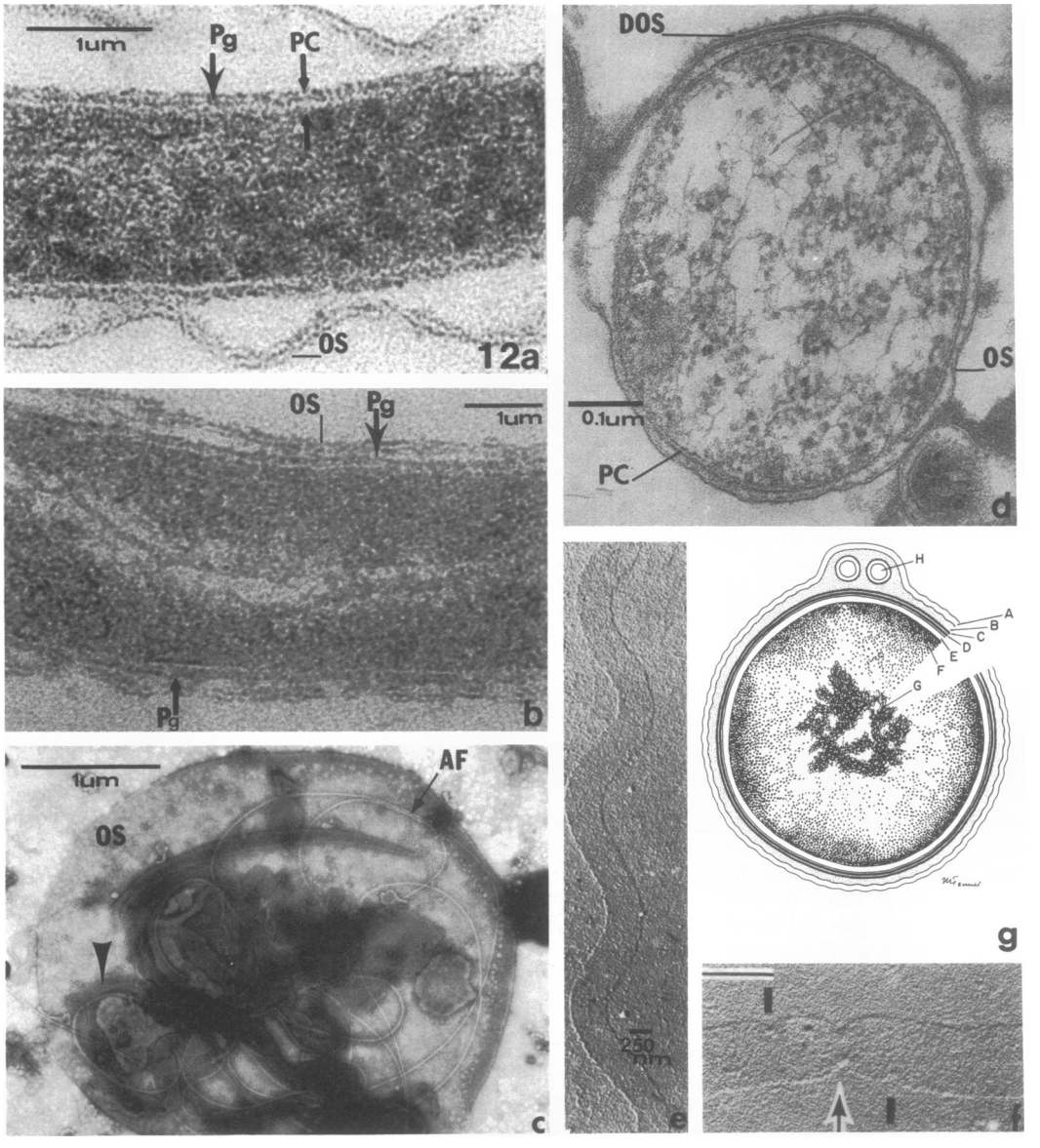

FIG. 12. *Electron micrographs (a through f) and interpretative drawing (g) of S. stenostrepta and S. litoralis revealing the location of the peptidoglycan layer. In glutaraldehyde + osmium-fixed cells (a, b), the peptidoglycan is below the outer sheath and outer membrane of the cell wall-cell membrane complex (protoplasmic-cylinder layers). In S. stenostrepta (c) penicillin G-treated cells, the protoplasmic cylinder is disrupted but remains within the outer sheath. Treatment of S. stenostrepta with lysozyme results in a swollen protoplasmic cylinder (d) that remains within an intact outer sheath; the peptidoglycan layer is not visible. An outer sheath from a nearby spirochete is present. In peptidoglycan fragments isolated by platinum-carbon shadow from S. stenostrepta (e), the helical shape has been maintained; in a constricted region of the peptidoglycan, presumably from a cell division area (f, arrow), an axial fibril pore adjacent to the division plane is seen. Thin fibrils (arrow) similar to cytoplasmic fibrils are seen (c). Diagrammatic representation (g) of a transverse section of S. stenostrepta depicts the various cell layers. The outermost layer, the outer sheath (A), envelopes the cell. Situated in the electron-opaque periplasmic region (B) are the axial fibrils (H). The layers of the protoplasmic cylinder consist of the outermost helical lipoprotein layer (C), a peptidoglycan layer (D), and internal to the peptidoglycan, the innermost layer of the cell, the cytoplasmic membrane (E). The cytoplasmic region contains ribosomes (F) and a centrally disposed nuclear region (G). (a, b, d) Glutaraldehyde + osmium fixed, UAC-lead citrate stained; (c) KPTA, negative stain—taken from reference 114.*

The precise location of the peptidoglycan layer and its chemical composition have been demonstrated only in *S. stenostrepta* by Joseph et al. (114). When exponentially growing cells of *S. stenostrepta* were treated with penicillin G, the protoplasmic cylinder became distorted and disrupted but remained within the apparently intact, but swollen, outer sheath (Fig. 12c), indicating that the peptidoglycan is associated with the protoplasmic cylinder and not the outer sheath. Even though treatment of cell suspensions with sodium deoxycholate results in removal of the outer sheath and portions of the cytoplasmic membrane, the cells retain their helical shape. Final proof for the peptidoglycan location came from lysozyme treatment of cell suspensions not previously exposed to sodium deoxycholate. In the presence of lysozyme, cells became distorted, even though the outer sheath remained intact. Chemical fixation of such treated cells in glutaraldehyde + osmium revealed the absence of the outermost electron-dense layer of the cell wall-cell membrane complex (cf. Fig. 12a and b with d). Thus, the outermost layer of the cell wall-cell membrane complex is peptidoglycan, and the inner triple-layered membrane is morphologically identical to, and the analog of, the procaryotic cytoplasmic membrane (Fig. 12g). Joseph and co-workers (114) successfully isolated this peptidoglycan layer (see below) from *S. stenostrepta* and showed that even in its isolated state it maintained a helical shape (Fig. 12e), thus unequivocally confirming its shape-conferring role in this spirochete.

Characteristics of Peptidoglycan

Isolated peptidoglycan accounts for 1% of the cell dry weight and is similar in chemical composition to that found in other gram-negative organisms (120, 135–137, 178, 223), with the exception that L-ornithine is the only diamino-amino acid, in contrast to the presence of either diaminopimelic acid or lysine found in eubacteria and, now, in some spirochetes. The isolated peptidoglycan from *S. stenostrepta* and *S. litoralis* contains as major constituents muramic acid, glucosamine, alanine, L-ornithine, and glutamic acid. Tinelli and Pillot (212) also found L-ornithine in the peptidoglycan of *T. phagedenis* Reiteri, along with equimolar amounts of muramic acid and glucosamine.

The molar ratios of L-ornithine, glutamic acid, glucosamine, and muramic acid relative to alanine in the purified peptidoglycan from *S. stenostrepta* are 1:1:1:1:1.4. This suggests that the peptide is composed of equimolar amounts of alanine, glutamic acid, and L-ornithine. The presence of larger amounts of alanine is thought to represent terminal alanine residues, which could be available for cross-linking the L-ornithine of adjacent peptide subunits (Fig. 13; references 114, 185). In a recent report, Azuma et al. (8) extracted cell wall fractions from *L. interrogans* biflexa Urawa and *T. pallidum* Reiter. In their extraction procedure they utilized NH_4OH to separate a polysaccharide fraction and a cell residue fraction; the latter fraction was broken at 28,000 to 45,000 lb/in^2. The resulting "cell wall" material was treated with an array of proteolytic enzymes and lipid solvents. Chemical analysis of this material revealed it to be rich in polysaccharide (90% of the fraction) with only 2 to 5% peptidoglycan. The cell walls of both organisms contained alanine, glutamic acid, glucosamine, and muramic acid. Of interest is that the *L. interrogans* biflexa Urawa peptidoglycan contained α,ϵ-diaminopimelic acid, whereas that recovered from *T. pallidum* Reiter contained L-ornithine as the only diamino-amino acid.

Fibrils

Several spirochetes, labeled *L. interrogans* pomona (*L. biflexa*) (235), *T. pallidum* Nichols (105, 119, 152, 153, 231), *T. pallidum* Reiter (99; R. H. Jones, F. Yoshii, and O. J. Carver, Proc. 28th Annu. Meet. Elec. Microsc. Soc. Am. 1970, p. 110–111), *B. recurrentis* (142), and *S. stenostrepta* (113), contain bundles of fine fibrils that seem in some way associated with the protoplasmic cylinder. Morphologically, the fibrils are of three types; one, referred to as perimural fibrils by Yanagawa and Faine (234), is seen associated with the outer layers of the protoplasmic cylinder (Fig. 14a and b), whereas the second class of fibrils (Fig. 14c and d) is associated with the cytoplasmic membrane (60, 93, 99–101, 105, 155, 201, 231). These two classes of fibrils have been referred to by a host of terms, including microtubulifilamente, deep filaments, body fibrils, fibrils, microtubules, and tubules.

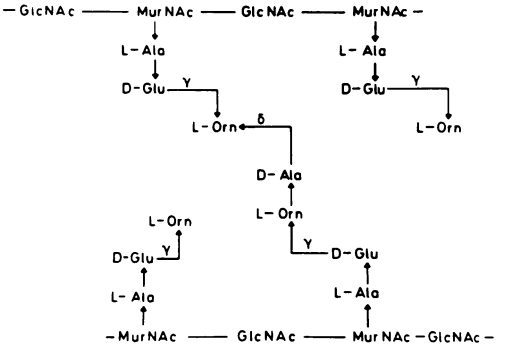

FIG. 13. *Chemical structure of the peptidoglycan from S. stenostrepta—taken from reference 185.*

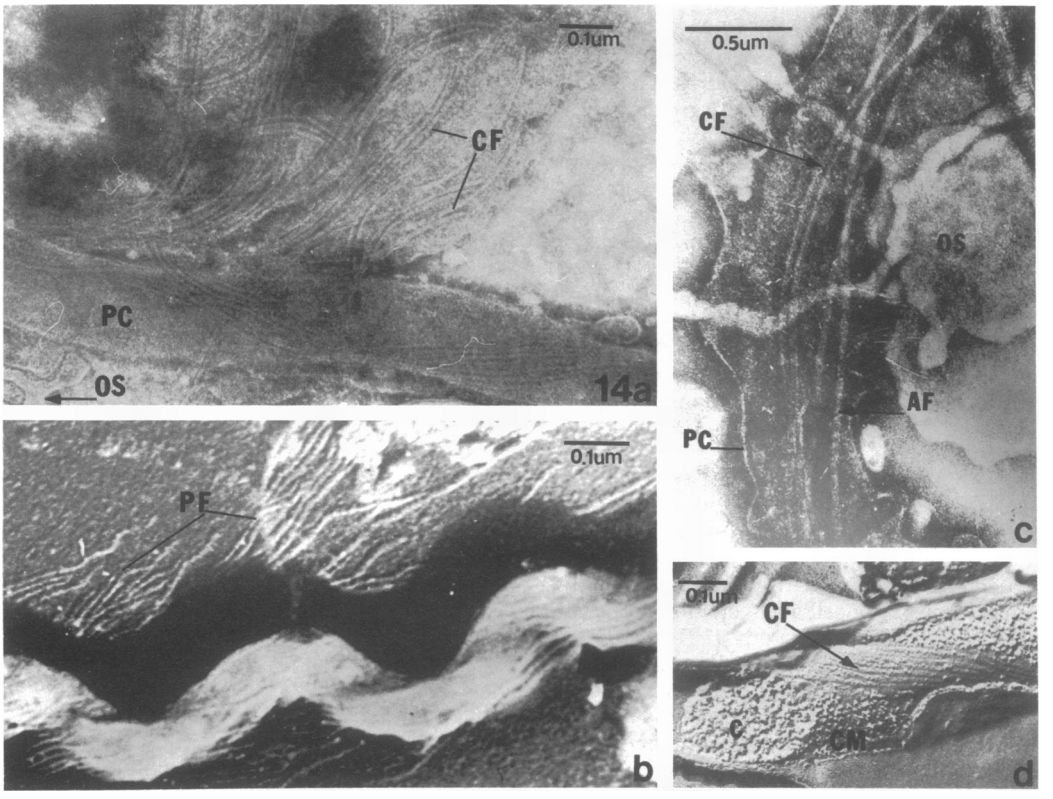

FIG. 14. *Electron micrographs showing protoplasmic cylinder-associated fibrils. An autolyzed cell of T. pallidum Nichols (a, KPTA, negative stain) reveals parallel arrays of cytoplasmic fibrils extending outward from the surface of the protoplasmic cylinder; fragments of outer sheath are evident. In L. interrogans biflexa (b, chromium shadowed), perimural fibrils are seen released from the protoplasmic cylinder after hyaluronidase treatment. In T. pallidum Nichols (d, freeze etch), cytoplasmic fibrils appear to be situated between the outer sheath and the outer layer of the cytoplasmic membrane. Disrupted S. stenostrepta (c, KPTA) with cytoplasmic fibrils, similar in dimension to cytoplasmic tubules (see Fig. 5b). (a, d) are from reference 106; (c) from reference 113; and (b) from reference 235.*

The third class of fibrils, helical, has to date been observed only on the surface of *S. stenostrepta* as longitudinally arranged helices (Fig. 15a and b; reference 90).

Chemical characteristics of purified fibrils are known only for the helical ones.

Perimural fibrils. These surface fibrils (Fig. 14a and b) in *L. icterohaemorrhagiae* (234) and *L. biflexa* (235, 236) are observed only when cells are exposed to dilute alkali (0.5 N NaOH) or hyaluronidase (0.5 mg/ml). In *L. biflexa*, the fibrils that are released by hyaluronidase treatment are 3 to 5 nm in diameter and may represent microfibers of the 6- to 8-nm perimural fibers.

Cytoplasmic fibrils. The cytoplasmic fibrils extend along the inner layer of the cytoplasmic membrane and are 6 to 9 nm in diameter. In transverse sections, the fibrils varied from comma-shaped (201), elongate (155), and triangular (59) to oblong (28). When negatively stained, the stain appears to penetrate the lumen of the fibril, thus indicating a tubular nature.

Freeze-etch replicas of fibrils from *T. pallidum* Nichols (Fig. 14d) show parallel arrays coursing along the inner surface (fractured sur-

FIG. 15. *Electron micrographs of ballistically disrupted cells of S. stenostrepta Z1. Where the outer sheath has been partially removed (a, b), the underlying helical lipoprotein layer is seen. More extensive disruption revealed individual globular units (b, open arrows), which form the helical layer; in some areas, the helices consist of four-sided interconnected structures. Purified helices (c, d) maintain their original in vivo structure, as well as their globular subunit structure (d, G). When viewed tangentially, the helices appear doughnut- to cogwheel-shaped (d, arrows). KPTA, negative stains. (a, b) are from reference 90; and (c, d) from Joseph, Ph.D. thesis, 1971.*

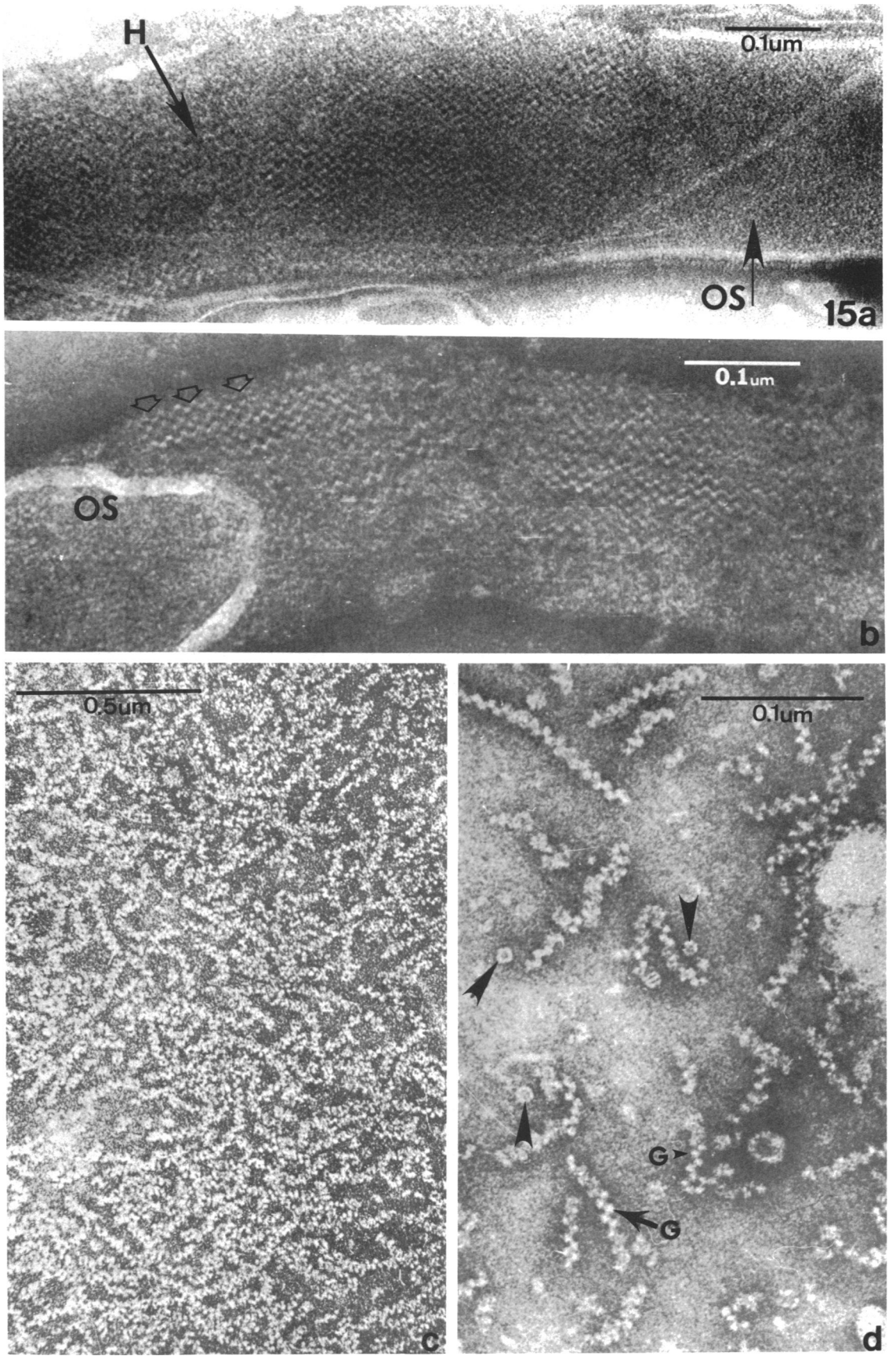
H
0.1um
OS
15a
0.1um
OS
b
0.5um
c
0.1um
G
G
d

face) of the plasma membrane. It is not clear from Fig. 14d how the fibrils could be in contact with the cytoplasm of the cell, as has been suggested earlier (59, 105).

Eipert and Black (59) have made an extensive examination of the ultrastructure of cytoplasmic fibrils found in *T. refringens,* and they locate the fibrils "on the inner sides of the helical treponemes and next to the nuclear area." The fibrils are composed of a complex network of strands, in contrast to the tubular fibrils observed in *T. pallidum* Nichols. The cytoplasmic fibrils are sensitive to the action of proteolytic enzymes, urea, HCl, dilute base (0.005 N NaOH), and SDS. In *T. refringens* fixed by the Kellenberger-Ryter procedure (118), the nucleoid has been found adjacent to the cytoplasmic fibrils. Whether there is some association between these fibrils and the nucleoid, or whether they take part in nuclear or cell division is unknown. Eipert and Black (60) suggest that the cytoplasmic fibrils may be involved in maintaining the spiral shape of *T. refringens*; however, since the fibrils do not appear to be fixed at the cell poles (terminal insertions have not been observed), it may be premature to assign them such a function.

These 7-nm-diameter cytoplasmic fibrils have been observed in a majority of the members of the genus *Treponema,* including *T. phagedenis, T. vincentii, T. refringens, T. calligyrum, T. minutum, T. microdentium, T. cuniculi, T. pallidum* Nichols, *T. pertenue, T. phagedenis* Reiteri (Fig. 5b and 12c; see reference 98 for a discussion of this subject), and in an organism termed "illini" (78, 98). The cytoplasmic fibrils usually occur in clusters of six to eight, and their number in the treponemes varies with the species: *T. zuelzerae* contains one cluster, whereas *T. phagedenis, T. vincentii, T. refringens,* and *T. phagedenis* Reiteri contain eight clusters. The clusters occur at the cell poles, in close association with the insertion apparatus of the axial fibril. Hovind-Hougen (98) has some preliminary chemical evidence (see Table 2 of reference 98) which indicates that these cytoplasmic fibrils are chemically different from the axial fibril. *T. genitalis* did not possess these cytoplasmic fibrils even after deoxycholate or AL-1 enzyme treatment, and Hovind-Hougen (98) considers that this may be of taxonomic significance, especially since these structures also could not be found in *Borrelia* or authentic *Leptospira* species. Whether they are present in *Spirochaeta* remains to be determined.

It is important to note, as has been done for the striated tubules associated with the axial fibrils and for perimural fibrils, that thus far these cytoplasmic fibrils were seen only when cells were chemically treated either with deoxycholate or with the myxobacter AL-1 or AL-2 proteases, or on occasion when cells were physically damaged during preparation for electron microscopy. The possibility that these fibrils represent artifacts and not in vivo anatomical structure must thus be entertained. However, the fact that *T. genitalis, Borrelia,* and *Leptospira* appear to lack these fibrils may indicate that they are significant in vivo structures, since, if they represent artifacts produced in response to chemical or physical treatment, they should be present in all strains unless profound compositional differences exist between the strains.

Helical fibrils. The only detailed chemical analyses of fibrils are of those found on the surface of the protoplasmic cylinder of *S. stenostrepta*, where they appear as a layer of longitudinally arranged helices (Fig. 15a and b). Purified (Fig. 15c) helices are approximately 0.25 nm in diameter, with an amplitude of 0.5 nm. In transverse or tangential aspect, the helices appear doughnut- or cogwheel-shaped (Fig. 15d).

The helices (Joseph, Ph.D. thesis, 1971) are composed of lipoprotein and have a buoyant density in sucrose of 1.16 g/cm^3, which is characteristic of isolated lipoprotein (62). The lipid content of the helices is approximately 10% of their dry weight, whereas the remainder is protein and a small (<2%) amount of carbohydrate. Aspartic and glutamic acids, as well as alanine, glycine, and leucine, are the predominant amino acids. Fatty acid analysis reveals the presence of three fatty acids—12-methyltetradecanoic acid, 13-methyltetradecanoic acid, and hexadecanoic acid—which account for 68% of the total fatty acids of the helices; 72% of the fatty acids consist of branched-chain acids.

The effect of enzymes, chemicals, and temperature on helix integrity has also been determined. Lysozyme, EDTA, ribonuclease, hydroxylamine, HCl, NaCl, benzene, diethyl ether, and petroleum ether have no visible effect on helical structure. The helices are stable over a temperature range of −20 to 37°C. Surface denaturants, cationic bond breakers, and protein denaturants have a marked effect on helix integrity. What significance, if any, these unusual structures have for the single species in which they have thus far been found remains to be determined.

Finally, in *S. litoralis,* rod-shaped structures (reference 113; Fig. 5c) similar in morphology to rhapidosomes (127, 163) found in some gram-negative cells have been observed. These rods are of a tubular construction, 25 nm in diameter and 100 to 800 nm in length. The tubules are released from the protoplasmic cylinder by deoxycholate treatment, and, when sedimented in KBr isopycnic density gradients, have a density

comparable to that of axial fibrils (1.29 g/cm^3). The function and occurrence of these entities in any other spirochetes are unknown.

"Intracellular tubular structures" of quite different dimensions (approximately 16 nm) and of uncertain location have been reported for "aged," treated leptospiral cells (165).

CYTOPLASMIC MEMBRANE

As already indicated, the innermost double-track membrane of the cell wall-cell membrane complex (Fig. 7a and c, 12a, b, and g) is morphologically similar to the plasma or cytoplasmic membrane found in both gram-positive and gram-negative cells (179), although the spirochetal inner membrane has not yet been isolated and thus not characterized chemically or physically. The membrane is of unit dimension, approximately 6 to 8 nm in thickness. Of interest is the observation that this cytoplasmic membrane in *L. interrogans* pomona and *T. genitalis* is asymmetric—the outer leaflet is thicker and more electron dense than the inner leaflet (18, 97).

CELL DIVISION

With the exception of several early reports indicating that leptospires may divide in a longitudinal plane (46, 47), all observations indicate transverse binary fission in the spirochetes so far examined (see, e.g., 95, 102, 147, 167, 173).

Selected electron micrographs (Fig. 16) support a model for the sequence of events that may occur in spirochete cell division that is similar to those proposed earlier by Listgarten and Socransky (128; see Fig. 18).

Very early in the division process, well before any cytological signs of cell constriction or membrane modification, new axial fibrils are formed at the approximate center of the mother cell and at a region slightly subterminal to the subsequent division plane (Fig. 16a and b). The newly synthesized axial fibrils appear to be completely formed before the constriction process itself starts. Thus, in cells normally possessing two axial fibrils, four axial fibrils —two at the cell poles and two on either side of the division plane—are apparent at this stage in cell division. The axial fibrils of the mother cell pass across the division plane, which has indicated to Hovind-Hougen (94) that the new axial fibrils may be formed de novo.

Prior to the visible constriction of the protoplasmic cylinder, a thin, dense line appears that delineates the subsequent division plane (Fig. 16a and c). Protoplasmic-cylinder constriction and cell separation occur along this plane, approximately midway between the new axial fibrils (Fig. 16d through f), and is almost completed when outer sheath constriction begins (Fig. 16f). In *B. merionesi* and *B. recurrentis,* the presence of tapered cell poles may be a necessary correlate of the division process (94).

HOST-ASSOCIATED SPIROCHETES

The morphology of eucaryotic and procaryotic organisms associated with numerous, different hosts has been examined for many years by light microscopy. It remained for the development of the electron microscope (both transmission and scanning) and associated ultrastructural techniques (e.g., thin sectioning, negative staining, cryomicrotomy, critical-point drying, and freeze-fracture etching) to demonstrate in a definitive way the physical relationship(s) that exists between these organisms and their hosts (e.g., 51, 182, 184, 207, 208, 218, 220). Host-associated organisms may be pathogenic or not, and the spirochetes provide no exception to this generalization. Breznak (28) has reviewed in great detail the biology of nonpathogenic, host-associated spirochetes, and the reader is referred to this review for a subject survey.

Host-associated spirochetes, as for host-associated microorganisms in general, have been shown to exist in a wide variety of host niches. These associations include: (i) both the survival and multiplication of *Cristispira* in the digestive tract, (ii) the crystalline style of a wide variety of mollusks (see reference 28), (iii) the recently observed "spontaneous" spirochetal infection of brine shrimp, *Artemia salina* (218–222), (iv) the spirochetes found in intestinal tracts of insects (Table 2 of reference 28) and ruminant (33, 103) and nonruminant vertebrates (51, 124, 141, 176, 180, 182–184, 208), and (v) the associations that exist in termite hindguts (28, 29, 42, 75). Advantages accrue to both the host and the resident spirochete in several of these latter associations (28, 29).

With the possible exception of the spirochete-*A. salina* association, all of the above appear to be nonpathogenic for the host. In *A. salina,* it is not clear that the association should be regarded as a true infection, with resultant pathogenesis, for it may represent some mutualistic relationship between shrimp and spirochetes.

There are, of course, well-known spirochete-host interactions that have adverse effects on the host. These include, for example, the production of syphilis and related diseases such as yaws and pinta by *T. pallidum* and *T. pertenue* in humans, and *T. carateum,* which produces venereal spirochetosis in rabbits. Infectious leptospiral jaundice (Weil's disease) caused by *L. icterohaemorrhagiae* and relapsing fever in humans are the result of infection with *B. recurrentis,* this latter infection occurring through an

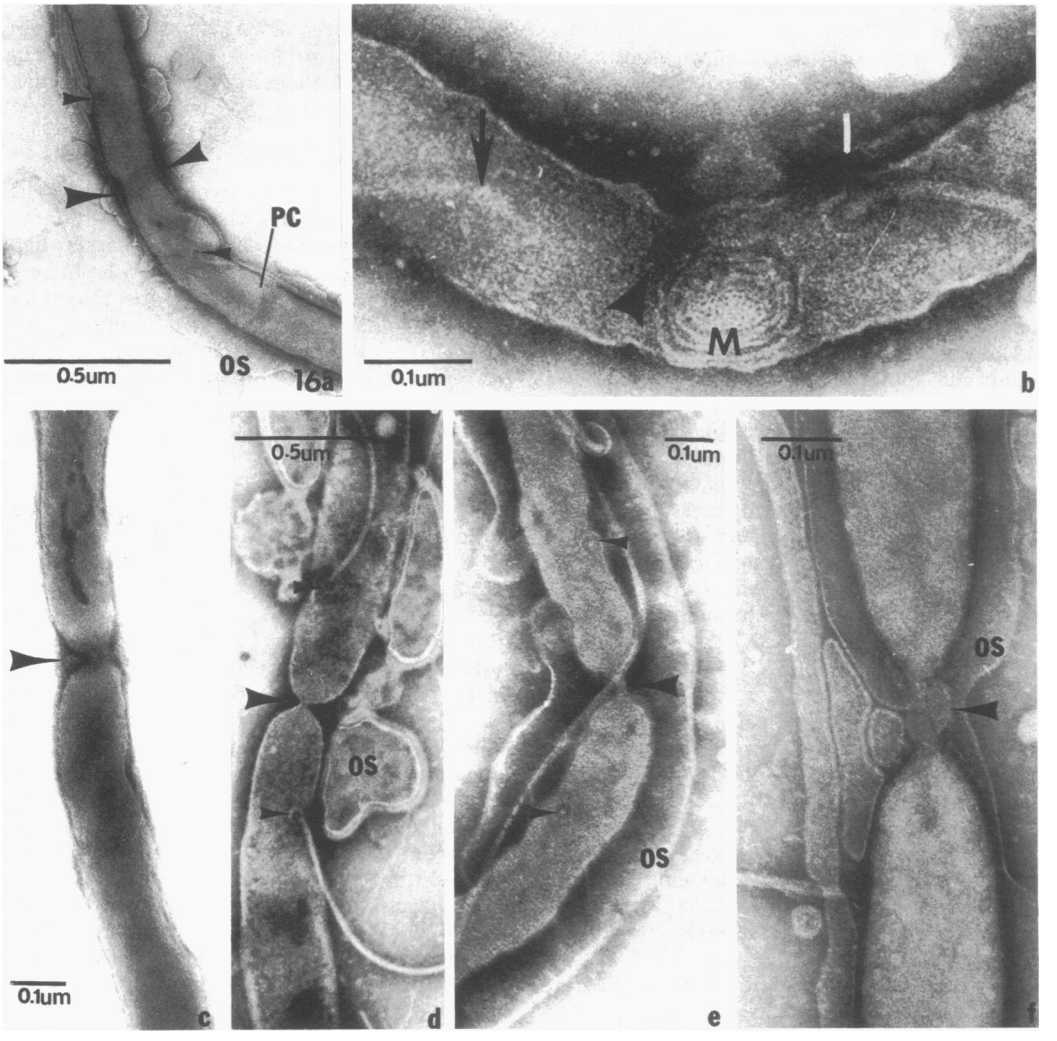

FIG. 16. *Electron micrographs of spirochetes selected to show possible sequence of cell division in spirochetes. Prior to any visible evidence of constriction, new axial fibrils are present (a and b, small arrows), and a lightly darkened (electron-opaque putative division plane) is seen (a, large arrows). A mesosome is present at such a division plane (b). Constricted protoplasmic cylinders (c through f). The outer sheath constriction appears to have taken place only during the final stages of division (c); cell separation probably occurs by the pinching-off of a thin thread of protoplasmic membrane. Protoplasmic cylinder constriction is complete prior to outer sheath constriction (d through f). KPTA, negative stains. (b) is from reference 147; and (a, c through f) from S. C. Holt, unpublished.*

intermediate host or vector.

In addition to these more severe disease states resulting from spirochete-host associations, there are those of the buccal cavity, including *Treponema* and *Borrelia* (80, 130, 149, 170, 196–198), which are on the whole still not well understood. Whether a specific organism acts alone, interacts with other spirochetes, or interacts with other procaryotes to produce diseases such as Vincent's infection (trench mouth) or various forms of gingivitis is not yet uncertain.

A small group of helically shaped microorganisms, *Spiroplasma,* found in the hemolymph of *Drosophila* species (151, 161, 177), associated with corn stunt and stubborn disease of citrus plants (52, 53, 175), and acting as suckling mouse cataract agent (40, 41, 61, 215) were thought in early investigations to be spirochetes. However, the absence of an axial fibril (Fig. 2b), lack of immunogenic cross-reactivity with species of *Leptospira, Spirochaeta,* or *Treponema,* and a low guanosine plus cytosine content (26% versus

35 to 39%, 38 to 40%, and 56 to 67%, respectively) exclude these microorganisms as members of the order *Spirochaetales*.

Morphological Studies of Spirochete-Host Interactions

In general, the morphology of spirochetes occurring within a host is similar to that already described for free-living spirochetes and for some host-associated treponemes examined in vitro. The only apparent morphological difference noted in spirochetes examined in situ occurs at their cell surface, especially at the poles. This polar differentiation undoubtedly permits spirochete-host cell interaction by way of spirochete adhesion to host tissue. In several instances the spirochete actually penetrates the host cell membrane.

Brine Shrimp Association

Spirochetes infecting *A. salina* are morphologically similar to those already described in this review and are found in both intra- and extracellular sites and in the hemocoel (see Fig. 20c), the cavity through which blood flows in arthropods. The hemocoel is not a true coelum, in that it is not entirely surrounded by mesodermal tissue, but is a cavity derived from the embryonic blastocoel. Spirochetes are also found in the three main parts of the maxillary (kidney) gland—the end sac, efferent muscle fibers, and hypodermal cells of *A. salina* (218), where they are closely associated with the basal lamina. Within the efferent tubule epithelium, the infecting spirochetes appear to occupy (are the cause of?) a "cave-like indentation" of the epithelium. The observation that in some areas the basal lamina is broken, or discontinuous, suggests some destructive interaction between the spirochete and the basal lamina. The spirochetes infecting *A. salina* usually possess two 15-nm-diameter axial fibrils per spirochete; although the number of fibrils varies, the apparent maximum is four. This seeming variability most probably results from differences in cell age, physiological condition, or the level at which the spirochetes were sectioned. When observed in ground cytoplasm of *A. salina*, the spirochetes have a tubular structure associated with them (221). These tubules appear nearly identical in morphology to the outer sheath seen in thin sections of these spirochetes and are only observed in the host-ground plasm. Tyson (221) suggests that the tubules may in some way be associated with the establishment and maintenance of an intracellular existence. They may well, however, represent only the sloughing-off of outer sheath material. Spirochetes are also found in *A. salina* amoebocytes, within membrane-limited digestive vacuoles where they appear to be partially digested; it is thus possible that the amoebocyte may be functioning as a phagocyte (221).

Swine Dysentery

One of the spirochetes implicated in swine dysentery may be *T. hyodysenteriae* (21, 65, 77, 83, 102, 166, 168, 210, 211, 213, 225), a large, loosely coiled spirochete, approximately 5 to 8 μm long and 300 to 800 nm in diameter. The number of axial fibrils inserted into each of the cell poles varied between 7 and 9, with 14 to 18 fibrils observed to overlap in the center of the cell (73, 85). These spirochetes may be morphologically identical to those originally described as being associated with swine dysentery (21, 83, 166, 168, 210). *T. hyodysenteriae* has been found in the lumen of intestine, in goblet cells, on luminal surfaces (see Fig. 19a), and in mucosal crypts (74, 83, 176, 210). As the disease progresses, more *T. hyodysenteriae* are found in intestinal epithelial cells. Specific attachment sites or attachment appendages are not observed in or on *T. hyodysenteriae*; thus, the spirochete may gain entrance to the host tissue by some form of endo- or phagocytosis. In pigs displaying swine dysentery, Harris et al. (84) have observed large spirochetes, presumed to be *T. hyodysenteriae*, on the colonic epithelium surface (see Fig. 19a). The spirochetes appear to be located between distorted or degenerate microvilli.

In addition to this large spirochete, both control and infected pigs contain on their mucosal surfaces small- and medium-sized spirochetes, approximately 4 to 5 by 0.2 to 0.21 nm, which are considered indigenous to the animal (176).

Syphilis

Some of the earliest ultrastructural studies of spirochete-host associations involved studies of *T. pallidum* from human syphilitic lesions (134, 162, 231, 232). For these morphological studies, material was removed from a lesion, placed in suspension, and then examined microscopically. Obviously, any anatomical relationship that existed between the microorganism and the host tissue was destroyed or completely disorganized.

The studies by Drusin et al. (58) and Ovcinnikov and Delektorskij (152–154) represent some of the earlier electron microscopic observations of *T. pallidum* in material taken directly from syphilitic lesions. These studies showed that *T. pallidum* in both human and rabbit lesions were located almost exclusively in the extracellular ground substance and in association with collagen fibrils of testicular tissue, and these studies

were soon followed by those of Lauderdale and Goldman (123), who employed serial thin sectioning to show clearly that some *T. pallidum* did penetrate fibroblasts, Leydig cells of monocytes, and mesenchymal cells in infected rabbits. Similar observations were made by Sykes and Miller (204), using *T. pallidum* Nichols-infected rabbits.

Examination of human biopsy material from a primary lesion revealed *T. pallidum* in fibroblasts, as well as in epithelial spaces (206). Recently, Sykes and Kalan (203) also showed *T. pallidum* in vacuoles of fibroblasts and epithelial cells and lying along and among collagen fibrils in a human syphilitic lesion (Fig. 17b and d). Ovcinnikov and Delektorskij (156) have also observed *T. pallidum* in the endo-, peri-, and epineurium of nerve fibers in experimental syphilomas of rabbits (Fig. 17a and c), whereas Wecke et al. (reference 229; Fig. 18a) have visualized *T. pallidum* in macrophages of a primary chancre, as well as embedded in collagen fibrils (Fig. 18b).

It is interesting that those *T. pallidum* found within cells are generally smaller and thicker (1 to 1.7 by 0.35 nm versus 5 by 0.1 nm) than those found in extracellular spaces. In addition, the intracellular *T. pallidum* cytoplasm was more electron dense. Similar observations have been made by Tyson (222) in brine shrimp-spirochete association. It is possible that the presence of the spirochetes intracellularly results in activation and/or release of chemical constituents (enzymes) that result in breakdown of procaryotic membrane permeability, and thus effect a loss of soluble spirochete components; hence, a compaction of macromolecular cytoplasmic constituents results in an increase in staining density of the microorganisms. Alternatively, the loss of membrane integrity may enable better stain penetration and thus increase stain density.

Skin Lesions: Yaws

When cultivated in skin and lymph nodes of hamsters, *T. pertenue*, the etiological agent of yaws, display an ultramicroscopic morphology (101) similar to that of *T. pallidum* Nichols and *T. cuniculi*; the cells are approximately 8 to 15 μm long and 0.15 μm wide and have at least three axial fibrils that insert into each of the pointed ends. Of interest is the observation that, in negatively stained *T. pertenue* Gauthier, thin, surface, or peripheral fibrils, 1 to 5 μm in length and 2 to 3 nm wide, are seen. Hovind-Hougen et al. (101) refer to these fibrils as "fimbriae"; however, they are not at all similar to the fimbriae (pili of reference 32) observed on the surface of *Escherichia* (32), *Pseudomonas* (26, 27), or *Neisseria* (202) species. These fimbriae are morphologically very reminiscent of the surface fibrils observed by Yanagihara et al. (235, 236) in *L. interrogans* biflexa Urawa. Similar "fimbriae" have not yet been observed in *T. pallidum* Nichols or in *T. cuniculi*. Thin-sectioned *T. pertenue* Gauthier-infected hamster skin reveals treponemes only within intercellular spaces in the stratum basale; they are never seen within or between cells of the dermal layer.

Gastrointestinal Tract

In a most interesting series of cytological investigations, Savage (180, 181), Savage and Blumershine (182), Savage et al. (184), Takeuchi and Zeller (207, 208), and Davis et al. (51) were able to show that morphologically distinct microorganisms inhabit different regions of the gastrointestinal tract of mice, rabbits, monkeys, and rats. In a given type of animal, not only are the microorganisms at an anatomical location of constant type, but they appear to "prefer" that anatomical location within the tract.

The rat cecum contains at least three recognizably different morphological microbial types, referred to as types I, II, and III (Fig. 19b; references 51, 208). The crypt of the cecum is heavily infested with microorganisms. One spirochetal type (type 1) is a *Borrelia*-like cell, measuring approximately 0.25 to 0.40 by 2.7 μm and containing 6 to 14 axial fibrils, each of which is 18 to 21 nm in diameter. These organisms occur at the base of goblet cells (Fig. 19b). Similar morphological types are observed in macrophages in the lamina propria. The two other morphological types are not spirochetes, are observed in macrophages in the lamina propria, and appear similar to spirilla.

Takeuchi and Zeller (208) have observed spirochetes similar to the Savage type I (51) organism. These occur at the brush border of the large intestinal epithelium of rhesus monkeys (Fig. 20a), are 3 to 6 by 0.2 to 0.4 μm, and contain 8 to 12 axial fibrils apparently crossing at the cell's mid-region. As is apparent in Fig. 20a, these spirochetes almost totally replace or at least mask the microvilli in the brush border. Erlandsen and Chase (63, 64) have observed what appear to be spirochetes (spiral microorganisms) in the crypt of Lieberkühn and within digestive vacuoles in Paneth cells in small intestine. It is not clear, however, whether these spiral microorganisms are indeed spirochetes.

The question as to whether or not spirochetes can be considered normal inhabitants of human intestine has recently been addressed by Minio et al. (141), who observed that colonic mucosa of healthy humans contains spirochetes at-

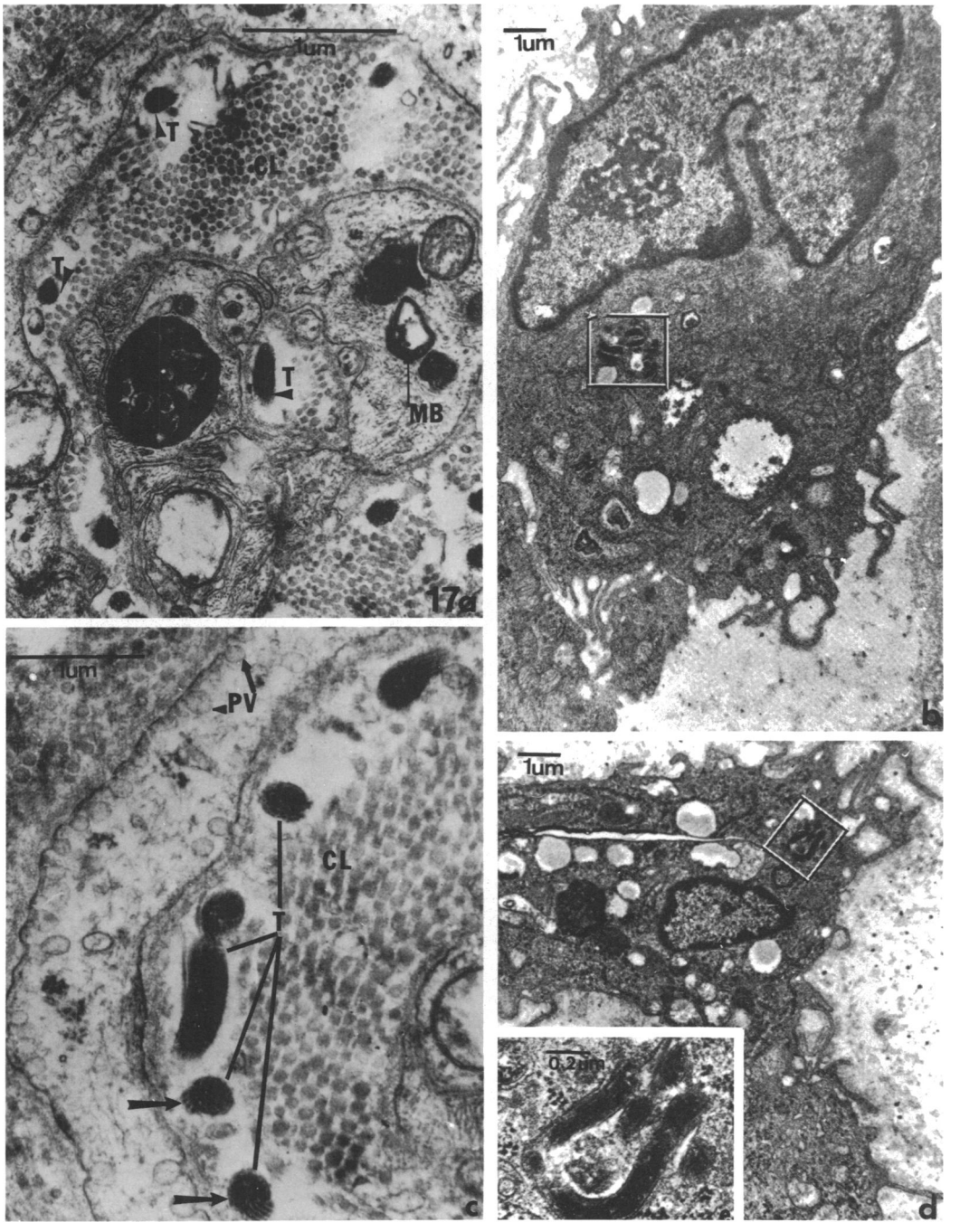

FIG. 17. *Electron micrographs of T. pallidum in rabbit tissue. T. pallidum in the endo-, peri-, and epineurium (a) and in a peripheral nerve fiber (c). In (a) and at high magnification (c), the treponemes have displaced a portion of the collagen fibers and appear in an electron-transparent space. Five treponemes may be present in the nerve fiber cross-section (c), in which there is massive destruction of collagen fibers. Note the many axial fibrils in cells sectioned transversely (c, arrows). T. pallidum is also seen localized within a fibroblast from the lamina propria (b) and a Leydig interstitial cell (d). The entrapped treponemes are outlined and are seen more clearly at high magnification in (e). (a, c) Glutaraldehyde + osmium fixation, UAC-lead citrate stained; (b, d) glutaraldehyde + osmium fixation, uranyl nitrate-lead citrate stained. (a, c) are from reference 156; and (b, d, e) from reference 204.*

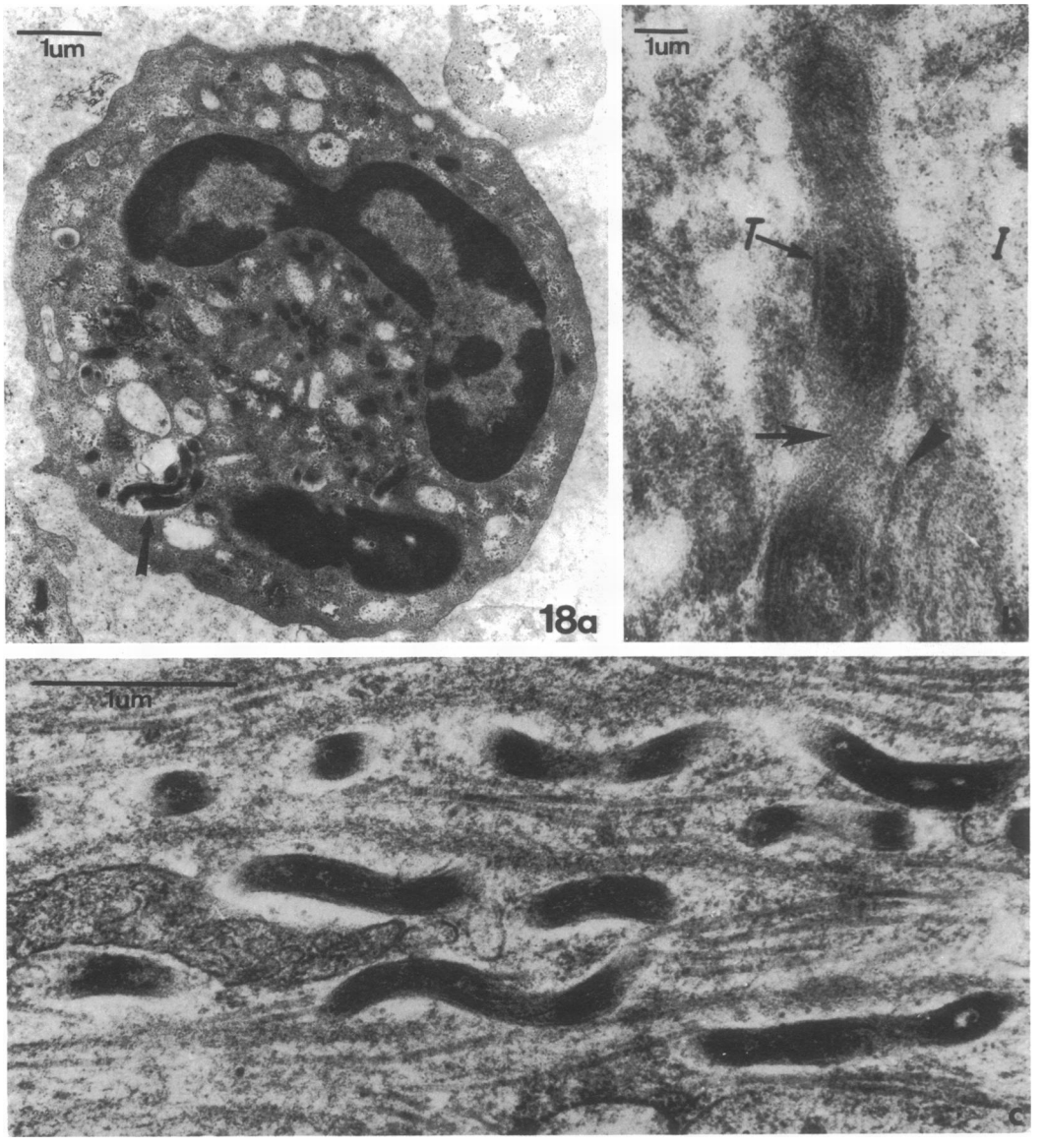

FIG. 18. *Electron micrographs of T. pallidum in a primary chancre of a human penis. T. pallidum, engulfed by a macrophage (a), appears to have been in the process of being phagocytized (arrow) at the time of fixation. T. pallidum, high magnification, in infected tissue (b); tailless arrow indicates the possible boundary between the intracellular space and tissue of the host cell. Note the multiple number of axial fibrils (tailed arrow) typical of T. pallidum. The treponemes have invaded the intercellular space (c). Glutaraldehyde + osmium-potassium chromate fixation, UAC-lead citrate stained; from reference 229.*

tached to superficial and cryptic cells (Fig. 20b). The spirochetes are slender (0.4 to 5 μm in diameter) with narrow tips or ends. Similar spirochetes are found between microvilli in contact with the epithelial plasmalemma, within patent intracellular spaces, and in close proximity to the opening of these spaces into the intestinal lumen. Morphologically similar spirochetes are also observed in the lamina propria and in the lumen of crypts, but they are present in smaller numbers than those associated with microvilli. There is no evidence of any phagocytic activity by epithelial cells or for that matter of inflammatory reactions against these spirochetes. The existing evidence of a nonspecific destruction of host epithelial cells needs further examination,

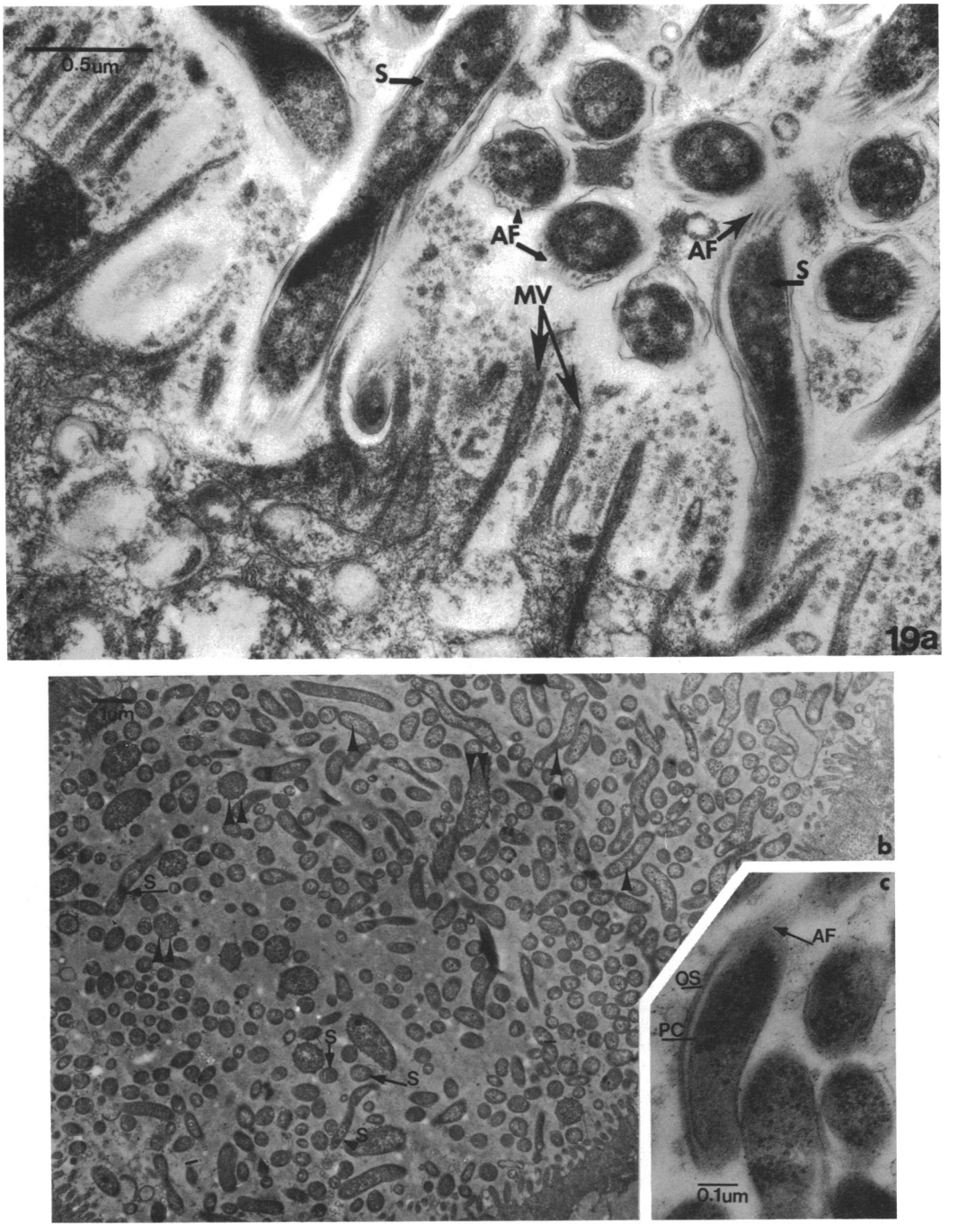

FIG. 19. *Electron micrographs of intestinal organisms. T. hyodysenteriae (a) on the intestinal surface of an afflicted pig. The cecal crypt (b) from a normal rat containing at least three distinctly different morphological types of bacteria. In (a), the spirochetes are located between distorted or disrupted microvilli and are in close proximity, but are not visibly attached, to the luminal surface. The cecal crypt of the normal rat (b) contains numerous spirochetes (Savage type I) as well as type II (double arrows) and III (arrows) organisms. The axial fibrils limiting outer sheath and protoplasmic cylinder membrane of a type I spirochete are seen in the high-magnification micrograph (c). Glutaraldehyde + osmium fixed, UAC-lead citrate stained. (a) is from reference 84; and (b) from reference 51.*

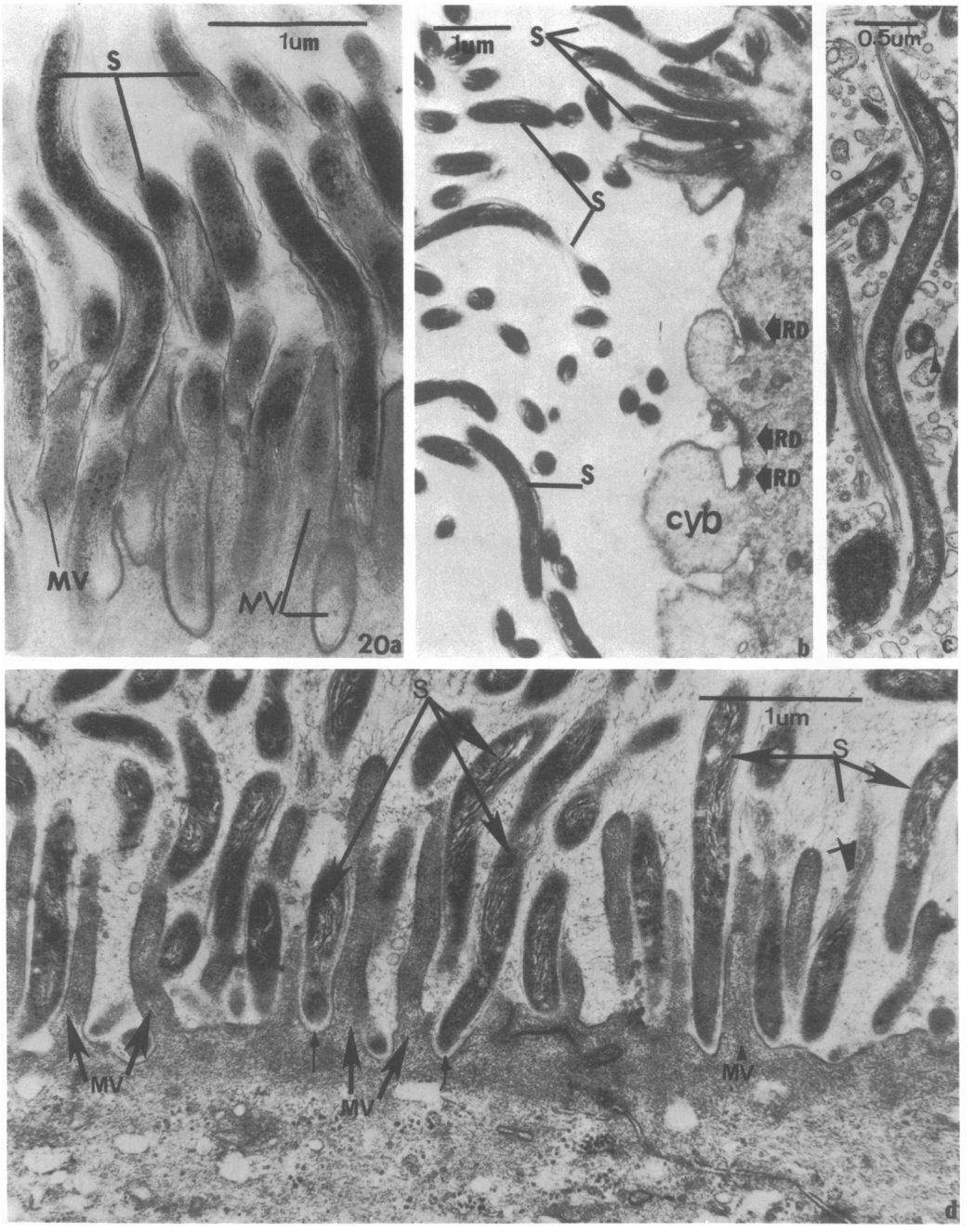

FIG. 20. *(a, b, d) Electron micrographs of intestinal spirochetes; (a) brush border of the large intestinal epithelium of a rhesus monkey; (b) a portion of an epithelial cell of a normal human colon; and (d) the apex of the colonic epithelium from a rectal biopsy from a patient with systemic lupus erythematosus. The spirochetes are either free within the intestinal lumen or in close association with the microvilli; in (a), they nearly replace the microvilli, and in (d) spirochetes and the epithelial surface are closely apposed but separated by a fine, fuzzlike material (arrows). Electron micrograph of the cytoplasmic region of the end-sac epithelium of the maxillary gland of brine shrimp, A. salina (c). In transverse section, one axial fibril (arrow) is apparent in the spirochete. (a) Glutaraldehyde + osmium fixation; (b, d) osmium fixation; (c) osmium-s-collidine fixation. All samples stained with UAC and lead citrate. (a) is from reference 207; (b) from reference 141; (c) from reference 220; and (d) from reference 68.*

inasmuch as only one method of tissue preparation was employed, and epithelial cell alteration due to other external stimuli cannot be ruled out. Harland and Lee (82) and Gear and Dobbins (68), in electron microscopic investigations of human intestinal spirochetosis, have observed spirochetes, morphologically similar to *Borrelia* species, approximately 3 μm in length, found between microvilli at the colonic epithelial cell apex (Fig. 20d). The spirochetes are separated from the surface of epithelial cells by an electron-transparent space, and thus there is no apparent physical attachment or invasion of host tissue. Lee et al. (125) and Toner et al. (214) have observed, in their study of human spirochetosis, attachment of spirochetes directly to the surface of the colonic epithelium, although the organisms did not appear in the cells. Whether the attachment may induce formation of spirochete-associated extracellular material (e.g., acid mucopolysaccharide), similar to that described recently by Zeigler et al. (237) for virulent *T. pallidum* Nichols, remains to be determined.

Xylophagous Insects

Extraordinarily interesting microbial associations are found to occur in guts of xylophagous insects such as termites, *Reticulitermes flavipes* (Kollar), and wood-eating roaches, *Cryptocercus punctulatus* (28). The hindgut of these animals contains a variety of small bacteria and large protozoa; the bacteria either are free within the gut, (Fig. 21i, 22d, and 23c), are physically attached to the linings of the gut, (Fig. 21i, 22f, 23a, and 24b), or occur on the surface of the protozoa (Fig. 21a and h). Outstanding among the protozoa is *Pyrsonympha,* which contains not only numerous microbial types within its cytoplasm but also very thin (0.2- to 0.25-μm diameter) spirochetes attached to its outer cell surface (Fig. 21a and h, 24). These spirochetes are of interest because of the tenacity with which they adhere to the protozoan surface. The presence of narrow, pointed ends in these spirochetes (Fig. 21f) is consistent with their insertion into the grooves or depressions in the protozoan cell surface, but this supposed interaction has not been observed clearly; instead, the narrow end of the spirochete comes only within 30 to 50 nm of the protozoan surface (Fig. 21f and i). It is possible that this 30- to 50-nm separation or space reflects the presence of adhesive or cementing material (glycocalyx) that could function to anchor the spirochete to the protozoan surface. Freeze-fracture (Fig. 21b and c) examination reveals the spirochete surface to be grooved and with equidistant ridges. Such grooves could also function to attach the spirochete at various points along the surface.

On another protozoan, *Barbulanympha,* which also inhabits the hindgut of *Cryptocercus* (reference 24a), spirochetes with similar narrow, pointed ends have been observed (Fig. 23). However, as is apparent in Fig. 23a and b, these spirochetes appear to insert directly into the surface membrane of *Barbulanympha.*

A similar polar differentiation has been observed in spirochetes from gut contents of *R. flavipes* (Kollar) termites (Fig. 22; S.C. Holt, unpublished). The cell poles were either long, slender structures, with the protoplasmic cylinder consisting of fine transverse striations (Fig. 22a), or flat to bullet-shaped structures (Fig. 22b and c). The amorphous material at the end of the cells (Fig. 22c) could represent an attachment material (either membrane, polysaccharide, or other cementing material).

Grimstone (75) and Cleveland and Grimstone (42) have observed spirochetes in hindguts of *C. punctulatus.* They describe, also, a large polymastigote flagellate, *Mixotricha paradoxa,* which inhabits the guts of wood-eating termites, *Mastotermes darwiniensis.* The more common and abundant spirochetes found associated with *C. punctulatus* are approximately 1 μm in diameter and 12 to 15 μm long. Many axial fibrils, numbering between 60 and 100, are observed (Fig. 24a). The remainder of the spirochetes found in the gut are small in size and number.

The surface of *M. paradoxa* is covered, both anteriorly and posteriorly, with microorganisms. These organisms adhere to the protozoan in specific association with its surface ridges (brackets); the anterior face of each bracket has an encapsulated bacterium lying in its shelter, whereas the posterior face of the bracket has a fringe of adhering spirochetes (Fig. 24b). The spirochetes attach or insert into depressions in the bracket and are in intimate contact with the plasma membrane of the flagellate. The spirochetes associated with *Mixotricha* are smaller than those seen in *C. punctulatus* (0.15 μm in diameter and 10 μm long, with one to two axial fibrils). A larger spirochete, 0.5 by 25 μm with 15 axial fibrils, is also seen adhering to *M. paradoxa.* An amorphous electron-dense material is noted on the outer sheath of the *Mixotricha*-associated spirochetes.

In an elegant study of the epi- and endobiotic bacteria associated with *Pyrsonympha vertans,* Smith and Arnott (194) have observed a highly differentiated region at one end of several gram-negative bacteria presumed to be spirochetes (Fig. 21d and e), although axial fibrils are not seen regularly. In Fig. 21d, an expansion of the

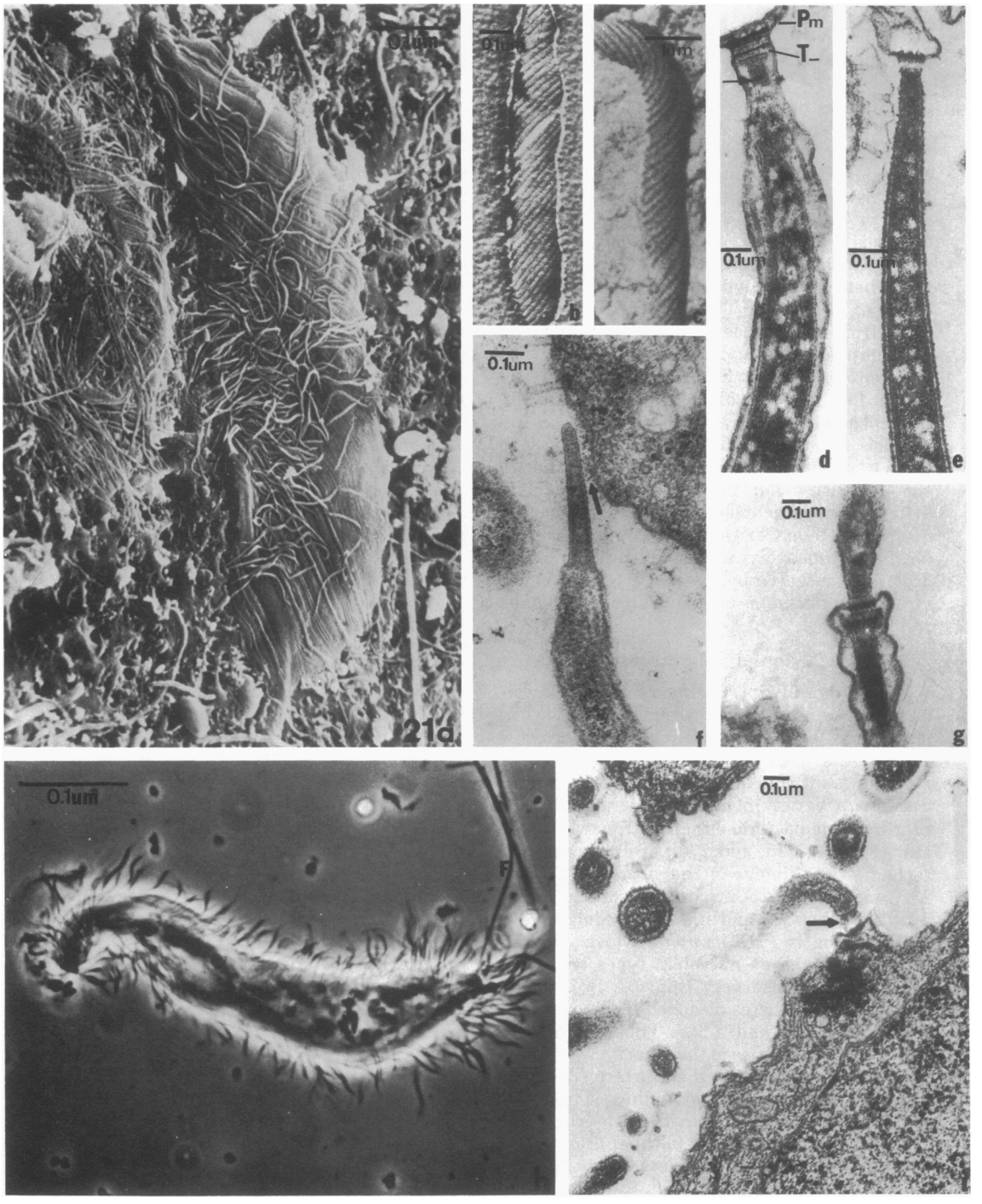

FIG. 21. *Spirochete-Pyrsonympha association. (a, h) are scanning electron micrograph and whole-cell mount of Pyrsonympha with numerous surface-associated spirochetes, respectively. Spirochetes protrude from the cell surface and are readily distinguished from the large terminal protozoan flagellum in (h). Freeze-etch replicas (b, c) show both the ridged surface of the spirochete as well as the narrow cell pole that is closely associated with the surface of the Pyrsonympha cell membrane. Spirochete may be separated from the protozoan surface by an electron-opaque space (f, arrow) or associated with the cell surface of Pyrsonympha through thin fibers (i, arrow). High-magnification micrographs (d, e, g) reveal that one pole of the spirochete consists of a specialized expanded region with parallel fibers that attach to a specialized region of the protozoan surface. This is clearly seen in (d), where the spirochete Pyrsonympha membrane is connected through a transition zone. The parallel fibers (d, arrow) may be extensions of the outer membrane of the spirochete and may be involved in attachment to the protozoan membrane. Thin sections: (d through g, i) glutaraldehyde + osmium fixed, UAC-lead stained. (a through c, f) are from reference 24; and (d, e, g through i) from reference 194.*

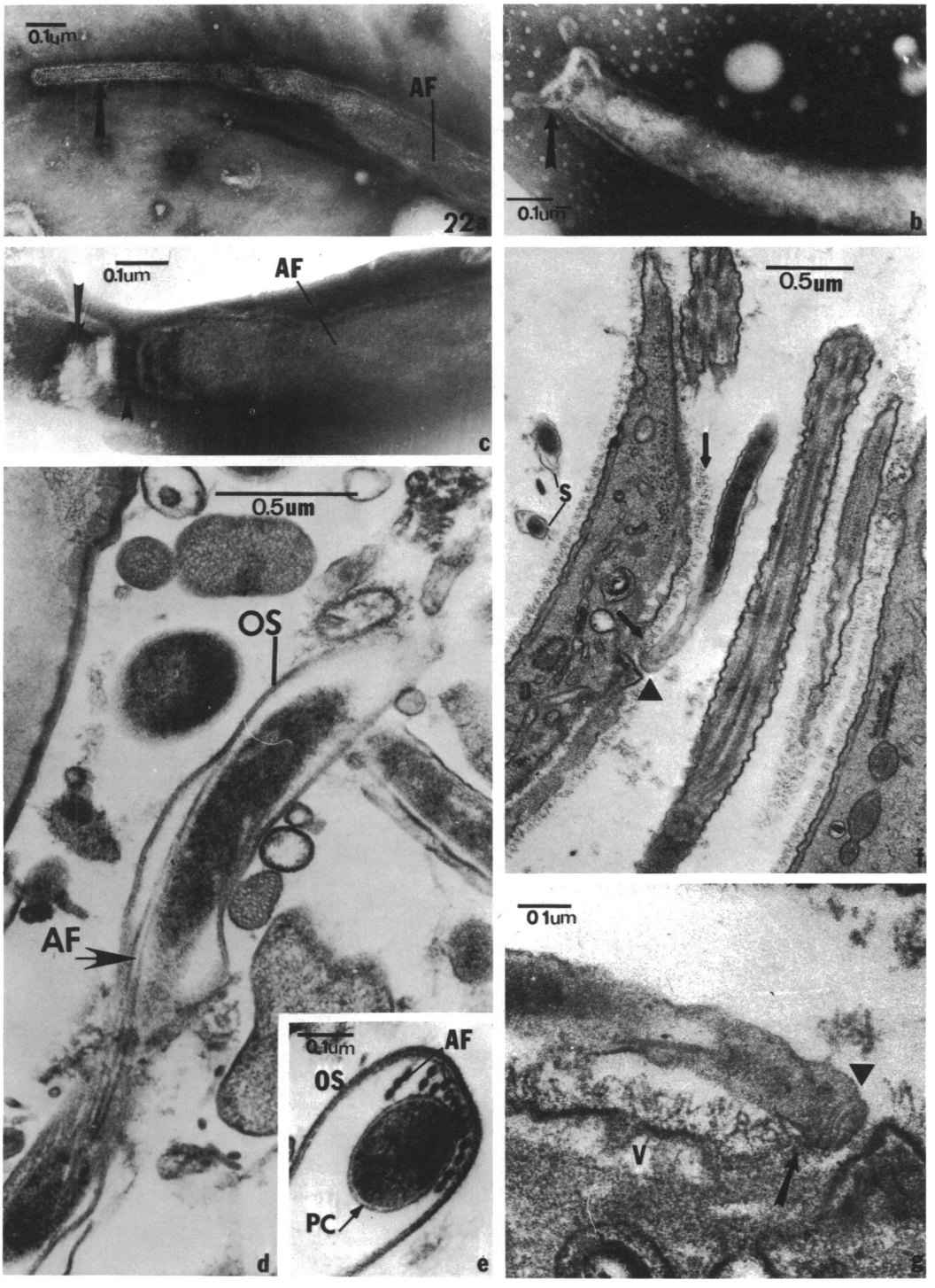

FIG. 22. *Electron micrographs of various spirochetes found in the hindgut of termites, R. flavipes. In (a through c) spirochete terminal cell poles are seen to vary from long, narrow striated structures (a, arrow) to flattened, plunger- or cuplike regions (b, c). In (c), the cell pole is flattened and contains parallel fibers (small arrow) and an attached electron-transparent material (large arrow) that may be a fragment of a host-cell membrane. Spirochetes are seen free in the lumen of the gut (d) as well as attached to host-cell membrane (f, triangle). Note the electron-dense fuzz in (f) and (g, arrow); the association of a spirochete through this fuzz to the protozoan membrane is seen more clearly in the high-magnification enlargement (g). The clear areas immediately below the host-cell membrane may represent vesicles involved in spirochete detachment. Transverse section: (e) numerous axial fibrils located between the outer sheath and the protoplasmic cylinder. (a through c) NH_4MoO_4, negative stain; (d through g) glutaraldehyde + osmium fixation, UAC-lead citrate stained (S. C. Holt and E. Canale-Parola, unpublished).*

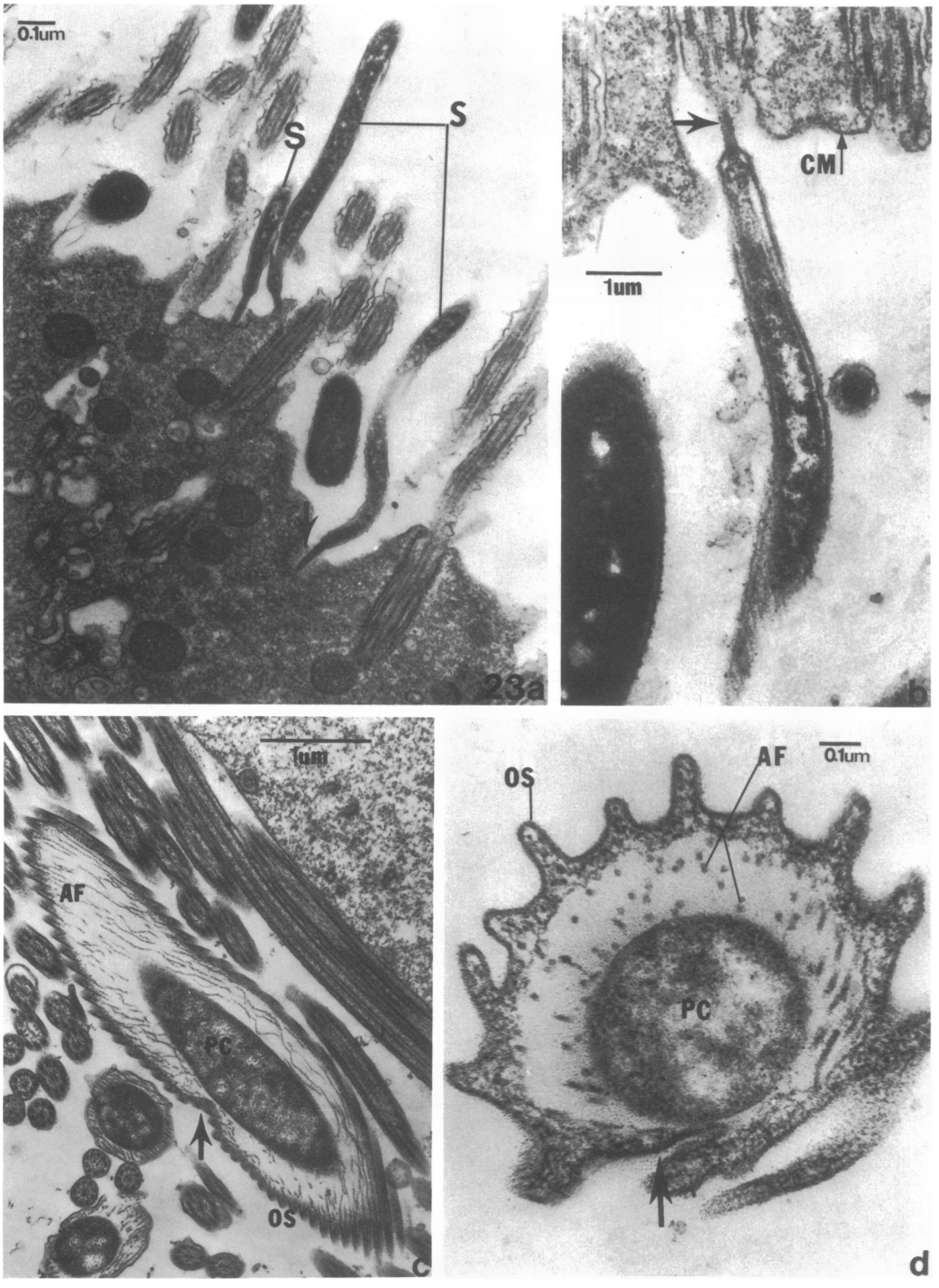

FIG. 23. *Electron micrographs of small spirochetes attached to the cell membrane of the flagellate protozoan Barbulanympha isolated from the hindgut of C. punctulatus (a, b) and Pillotina spirochetes (c, d) from the hindgut of R. flavipes. In (a), three slender spirochetes have their narrow, pointed ends inserted directly into the cell membrane; note that only one end of the spirochetes is so differentiated. One spirochete appears associated with the protozoan surface by its pointed end, which is enmeshed in a slightly electron-dense matrix (a, arrow). At higher magnification, the differentiated end (b, arrow) of the spirochete is seen in direct contact with the protozoan cell membrane; this end is electron dense, with some banding apparent within the outer sheath. The Pillotina spirochete seen in longitudinal section (c) is representative of these large spirochetes, contains numerous axial fibrils, has a wrinkled or crenated outer sheath, and a groove, or sillon (c, d, arrow), characteristic of this proposed genus. The sillon may be continuous with the interior of the protoplasmic cylinder. Glutaraldehyde + osmium fixation, UAC-lead citrate stained. (a, b) are from reference 24a; and (c, d) courtesy of R. A. Bloodgood.*

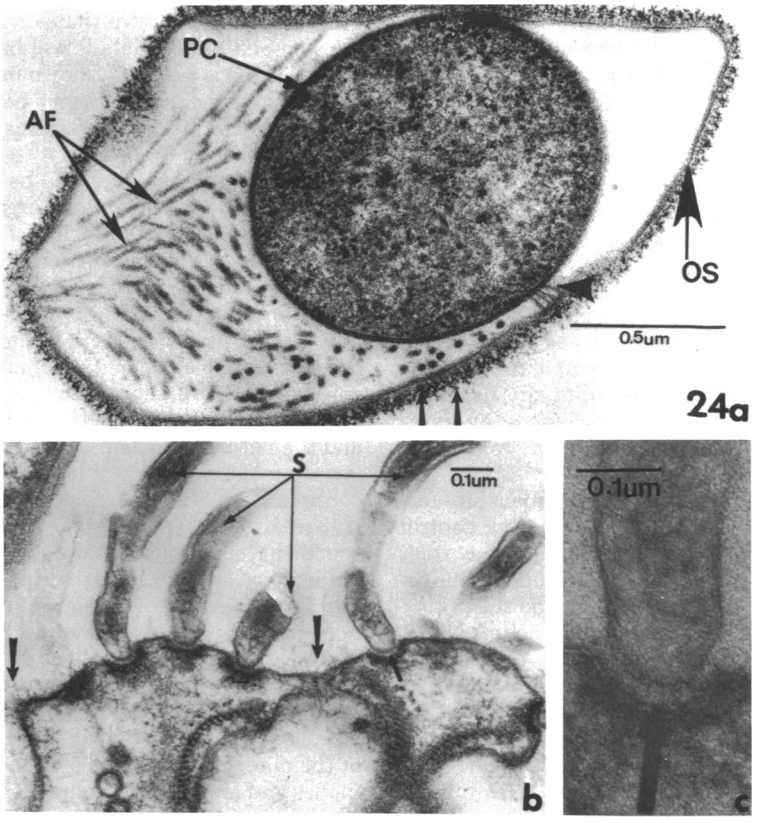

FIG. 24. *Electron micrograph (a) of a transverse section of a large spirochete associated with C. punctulatus. The spirochete contains an outer sheath with attached electron-dense fibers (a, arrows). Numerous axial fibrils are present between the outer sheath and protoplasmic cylinder, which is connected to the outer sheath (large arrow) by several fibers. In (b), four spirochetes are associated with brackets in the cell membrane of the protozoan M. paradoxa; the spirochetes are separated from the protozoan bracket by a slightly electron-opaque fibrous region (b, arrows, a through d [high magnification], c). No terminal specialization is noted in these spirochetes. Osmium fixation, UAC stained. (a) is from reference 75; and (b) from reference 42.*

end of the cell into a cup- or plunger-like structure, together with a series of parallel fibers and disks, is apparent. This flat end of the spirochete attaches to the surface membrane of the protozoan through a series of dense fibers (Fig. 21e and g) and comes to a point of attachment on brackets in the protozoan surface that extended outward from the cell body (Fig. 21i, arrow).

In contrast to the highly differentiated ends of spirochetes found associated with *Pyrsonympha,* the ends of spirochetes associated with *Mixotricha* and *Cryptocercus* appear to be undifferentiated (Fig. 24b). Careful examination of the interface between the plasma membrane of the bracket and the spirochete pole reveals the presence of a densely staining material that, again, may function in cell-cell adhesion (Fig. 24c).

A spirochete of unusual morphology has been observed within the hindguts of *R. flavipes* and *Cryptocercus* (Fig. 23c and d; R. A. Bloodgood, personal communication; reference 212a). This large spirochete is approximately 1 μm in diameter, contains numerous axial fibrils, and is considered by Margulis and Bloodgood (personal communication) to be a member of a new genus, *Pillotina* (89); in contrast to the other free-living and host-associated spirochetes so far examined, these spirochetes have a characteristically wrinkled or crenated outer sheath (Fig. 23d). In longitudinal section (Fig. 23c), the numerous axial fibrils are threadlike. The extensive space between the outer sheath and the protoplasmic cylinder may be a consequence of preparative procedures employed.

Smith et al. (195) have attempted to describe a morphological sequence in the formation of the spirochete attachment site in the polymastigote flagellate of *R. flavipes.* Although a synchronized developmental sequence was not ob-

served, some reconstruction of the sequence of events in attachment site development is possible. The primary event in attachment site formation appears to involve differentiation of localized regions of the flagellate surface (plasma membrane) into surface protrusions. These protrusions enlarge into brackets by the uneven growth of the plasma membrane and result in formation of a raised region, "the mature attachment site." When viewed longitudinally, the attachment site resembles a screw, the head of which projects posteriorly along the flagellate surface, as the screw shaft acts to reinforce the site anteriorly. The attachment sites may be transitory, for they detach from the flagellate surface at random. The actual mode of spirochete recognition of, or attachment to, the attachment site is unknown.

This transitory nature of attachment site formation seems to present an interesting control problem for the protozoan; how do the correct number of sites arise to accommodate the required number of spirochetes? Or do the "sites" arise in response to spirochetal attachment?

Spirochete and attachment site detachment from the flagellate surface is postulated to occur by the formation of vesicles just internal to the attachment site (Fig. 22f and g). The vesicles appear to grow, fuse, and eventually undercut the attachment site, enabling its release from the protozoan surface, perhaps aided by movement or rotation of the attached spirochete.

The presence of these spirochetes on the protozoan surface and within the guts of termites and other animals lends itself to interesting and provocative interpretations regarding function, several of which have been discussed by Breznak (28). So, for example, surface-associated spirochetes may be involved in protozoan motility or as chemoreceptors for scavenging for nutrients. They could also act in tactic phenomena, moving the protozoan out of areas of discomfort or danger. Within the gut, the spirochetes as well as the large number of other microbial types could function in the breakdown of ingested substrates, especially non-metabolizable large molecules, or they could function in nitrogen fixation (28, 30). In this way, energy and macromolecules generated by the spirochetes could be shared or utilized by the host.

CONCLUDING REMARKS

Ultrastructural examination of spirochetes has established their procaryotic nature and the one ultrastructural feature—the axial fibril—that sets them apart from other procaryotes. But organisms of quite different physiological states have been examined, and there is every reason to believe that environmental effects on anatomical details will be important in this group as is regularly shown in other groups. Hence, detailed comparisons possible at this time may not be as realistic as those of the future.

Such comparisons may well be especially significant when host-associated organisms are examined vis-a-vis free-living forms in attempts to discern possible ultrastructural bases and correlates for their respective life styles.

The interrelationship of structure and function may be of profound importance in terms of the localization and chemical characterization of spirochetal LPS, the quality and quantity of enzymes likely present in the periplasmic space, and the nature of the surfaces of the cells' outer layers. In part or in whole, these features undoubtedly play cardinal roles in determining the nature of host-spirochete relationships. The specificity of spirochetal attachment to particular host cells and the potential of spirochetal periplasmic enzymes, for example, to degrade host barriers directly, or of LPSs of differing chemical composition to elicit different host responses, are of obvious import in the ecology of host-associated forms.

A clear understanding of the chemical nature of the outer sheath, its biosynthetic origins, and modes and locales of attachment to the classical gram-negative outer membrane may be instructive in perceiving, again, attachment/invasiveness relationships not only to host cells or to survival in other environments, but also to the mechanisms of spirochetal movements. Structures other than the axial fibrils may have roles in such movements, and thus the nature and activity of the microtubule-like protoplasmic structures, the helical, cytoplasmic, and perimural fibrils, and the sheath itself must be assessed in this vein.

One can be confident, accordingly, that with the basic anatomical details now charted, future scrutinizing of spirochetal structure will be accompanied by enhanced comprehension of organismal function(s) and, hence, the eventual perception of why a given organism occupies a particular habitat.

ACKNOWLEDGMENTS

This work was supported by Public Health Service grants DE 03512 and DE 04383 from the National Institute of Dental Research and by the Research Corporation.

This work could not have been completed without the expert technical assistance of Erika Musante. I am indebted to E. R. Leadbetter for his assistance in bringing this work to completion and to Gloria Holt for her continued interest in my work. Thanks to M. Fenner for the preparation of Fig. 2f, 3, 11d, and 12g.

LITERATURE CITED

1. **Abram, D., and H. Koffler.** 1964. *In vitro* formation of flagella-like filaments and other structures from flagellin. J. Mol. Biol. **9**:168–185.
2. **Abram, D., J. R. Mitchen, H. Koffler, and A. E. Vatter.** 1970. Differentiation within the bacterial flagellum and isolation of the proximal hook. J. Bacteriol. **101**:250–261.
3. **Abram, D., A. E. Vatter, and H. Koffler.** 1966. Attachment and structural features of flagella of certain bacilli. J. Bacteriol. **91**:2045–2068.
4. **Adams, G. A., T. G. Tornabene, and M. Yaguchi.** 1969. Cell wall lipopolysaccharides from *Neisseria catarrhalis*. Can. J. Microbiol. **15**:365–374.
5. **Aeschlimann, A., R. Geigy, and H. Hecker.** 1968. Observations on the ultrastructure of various *Borrelia* species (blood and tissue forms). Acta Trop. **25**:176–181.
6. **Anderson, D. C., and R. C. Johnson.** 1968. Electron microscopy of immune disruption of leptospires: action of complement and lysozyme. J. Bacteriol. **95**:2293–2309.
7. **Auran, N. E., R. C. Johnson, and D. M. Ritzi.** 1972. Isolation of the outer sheath of *Leptospira* and its immunogenic properties in hamsters. Infect. Immun. **5**:968–975.
8. **Azuma, I., T. Taniyama, Y. Yamamura, Y., Yanagihara, Y. Hattori, S. Yasuda, and I. Mifuchi.** 1975. Chemical studies on the cell walls of *Leptospira biflexa* strain Urawa and *Treponema pallidum* strain Reiter. Jpn. J. Microbiol. **19**:45–51.
9. **Babudieri, B.** 1948. Ricerche di microscopia elettronica. III. Studio del genere *Leptospira*. Rend. Ist. Super. Sanita (Ital. Ed.) **11**:1046–1066.
10. **Babudieri, B.** 1958. Die Feinstruktur der leptospiren und anderer Spirochaeten. Zentralbl. Bakteriol. Parasitenkd. Infectionskr. Hyg. Abt. 2 **173**:386–406.
11. **Babudieri, B.** 1960. Die Zellstruktur und die serologie der Leptospiren. Ergeb. Mikrobiol. Immunitaetsforsch. Exp. Ther. **33**:259–306.
12. **Babudieri, B.** 1968. The axistyle of Leptospira. p. 93–114. *In* B. Babudieri (ed.), The fine morphology of spirochaetas. Leonardo Editioni Scientifiche, Rome.
13. **Baker, R. F., and C. G. Loosli.** 1966. The ultrastructure of encapsulated *Diplococcus pneumoniae* type 1 before and after exposure to type specific antibody. Lab. Invest. **15**:716–730.

13a. **Berg, H. C.** 1976. How spirochetes may swim. J. Theor. Biol. **56**:269–273.

14. **Bharier, M., and D. Allis.** 1974. Purification and characterization of axial filaments from *Treponema phagedenis* biotype *Reiterii* (the Reiter treponeme). J. Bacteriol. **120**:1434–1442.
15. **Bharier, M. A., F. A. Eiserling, and S. C. Rittenberg.** 1971. Electron microscopic observations on the structure of *Treponema zuelzerae* and its axial filaments. J. Bacteriol. **105**:413–421.
16. **Bharier, M. A., and S. C. Rittenberg.** 1971. Chemistry of axial filaments of *Treponema zuelzerae*. J. Bacteriol. **105**:422–429.
17. **Bharier, M. A., and S. C. Rittenberg.** 1971. Immobilization effects of anticell and antiaxial filament sera on *Treponema zuelzerae*. J. Bacteriol. **105**:430–437.
18. **Birch-Andersen, A., K. Hovind-Hougen, and C. Borg-Petersen.** 1973. Electron microscopy of *Leptospira*. I. *Leptospira* strain *Pomona*. Acta Pathol. Microbiol. Scand. Sect. B **81**:665–676.
19. **Bladen, H. A., and E. G. Hampp.** 1964. Ultrastructure of *Treponema microdentium* and *Borrelia vincentii*. J. Bacteriol. **87**:1180–1191.
20. **Blakemore, R. P., and E. Canale-Parola.** 1973. Morphological and ecological characteristics of *Spirochaeta plicatilis*. Arch. Mikrobiol. **89**:273–289.
21. **Blakemore, W. F., and D. J. Taylor.** 1970. An agent possibly associated with bovine dysentery. Vet. Rec. **87**:59–60.
22. **Blanquet, P. R.** 1976. Ultrahistochemical study on the ruthenium red surface staining. I. Procèsses which give rise to electron-dense marker. Histochemistry **47**:63–78.
23. **Blanquet, P. R.** 1976. Ultrahistochemical study on the ruthenium red surface staining. II. Nature and affinity of the electron-dense marker. Histochemistry **47**:175–189.
24. **Bloodgood, R. A., K. R. Miller, T. P. Fitzharris, and J. R. McIntosh.** 1974. The ultrastructure of *Pyrsonympha* and its associated microorganisms. J. Morphol. **143**:77–105.

24a. **Bloodgood, R. A., and T. P. Fitzharris.** 1976. Specific associations of prokaryotes with symbiotic flagellate protozoa from the hindgut of the termite *Reticulitermes* and the wood-eating roach *Cryptocercus*. Cytobios **17**:103–122.

25. **Bocciarielli, D. S.** 1968. General methods in e. m. study of spirochaetas and interpretation of the findings, p. 9–25. *In* S. Babudieri (ed.), The fine morphology of spirochaetas. Leonardo Edizioni Scientifiche, Rome.
26. **Bradley, D. E.** 1972. Shortening of *Pseudomonas aeruginosa* pili after RNA phage absorption. J. Gen. Microbiol. **72**:303–319.
27. **Bradley, D. E.** 1966. The structure and infective process of a *Pseudomonas aeruginosa* bacteriophage containing ribonucleic acid. J. Gen. Microbiol. **45**:83–96.
28. **Breznak, J. A.** 1973. Biology of nonpathogenic, host associated spirochetes. CRC Crit. Rev. Microbiol. **2**:457–489.
29. **Breznak, J. A.** 1975. Symbiotic relationships between termites and their intestinal microbiota. Symp. Soc. Exp. Biol. **29**:559–580.
30. **Breznak, J. A., W. J. Brill, J. W. Mertins, and H. C. Coppel.** 1973. Nitrogen fixation in termites. Nature (London) **244**:577–580.
31. **Breznak, J. A., and E. Canale-Parola.** 1969. *Spirochaeta aurantia*, a pigmented, facultatively anaerobic spirochete. J. Bacteriol.

97:386-395.

32. **Brinton, C. C.** 1965. The structure, function, synthesis and genetic control of the bacterial pilus and a molecular model for DNA and RNA transport in gram negative bacteria. Trans. N.Y. Acad. Sci. **27**:1003-1054.
33. **Bryant, M. P.** 1952. The isolation and characteristics of a spirochete from the bovine rumen. J. Bacteriol. **64**:325-335.
34. **Canale-Parola, E., Z. Udris, and M. Mandel.** 1968. The classification of free-living spirochetes. Arch. Mikrobiol. **63**:385-397.
35. **Chang, J. Y., D. M. Brown, and A. N. Glazer.** 1969. Characterization of the subunits of the flagella of *Proteus vulgaris*. J. Biol. Chem. **244**:5196-5200.
36. **Chang, A., and S. Faine.** 1970. Electron microscopic evidence for reactions of axial filaments of *Leptospira* with IgM and IgG antibodies. Bull. W.H.O. **43**:571-577.
37. **Cheng, K.-J., and J. W. Costerton.** 1973. Localization of alkaline phosphatase in three gram-negative rumen bacteria. J. Bacteriol. **116**:424-446.
38. **Cheng, K.-J., J. M. Ingram, and J. W. Costerton.** 1970. Alkaline phosphatase localization and spheroplast formation of *Pseudomonas aeruginosa*. Can. J. Microbiol. **16**:1319-1324.
39. **Christiansen, A. H.** 1962. Studies on the antigenic structure of *Treponema pallidum*. II. Isolation and purification of polysaccharides from Reiter's pathogenic strain. Acta Pathol. Microbiol. Scand. **56**:166-176.
40. **Clark, H. F.** 1964. Suckling mouse cataract agent. J. Infect. Dis. **114**:476-487.
41. **Clark, H. F., and D. T. Karzon.** 1969. Growth curve studies of the suckling mouse cataract agent in individual compartments of the eye. Proc. Soc. Exp. Biol. Med. **131**:693-696.
42. **Cleveland, L. R., and A. V. Grimstone.** 1964. The fine structure of the flagellate *Mixotricha paradoxa*. Proc. R. Soc. London Ser. B **159**:668-686.
43. **Cohen-Bazire, G., and J. London.** 1967. Basal organelles of bacterial flagella. J. Bacteriol. **94**:458-465.
44. **Costerton, J. W., J. M. Ingram, and K.-J. Cheng.** 1974. Structure and function of the cell envelope of gram-negative bacteria. Bacteriol. Rev. **38**:87-110.
45. **Cox, C. D.** 1972. Shape of *Treponema pallidum*. J. Bacteriol. **109**:943-944.
46. **Czekalowski, J. W.** 1960. Leptospirae and leptospirosis in man and animals. Infl. Symp. Lublin, Poland, December 1958. *In* The problem sessions series of the Polish Academy of Science **19**:22.
47. **Czekalowski, J. W.** 1963. Electron microscope study of *Leptospira*. Antonie van Leeuwenhoek J. Microbiol. Serol. **29**:29-34.
48. **Czekalowski, J. W.** 1968. Staining with heavy metals for e.m. of *leptospirae*, p. 27-58. *In* B. Babudieri (ed.), The fine morphology of spirochaetas. Leonardo Edizioni Scientifiche, Rome.
49. **Czekalowski, J. W., and G. Eaves.** 1955. The structure of leptospirae as revealed by electron microscopy. J. Pathol. Bacteriol. **69**:129-132.
50. **D'Alessandro, G., and C. del Carpio.** 1958. A lipopolysaccharide antigen of the *Treponema*. Nature (London) **181**:991-992.
51. **Davis, C. P., D. Mulcahy, A. Takeuchi, and D. C. Savage.** 1972. Location and description of spiral-shaped microorganisms in the normal rat cecum. Infect. Immun. **6**:184-192.
52. **Davis, R. E., and J. F. Worley.** 1973. *Spiroplasma*: motile, helical microorganism associated with corn stunt disease. Phytopathology **63**:403-408.
53. **Davis, R. E., J. F. Worley, R. F. Whitcomb, T. Ishijima, and R. L. Steere.** 1972. Helical filaments produced by a mycoplasma-like organism associated with corn stunt disease. Science **176**:521-523.
54. **DeBrujin, J. H.** 1959. Investigations into the antigenic structure of the Reiter strain of *Treponema pallidum*. II. The complex nature of the protein fraction. Antonie van Leeuwenhoek J. Microbiol. Serol. **25**:41-45.
55. **DePamphilis, M. L., and J. Adler.** 1971. Fine structure and isolation of the hook-basal body complex of flagella from *Escherichia coli* and *Bacillus subtilis*. J. Bacteriol. **105**:384-395.
56. **Dobell, C.** 1912. Researches on the spirochaetas and related organisms. Arch. Protistenkd. **26**:117-240.
57. **Dobell, C.** 1932. Antony van Leeuwenhoek and his "little animals," p. 217-255. Harcourt Brace & Co, New York.
58. **Drusin, L. M., G. C. Rouiller, and G. B. Chapman.** 1969. Electron microscopy of *Treponema pallidum* occurring in a human primary lesion. J. Bacteriol. **97**:951-955.
59. **Eipert, S. R., and S. H. Black.** 1976. The cytoplasmic fibrils of *Treponema refringens*. I. Isolation and ultrastructure of the fibrils. Arch. Microbiol. In press.
60. **Eipert, S. R., and S. H. Black.** 1976. The cytoplasmic fibrils of *Treponema refringens*. II. Relationship of the fibrils to the helical shape of the cell and the association of the fibrils with DNA. Arch. Microbiol. In press.
61. **Elizan, T. S., A. Fabryi, and H. F. Clark.** 1972. Suckling mouse cataract agent (SMCA)-induced hydrocephalus and chronic brain infection in newborn rats. Proc. Soc. Exp. Biol. Med. **139**:51-55.
62. **Engleman, D. M., and H. J. Morowitz.** 1968. Characterization of the plasma membrane of *Mycoplasma laidlawii*. IV. Structure and composition of membrane and aggregated components. Biochim. Biophys. Acta **150**:385-396.
63. **Erlandsen, S. L., and D. G. Chase.** 1972. Paneth cell function: phagocytosis and intracellular digestion of intestinal microorganisms. I. Hexamita muris. J. Ultrastr. Res. **41**:296-318.
64. **Erlandsen, S. L., and D. G. Chase.** 1972. Paneth cell function: phagocytosis and intracellular digestion of intestinal microorganisms. II. Spiral microorganism. J. Ultrastruct. Res.

41:319-333.
65. **Espinasse, J., and P. Redon.** 1970. The control of swine dysentery. Vet. Rec. **86**:24.
66. **Finco, D. R., and D. G. Low.** 1967. Endotoxin properties of *Leptospira canicola*. Am. J. Vet. Res. **28**:1863-1872.
67. **Fox, E. N.** 1974. M proteins of group A streptococci. Bacteriol. Rev. **38**:57-86.
68. **Gear, E. V., and W. O. Dobbins.** 1968. Rectal biopsy. A review of its diagnostic usefulness. Gastroenterology **55**:522-543.
69. **Gibbons, R. J., and J. van Houte.** 1975. Bacterial adherence in oral microbial ecology. Annu. Rev. Microbiol. **29**:19-44.
70. **Ginger, C. D.** 1963. Isolation and characterization of muramic acid from two spirochaetes: *Borrelia duttoni* and *Leptospira biflexa*. Nature (London) **199**:159.
71. **Glauert, A. M.** 1974. Practical methods in electron microscopy, vol. 3. North Holland Publishing Co., Amsterdam.
72. **Glauert, A. M., and J. A. Lucy.** 1969. Electron microscopy of lipids: effects of pH and fixatives on the appearance of a macromolecular assembly of lipid micelles in negatively stained preparations. J. Microsc. **89**:1-18.
73. **Glock, R. D., and D. L. Harris.** 1972. Swine dysentery. II. Characterization of lesions in pigs inoculated with *Treponema hyodysenteriae* in pure and mixed culture. Vet. Med. Small Anim. Clin. **67**:65-68.
74. **Glock, R. D., D. L. Harris, and J. P. Kluge.** 1974. Localization of spirochetes with the structural characteristics of *Treponema hyodysenteriae* in the lesions of swine dysentery. Infect. Immun. **9**:167-178.
75. **Grimstone, A. V.** 1963. A note on the fine structure of a spirochete. Q. J. Microsc. Sci. **104**:145-153.
76. **Habeeb, A. F. S. A., and R. Hiramoto.** 1968. Reactions of proteins with glutaraldehyde. Arch. Biochem. Biophys. **126**:16-26.
77. **Hamdy, A. J., and M. W. Glenn.** 1974. Transmission of swine dysentery with *Treponema hyodysenteriae* and *Vibrio coli*. Am. J. Vet. Res. **35**:791-797.
78. **Hanson, L. E., D. N. Tripathy, L. B. Evans, and A. D. Alexander.** 1974. An unusual leptospira, serotype *illini* (a new serotype). Int. J. Syst. Bacteriol. **24**:355-357.
79. **Hardy, P. H., W. R. Fredericks, and E. E. Nell.** 1975. Isolation and antigenic characteristics of axial filaments from the Reiter treponeme. Infect. Immun. **11**:380-386.
80. **Hardy, P. H., Y. C. Lee, and E. E. Nell.** 1964. Use of a bacterial culture filtrate as an aid to the isolation and growth of anaerobic spirochetes. J. Bacteriol. **87**:1521-1525.
81. **Hardy, P. H., and E. E. Nell.** 1957. Study of the antigenic structure of *T. pallidum* by specific agglutination. Am. J. Hyg. **66**:160-172.
82. **Harland, W. A., and F. D. Lee.** 1967. Intestinal spirochaetosis. Br. Med. J. **2**:718-719.
83. **Harris, D. L., R. D. Glock, C. R. Christensen, and J. M. Kinyon.** 1972. Swine dysentery. I. Inoculation of pigs with *Treponema hyodysenteriae* (new species) and reproduction of the disease. Vet. Med. Small Anim. Clin. **67**:61-64.
84. **Harris, D. L., R. D. Glock, and J. M. Kinyon.** 1976. Intestinal treponematoses, p. 277-293. *In* R. C. Johnson (ed.), The biology of parasitic spirochetes. Academic Press, Inc., New York.
85. **Harris, D. L., J. M. Kinyon, M. T. Mullin, and R. D. Glock.** 1972. Isolation and propagation of spirochetes from the colon of swine dysentery affected pigs. Can. J. Comp. Med. **36**:74-76.
86. **Heppel, L. A.** 1967. Selective release of enzymes from bacteria. Science **156**:1451-1455.
87. **Heppel, L. A.** 1969. The effect of osmotic shock on release of bacterial proteins and on active transport. J. Gen. Physiol. **54**:95-109.
88. **Hespell, R. B., and E. Canale-Parola.** 1970. *Spirochaeta litoralis* sp. n., a strictly anaerobic marine spirochete. Arch. Mikrobiol. **74**:1-18.
89. **Hollande, A., and I. Gharagozlou.** 1967. Morphologie infra structurale de *Pillotina calotermitidis*, nov. gen., nov. sp., spirochaetale de l'intestin de *Calotermes praecox*. C. R. Acad. Sci. **265**:1309-1313.
90. **Holt, S. C., and E. Canale-Parola.** 1968. Fine structure of *Spirochaeta stenostrepta*, a free-living, anaerobic spirochete. J. Bacteriol. **96**:822-835.
91. **Horne, R. W.** 1967. The examination of small particles, p. 311-327. *In* D. Kay (ed.), Techniques for electron microscopy. Blackwell Scientific Publishers, Oxford.
92. **Horne, R. W.** 1967. Negative staining methods, p. 328-355. *In* D. Kay (ed.), Techniques for electron microscopy. Blackwell Scientific Publishers, Oxford.
93. **Hovind-Hougen, K.** 1972. Further observations on the ultrastructure of *Treponema pallidum* Nichols. Acta Pathol. Microbiol. Scand. Sect. B **80**:297-304.
94. **Hovind-Hougen, K.** 1974. Electron microscopy of *Borrelia merionesi* and *Borrelia recurrentis*. Acta Pathol. Microbiol. Scand. Sect. B **82**:799-809.
95. **Hovind-Hougen, K.** 1974. The ultrastructure of cultivable treponemes. I. *Treponema phagedenis, Treponema vincentii* and *Treponema refringens*. Acta Pathol. Microbiol. Scand. Sect. B **82**:329-344.
96. **Hovind-Hougen, K.** 1974. The ultrastructure of cultivable treponemes. II. *Treponema calligyrum, Treponema minutum* and *Treponema microdentium*. Acta Pathol. Microbiol. Scand. Sect. B **82**:495-507.
97. **Hovind-Hougen, K.** 1975. The ultrastructure of cultivable treponemes. III. *Treponema genitalis*. Acta Pathol. Microbiol. Scand. Sect. B **83**:91-99.
98. **Hovind-Hougen, K.** 1976. Determination by means of electron microscopy of morphological criteria of value for classification of some spirochetes, in particular treponemes. Acta Pathol. Microbiol. Scand. Sect. B **255** (Suppl.): 1-41.

99. **Hovind-Hougen, K., and A. Birch-Andersen.** 1971. Electron microscopy of endoflagella and microtubules in *Treponema* Reiter. Acta Pathol. Microbiol. Scand. Sect. B **79**:37-50.
100. **Hovind-Hougen, K., A. Birch-Andersen, and J.-J. Skovgaard Jensen.** 1973. Electron microscopy of *Treponema cuniculi*. Acta Pathol. Microbiol. Scand. Sect. B **81**:15-26.
101. **Hovind-Hougen, K., A. Birch-Andersen, and H.-J. Skovgaard Jensen.** 1976. Ultrastructure of cells of *Treponema pertenue* obtained from experimentally infected hamsters. Acta Pathol. Microbiol. Scand. Sect. B **84**:101-108.
102. **Hughes, R., H. J. Olander, and C. B. Williams.** 1975. Swine dysentery: pathogenicity of *Treponema hyodysenteriae*. Am. J. Vet. Res. **36**:971-977.
103. **Hungate, R. E.** 1966. The rumen and its microbes. Academic Press, Inc., New York.
104. **Iino, T.** 1969. Genetics and chemistry of bacterial flagella. Bacteriol. Rev. **33**:454-475.
105. **Jackson, S., and S. H. Black.** 1971. Ultrastructure of *Treponema pallidum* Nichols following lysis by physical and chemical methods. I. Envelope, wall, membrane and fibrils. Arch. Mikrobiol. **76**:308-324.
106. **Jackson, S., and S. H. Black.** 1971. Ultrastructure of *Treponema pallidum* Nichols following lysis by physical and chemical methods. II. Axial filaments. Arch. Mikrobiol. **76**:325-340.
107. **Jackson, S. W., and P. N. Zey.** 1973. Ultrastructure of lipopolysaccharide isolated from *Treponema pallidum*. J. Bacteriol. **114**:838-844.
108. **Jepsen, O. B., K. Hovind-Hougen, and A. Birch-Andersen.** 1968. Electron microscopy of *Treponema pallidum* Nichols. Acta Pathol. Microbiol. Scand. **74**:241-258.
109. **Johnson, R. C., D. M. Ritzi, and B. P. Livermore.** 1973. Outer envelope of virulent *Treponema pallidum*. Infect. Immun. **8**:291-295.
110. **Johnson, R. C., M. S. Wachter, and D. M. Ritzi.** 1973. Treponeme outer cell envelope: solubilization and reaggregation. Infect. Immun. **7**:249-258.
111. **Jones, R. H., T. A. Nevin, W. J. Guest, and L. C. Logan.** 1968. Lytic effect of trypsin, lysozyme and complement of *Treponema pallidum*. Br. J. Vener. Dis. **44**:193-200.
112. **Jones, A. M., J. A. Zeigler, and R. H. Jones.** 1976. Experimental syphilis vaccines in rabbits. I. Differential protection with an adjuvant spectrum. Br. J. Vener. Dis. **52**:9-17.
113. **Joseph, R., and E. Canale-Parola.** 1972. Axial fibrils of anaerobic spirochetes: ultrastructure and chemical characteristics. Arch. Mikrobiol. **81**:146-168.
114. **Joseph, R., S. C. Holt, and E. Canale-Parola.** 1973. Peptidoglycan of free-living anaerobic spirochetes. J. Bacteriol. **115**:426-435.
115. **Katz, L. N., N. D. Konstantinova, and A. A. Ananyin.** 1968. Some features of submicroscopic structure of the cytoplasmic cylinder in leptospirae. Zh. Mikrobiol. Epidemiol. Immunobiol. **45**:64-67.
116. **Kawata, T.** 1957. Electron microscopic studies on the cellular structure of Reiter spirochete. Nippon Saikingaku Zasshi **11**:547-560.
117. **Kawata, T., and T. Inoue.** 1964. Fine structure of the Reiter treponeme as revealed by electron microscopy using thin sectioning and negative staining techniques. Nippon Saikingaku Zasshi **8**:49-65.
118. **Kellenberger, E., A. Ryter, and J. Séchaud.** 1958. Electron microscopy of DNA-containing plasms. II. Vegetative and mature phage DNA compared with normal bacterial nucleoids in different physiological states. J. Biophys. Biochem. Cytol. **4**:671-675.
119. **Klingmüller, G., Y. Ishibashi, and K. Radke.** 1968. Der elektronenikroskopische Aufbau des *Treponema pallidum*. Arch. Klin. Exp. Dermatol. **233**:197-205.
120. **Kolenbrander, P. E., and J. C. Ensign.** 1968. Isolation and chemical structure of the peptidoglycan of *Spirillum serpens* cell walls. J. Bacteriol. **95**:201-210.
121. **Kondo, E., and N. Ueta.** 1972. Composition of fatty acids and carbohydrates in *Leptospira*. J. Bacteriol. **110**:459-467.
122. **Lataste-Dorolle, C. L.** 1968. Structure and nature of the membrane of *Treponemes*, p. 59-62. *In* B. Babudieri (ed.), The fine morphology of spirochaetas. Leonardo Edizioni Scientifiche, Rome.
123. **Lauderdale, V., and J. N. Goldman.** 1972. Serial ultrathin sectioning demonstrating the intracellularity of *T. pallidum*. An electron microscopic study. Br. J. Vener. Dis. **48**:87-97.
124. **Leach, W. D., A. Lee, and R. P. Stubbs.** 1973. Localization of bacteria in the gastrointestinal tract: a possible explanation of intestinal spirochaetosis. Infect. Immun. **7**:961-972.
125. **Lee, F. D., A. Kraszewski, J. Gordan, J. G. R. Howie, D. McSeveney, and W. A. Hanlard.** 1971. Intestinal spirochaetosis. Gut **12**:126-133.
126. **Leibowitz, P. J., and M. Schaechter.** 1975. The attachment of the bacterial chromosome to the cell membrane. Int. Rev. Cytol. **41**:1-28.
127. **Lewin, R. A.** 1963. Rod-shaped particles in *Saprospira*. Nature (London) **198**:103-104.
128. **Listgarten, M. A., and S. S. Socransky.** 1964. Electron microscopy of axial fibrils, outer envelope, and cell division of certain oral spirochetes. J. Bacteriol. **88**:1087-1103.
129. **Listgarten, M. A., and S. S. Socransky.** 1965. Electron microscopy as an aid in the taxonomic differentiation of oral spirochetes. Arch. Oral Biol. **10**:127-138.
130. **Loesche, W. J.** 1968. Importance of nutrition of gingival crevice microbial ecology. Periodontics **6**:245-249.
131. **Lopes, J., and W. E. Inniss.** 1970. Electron microscopic study of lipopolysaccharide from an avian strain of *Escherichia coli* O18. J. Bacteriol. **103**:238-243.
132. **Luft, J. H.** 1966. Fine structure of capillary and endocapillary layer as revealed by ruthenium red. Fed. Proc. Fed. Am. Soc. Exp.

25:1773–1783.

133. **Luft, J. H.** 1971. Ruthenium red and violet. I. Chemistry, purification, methods of use for electron microscopy and mechanism of action. Anat. Rec. **171**:347–368.
134. **Magerstedt, C.** 1944. Ein Beitrag zur Morphologie der Syphilis spirochäete. Dermatol. Z. **185**:272–280.
135. **Mandelstam, J.** 1962. Preparation and properties of the mucopeptides of cell walls of gram-negative bacteria. Biochem. J. **84**:294–299.
136. **Martin, H. H., and H. Frank.** 1962. Die Mucopeptid-Grundstrucktur in der Zellwand Gram-Negativer Bakterien. Zentralbl. Bakteriol. Parasitenkd. Abt. 1 Orig. **184**:306–311.
137. **Martin, H. H., H. D. Heilmann, and H. J. Preusser.** 1972. State of the rigid-layer in cell walls of some gram-negative bacteria. Arch. Mikrobiol. **83**:332–346.
138. **Martinez, R. J., D. M. Brown, and A. N. Glazer.** 1967. The formation of bacterial flagella. III. Characterization of the subunits of the flagella of *Bacillus subtilis* and *Spirillum serpens*. J. Mol. Biol. **28**:45–51.
139. **Martinez, R. J., and E. Rosenberg.** 1964. Thermal transition of *Spirillum serpens* flagella. J. Mol. Biol. **8**:702–707.
140. **Miller, N. G., and R. B. Wilson.** 1962. *In vivo* and *in vitro* observation of *Leptospira pomona* by electron microscopy. J. Bacteriol. **84**:569.
141. **Minio, F., G. Tonietti, and A. Torsoli.** 1973. Spontaneous spirochete infestation in the colonic mucosa of healthy men. Rend. Gastroenterol. **5**:183–195.
142. **Mölbert, E.** 1956. Elektonenmikroskopischer Beitrag zur Morphologie des Bewegundsapparates von Borrelien. Z. Hyg. **142**:203–212.
143. **Morton, H. E., and T. F. Anderson.** 1942. Observations on the morphology of *leptospira* and the Nichols' strain of *Treponema pallidum* with the aid of the RCA electron microscope. J. Bacteriol. **43**:64–65.
144. **Morton, H. E., and T. F. Anderson.** 1942. Some morphological features of the Nichols' strain of *Treponema pallidum* as revealed by the electron microscope. Am. J. Syph. Gonorrhea Vener. Dis. **26**:565–573.
145. **Mudd, S., K. Polevitzky, and T. F. Anderson.** 1943. Bacterial morphology as shown by the electron microscope. V. *Treponema pallidum, T. macrodentium,* and *T. microdentium*. J. Bacteriol. **46**:15–24.
146. **Murray, R. G. E., and A. Birch-Andersen.** 1963. Specialized structure in the region of the flagella tuft in *Spirillum serpens*. Can. J. Microbiol. **9**:393–401.
147. **Nauman, R. K., S. C. Holt, and C. D. Cox.** 1969. Purification, ultrastructure and composition of axial filaments from *Leptospira*. J. Bacteriol. **98**:264–280.
148. **Neu, H. C., and L. A. Heppel.** 1965. The release of enzymes from *Escherichia coli* by osmotic shock and during the formation of spheroplasts. J. Biol. Chem. **240**:3685–3692.
149. **Nevin, T. A., E. G. Hampp, and B. V. Duey.** 1960. Interaction between *Borrelia vincentii* and an oral diphtheroid. J. Bacteriol. **80**:783–786.
150. **Noguchi, H.** 1928. The spirochetes. The University of Chicago Press, Chicago.
151. **Oishi, K., and D. F. Poulson.** 1970. A virus associated with SR-spirochetes of *Drosophila nebulosa*. Proc. Natl. Acad. Sci. U.S.A. **67**:1565–1572.
152. **Ovcinnikov, N. M., and V. V. Delektorskij.** 1966. Morphology of *Treponema pallidum*. Bull. W.H.O. **35**:223–229.
153. **Ovcinnikov, N. M., and V. V. Delektorskij.** 1968. Further study of ultrathin sections of *Treponema pallidum* under the electron microscope. Br. J. Vener. Dis. **44**:1–34.
154. **Ovcinnikov, N. M., and V. V. Delektorskij.** 1969. Further studies of the morphology of *Treponema pallidum* under the electron microscope. Br. J. Vener. Dis. **45**:87–116.
155. **Ovcinnikov, N. M., and V. V. Delektorskij.** 1970. *Treponema pertenue* under the electron microscope. Br. J. Vener. Dis. **46**:349–379.
156. **Ovcinnikov, N. M., and V. V. Delektorskij.** 1975. *Treponema pallidum* in nerve fibres. Br. J. Vener. Dis. **51**:10–18.
157. **Palit, A., R. C. Hamilton, and J. Gulasekharam.** 1974. Further studies on leptospiral genus-specific antigen: its ultrastructure and immunochemistry. J. Gen. Microbiol. **82**:223–236.
158. **Pate, J. L., and E. J. Ordal.** 1967. The fine structure of *Chondrococcus columnaris*. III. The surface layers of *Chondrococcus columnaris*. J. Cell Biol. **35**:37–50.
159. **Pillot, J., and P. Dupouey.** 1964. Composition antigenique de treponemes. IV. Solubilisation et purification des antigens polyosidiques du *Treponeme* Reiter. Ann. Inst. Pasteur (Paris) **106**:456–468.
160. **Pillot, J., and A. Ryter.** 1965. Structure des spirochetes. I. Etude des genres *Treponema, Borrelia* et *Leptospira* au microscope electronique. Ann. Inst. Pasteur (Paris) **108**:791–804.
161. **Poulson, D. F., and B. Sakaguchi.** 1961. Nature of "sex-ratio" agent in *Drosophila*. Science **133**:1489–1490.
162. **Prokopchuk, A. Y., V. A. Prokopchuk, and A. G. Bondarovitch.** 1951. Causative agents of skin and venereal diseases as they appear in the electron microscope. Observation I. *Spirocheta pallida* as it appears in the electron microscope. Vestn. Dermatol. Venerol. **3**:20–23.
163. **Reichle, R. E., and R. A. Lewin.** 1968. Purification and structure of rhapidosomes. Can. J. Microbiol. **14**:211–213.
164. **Ritchie, A. E.** 1968. A brief consideration of anatomic features of the spirochaetas as revealed by e.m., p. 77–92. *In* B. Babudieri (ed.), The fine morphology of spirochaetas. Leonardo Edizioni Scientifiche, Rome.
165. **Ritchie, A. E.** 1976. Morphology of leptospires, p. 19–37. *In* R. C. Johnson (ed.), The biology of parasitic spirochetes. Academic Press, Inc.,

New York.
166. **Ritchie, A. E., and L. N. Brown.** 1971. An agent possibly associated with swine dysentery. Vet. Rec. **89**:608–609.
167. **Ritchie, A. E., and H. C. Ellinghausen.** 1965. Electron microscopy of leptospires. I. Anatomical features of *Leptospira pomona*. J. Bacteriol. **89**:223–233.
168. **Roberts, R. M., and J. R. Simmons.** 1970. An agent possibly associated with swine dysentery. Vet. Rec. **86**:22.
169. **Robertson, J. D.** 1959. The ultrastructure of cell membranes and their derivatives. Symp. Biochem. Soc. **16**:3.
170. **Rosebury, T.** 1962. Microorganisms indigenous to man. McGraw-Hill, New York.
171. **Rosenfelder, G., O. Lüderitz, and O. Westphal.** 1974. Composition of lipopolysaccharides from *Myxococcus fulvus* and other fruiting and nonfruiting myxobacteria. Eur. J. Biochem. **44**:411–420.
172. **Rothstein, N., and C. W. Hiatt.** 1956. Studies of the immunochemistry of leptospires. J. Immunol. **79**:276–280.
173. **Ryter, A., and J. Pillot.** 1963. Etude au microscope electronique de la structure externe et interne du *Treponema Reiter*. Ann. Inst. Pasteur (Paris) **104**:486–501.
174. **Ryter, A., and J. Pillot.** 1965. Structure des spirochetes. II. Etude du genre *Cristispira* au microscope optique et au microscope electronique. Ann. Inst. Pasteur (Paris) **109**:552–562.
175. **Saglio, P., M. Lhospital, D. Lafleche, G. Dupont, J. M. Bove, J. G. Tully, and E. A. Freundt.** 1973. *Spiroplasma citri* gen. and sp. n.: a mycoplasma-like organism associated with "stubborn" disease of citrus. Int. J. Syst. Bacteriol. **23**:191–204.
176. **Saheb, S. A., and L. Berthliaume.** 1973. Etude au microscope electronique d'un spirochete isole du porc. Rev. Can. Biol. **32**:3–9.
177. **Sakaguchi, B., K. Oishi, and S. Kobayashi.** 1965. Interference between "sex-ratio" agents of *Drosophila willistoni* and *Drosophila nebulosa*. Science **147**:160–162.
178. **Salton, M. R. J.** 1964. Physico-chemical properties and chemical composition of walls, p. 92–132. *In* Bacterial cell wall. Elsevier Publishing Co., New York.
179. **Salton, M. R. J.** 1967. Structure and function of bacterial cell membranes. Annu. Rev. Microbiol. **21**:413–442.
180. **Savage, D. C.** 1969. Localization of certain indigenous microorganisms on the ileal villi of rats. J. Bacteriol. **97**:1505–1506.
181. **Savage, D. C.** 1970. Associations of indigenous microorganisms with gastrointestinal mucosal epithelia. Am. J. Clin. Nutr. **23**:1495–1501.
182. **Savage, D. C., and R. V. H. Blumershine.** 1974. Surface-surface associations in microbial communities populating epithelial habitats in the murine gastrointestinal ecosystem: scanning electron microscopy. Infect. Immun. **10**:240–250.
183. **Savage, D. C., R. Dubos, and R. W. Schaedler.** 1967. The gastrointestinal epithelium and its autochthonous bacterial flora. J. Exp. Med. **127**:67–76.
184. **Savage, D. C., J. S. McAllister, and C. P. Davis.** 1971. Anaerobic bacteria on the mucosal epithelium of the murine large bowel. Infect. Immun. **4**:492–502.
185. **Schleiffer, K. H., and R. Joseph.** 1973. A directly cross-linked L-ornithine-containing peptidoglycan in cell walls of *Spirochaeta stenostrepta*. FEBS Lett. **36**:83–86.
186. **Schneider, M. D.** 1954. Isolation and chemical composition of complement-fixing antigens from leptospires. Proc. Soc. Exp. Biol. Med. **85**:32–37.
187. **Schricker, R. L., and L. E. Hanson.** 1963. Precipitating antigens of leptospires. I. Chemical properties and serological activity of soluble fractions of *Leptospira pomona*. Am. J. Vet. Res. **24**:854–860.
188. **Sequeira, P. J. L.** 1956. The morphology of *Treponema pallidum*. Lancet **ii**:749.
189. **Shands, J. W., Jr.** 1971. The physical structure of bacterial lipopolysaccharides, p. 127–144. *In* G. Weinbaum, S. Kadis, and S. J. Ajl (ed.), Microbial toxins: bacterial endotoxins, vol. 4. Academic Press, Inc., New York.
190. **Shinagawa, M., and R. Yanagawa.** 1972. Isolation and characterization of a leptospiral type-specific antigen. Infect. Immun. **5**:12–19.
191. **Simpson, C. F., and F. H. White.** 1961. Electron microscope studies and staining reactions of leptospires. J. Infect. Dis. **109**:243–250.
192. **Smibert, R. M.** 1973. Spirochaetales, a review. CRC Crit. Rev. Microbiol. **2**:491–552.
193. **Smibert, R. M.** 1974. The spirochetes, p. 167–194. *In* R. E. Buchanan and N. E. Gibbons (ed.), Bergey's manual of determinative bacteriology, 8th ed. The Williams and Wilkins Co., Baltimore.
194. **Smith, H. E., and H. J. Arnott.** 1974. Epi- and endobiotic bacteria associated with *Pyrsonympha vertens*, a symbiotic protozoon of the termite *Reticulitermes flavipes*. Trans. Am. Microsc. Soc. **93**:180–194.
195. **Smith, H. E., H. E. Buhse, Jr., and S. J. Stamler.** 1975. Possible formation and development of spirochaete attachment sites found on the surface of symbiotic polymastigote flagellates of the termite *Reticulitermes flavipes*. Biosystems **7**:374–379.
196. **Socransky, S. S.** 1970. Relationship of bacteria to the etiology of periodontal disease. J. Dent. Res. **49**:203–222.
197. **Socransky, S. S., R. J. Gibbons, A. C. Dale, L. Bortwick, E. Rosenthal, and J. B. Macdonald.** 1963. The microbiota of the gingival crevice area of man. I. Total microscopic and viable counts on specific organisms. Arch. Oral Biol. **8**:275–280.
198. **Socransky, S. S., W. J. Loesche, C. Hubersak, and J. B. Macdonald.** 1964. Dependency of *Treponema microdentium* on other oral organisms for isobutyrate, polyamines, and a controlled oxidation-reduction potential. J. Bac-

teriol. **88**:200–209.

199. **Springer, L., and I. C. Roth.** 1973. The ultrastructure of the capsules of *Diplococcus pneumoniae* and *Klebsiella pneumoniae* stained with ruthenium red. J. Gen. Microbiol. **74**:21–31.
200. **Stead, A., J. S. Main, M. E. Ward, and P. J. Watt.** 1975. Studies on lipopolysaccharides isolated from strains of *Neisseria gonorrhoeae*. J. Gen. Microbiol. **88**:123–131.
201. **Swain, R. H. A., and N. Anderson.** 1972. The ultrastructure of species of treponemas and borreliae, p. 115–139. *In* B. Babudieri (ed.), The fine morphology of spirochaetas. Leonardo Edizioni Scientifiche, Rome.
202. **Swanson, J., S. J. Kraus, and E. C. Gotschlich.** 1971. Studies on gonococcus infection. I. Pili zones of adhesion: their relation to gonococcal growth patterns. J. Exp. Med. **134**:886–906.
203. **Sykes, J. A., and J. Kalan.** 1975. Intracellular *Treponema pallidum* in cells of a syphilitic lesion of the uterine cervix. Am. J. Obstet. Gynecol. **122**:361–367.
204. **Sykes, J. A., and J. N. Miller.** 1971. Intracellular location of *Treponema pallidum* (Nichols strain) in the rabbit testis. Infect. Immun. **4**:307–314.
205. **Sykes, J. A., and J. N. Miller.** 1973. Ultrastructural studies of treponemes: location of axial filaments and some dimensions of *Treponema pallidum* (Nichols strain), *Treponema denticola*, and *Treponema reiteri*. Infect. Immun. **7**:100–110.
206. **Sykes, J. A., J. N. Miller, and A. J. Galan.** 1924. *Treponema pallidum* within cells of a primary chancre from a human female. J. Vener. Dis. **50**:40–44.
207. **Takeuchi, A., and J. A. Zeller.** 1972. Scanning electron microscopic observations on the surface of the normal and spirochete infested colonic mucosa of the rhesus monkey. J. Ultrastruct. Res. **40**:313–324.
208. **Takeuchi, A., and J. A. Zeller.** 1972. Ultrastructural identification of spirochetes and flagellated microbes at the brush border of the large intestinal epithelium of the rhesus monkey. Infect. Immun. **6**:1008–1018.
209. **Takeya, K., R. Morei, and T. Toda.** 1957. Studies on the structure of leptospira as revealed by electron microscopy. Jpn. J. Microbiol. **1**:99–104.
210. **Taylor, D. J.** 1970. An agent possibly associated with swine dysentery. Vet. Rec. **86**:416.
211. **Taylor, D. J., and W. F. Blakemore.** 1971. Spirochaetal invasion of the colonic epithelium of swine dysentery. Res. Vet. Sci. **12**:177–179.
212. **Tinelli, R., and J. Pillot.** 1966. Etude de la composition du glycopeptide de *Treponema reiteri*. C. R. Acad. Sci. (Paris) **263**:739–741.

212a. **To, L., L. Margulis, and A. T. W. Cheung.** 1978. *Pillotinas* and *Hollandinas*: distribution and behaviour of large spirochaetes symbiotic in termites. Proc. R. Soc. London Ser. B. In press.

213. **Todd, J. N., D. Hunter, and A. Clark.** 1970. An agent possibly associated with swine dysentery. Vet. Rec. **86**:228.
214. **Toner, P. G., K. E. Carr, and G. M. Wyburn.** 1971. The digestive system. An ultrastructural atlas and review, p. 107–127. Butterworths, London.
215. **Tully, J. G., R. F. Whitcomb, D. L. Williamson, and H. Fred Clark.** 1977. Suckling mouse cataract agent is a helical wall—free procaryote (spiroplasma) pathogenic for vertebrates. Nature (London) **259**:112–120.
216. **Turner, T. B., and D. H. Hollander.** 1950. Cortisone in experimental syphilis. (A preliminary note). Bull. Johns Hopkins Hosp. **87**:503–509.
217. **Turner, T. B., and D. H. Hollander.** 1954. Studies on the mechanism of action of cortisone in experimental syphilis. Am. J. Syph. Gonorrhea Vener. Dis. **38**:371–387.
218. **Tyson, G. E.** 1970. The occurrence of a spirochete-like organism in tissues of the brine shrimp *Artemia salina*. J. Invert. Pathol. **15**:145–147.
219. **Tyson, G. E.** 1974. Distinctive renal lesion of spirochete-infected brine shrimp. J. Bacteriol. **119**:629–631.
220. **Tyson, G. E.** 1974. Ultrastructure of a spirochete found in tissues of the brine shrimp, *Artemia salina*. Arch. Microbiol. **99**:281–294.
221. **Tyson, G. E.** 1975. Tubular structures associated with intracytoplasmic spirochetes. Cell Tissue Res. **158**:333–337.
222. **Tyson, G. E.** 1975. Phagocytosis and digestion of spirochetes by amebocytes of infected brine shrimp. J. Invert. Pathol. **26**:105–111.
223. **Ushijima, T.** 1970. Morphology and chemistry of the bacterial cell wall. I. The location of mucopeptide in the cell wall of *Bacteroides convexus* and its chemical composition. Jpn. J. Microbiol. **14**:15–25.
224. **Valentine, R. C.** 1961. Contrast enhancement in the electron microscopy of viruses, p. 287–318. *In* K. M. Smith and M. A. Lauffer (ed.), Advances in virus research, vol. 8. Academic Press, Inc., New York.
225. **Vallejo, M. T.** 1969. Spirochaetales microorganisms: an agent possibly associated with swine dysentery. Vet. Rec. **85**:562–563.
226. **Van Thiel, P. H.** 1948. The leptospiroses. University of Leiden.
227. **Volk, W. A.** 1966. Cell wall lipopolysaccharides from *Xanthomonas* species. J. Bacteriol. **91**:39–42.
228. **Wachter, M. S., and R. C. Johnson.** 1975. Treponeme outer envelope: chemical analysis (39151). Proc. Soc. Exp. Biol. Med. **151**:97–100.
229. **Wecke, J., J. Bartunek, and G. Stüttgen.** 1976. *Treponema pallidum* in early syphilitic lesions in humans during high-dosage penicillin therapy. Arch. Dermatol. Res. **257**:1–15.
230. **Westphal, O., and K. Jahn.** 1965. Bacterial lipopolysaccharides, p. 83–91. *In* R. L. Whistler (ed.), Methods in carbohydrate chemistry, vol. 5. Academic Press, Inc., New York.

231. **Weigand, S. E., P. L. Strobel, and L. H. Glassman.** 1972. Electron microscopic anatomy of pathogenic *Treponema pallidum*. J. Invest. Dermatol. **58**:186–204.
232. **Wile, U. J., and E. B. Kearney.** 1943. The morphology of *T. pallidum* in the electron microscope. Demonstration of flagella. J. Am. Med. Assoc. **122**:167–168.
233. **Wile, U. J., R. G. Picard, and E. B. Kearney.** 1942. The morphology of *Spirochaeta pallida* in the electron microscope. J. Am. Med. Assoc. **119**:880–881.
234. **Yanagawa, R., and S. Faine.** 1966. Morphological and serological analysis of leptospiral structure. Nature (London) **211**:823–826.
235. **Yanagihara, Y., and I. Mifuchi.** 1968. Microfibers present in surface structure of *Leptospira*. J. Bacteriol. **95**:2403–2406.
236. **Yanagihara, Y., K. Saito, and I. Mifuchi.** 1974. Studies on microfiber present in surface structure of *leptospira* and other spirochetes. Folia Fac. Med. Univ. Comenianae Bratisl. **12** (Suppl.): 25–35.
237. **Zeigler, J. A., A. M. Jones, R. H. Jones, and K. M. Kubica.** 1976. Demonstration of extracellular material at the surface of pathogenic *T. pallidum* cells. Br. J. Vener. Dis. **52**:1–8.
238. **Zeigler, J. A., and W. P. Van Eseltine.** 1975. Isolation and chemical characterization of outer envelope of *Leptospira pomona*. Can. J. Microbiol. **21**:1102–1112.
239. **Zuelzer, M.** 1911–1912. Über *Spirochaeta plicatilis* Ehrbg. und deren Verwandtschaftsbeziehungen. Arch. Protistenkd. **24**:1–59.